Stimuli-Responsive Hydrogel Microlenses

A Thesis
Presented to
The Academic Faculty

by

Jongseong Kim

In Partial Fulfillment
of the Requirements for the Degree
Doctor of Philosophy in the
School of Chemistry and Biochemistry

Georgia Institute of Technology
May 2007

Stimuli-Responsive Hydrogel Microlenses

Approved by:

Dr. L. Andrew Lyon, Advisor
(School of Chemistry and Biochemistry)

Dr. Jiri Janata
(School of Chemistry and Biochemistry)

Dr. Robert M. Dickson
(School of Chemistry and Biochemistry)

Dr. Marcus Weck
(School of Chemistry and Biochemistry)

Dr. Mohan Srinivasarao
(School of Polymer, Textile & Fiber Engineering)

January 2, 2007

ACKNOWLEDGEMENTS

There are numerous people that have to be thanked for helping me through my graduate study, most of which cannot be mentioned in this short space. I would like to thank my advisor Prof. L. Andrew Lyon for giving me the opportunity to work in his lab. He always gave me advices about my research and also science. Throughout the four years in his lab, Andrew gave me the freedom to pursue the research that I was interested in. His excitement about science and chemistry guided me to think about my future career. I would like to thank my PhD committee; Prof. Jiri Janata, Prof. Robert M. Dickson, Prof. Marcus Weck, and Prof. Mohan Srinivasarao. I would like to thank the Lyon group especially Michael J. Serpe, Satish Nayak, and Neetu Singh. The friendships and collaboration we have made from this experience are very valuable to me. I would like to thank my wife, Heejoo, for everything she has sacrificed for me to make it this far in my career. For the past 5 years of marriage she has shown me extreme patience as well as offered unconditional love and support when I needed it most. I would like to thank all of my family members who supported me throughout the years. I thank God everyday for giving me a chance to do this work.

TABLE OF CONTENTS

LIST OF TABLES

LIST OF FIGURES

LIST OF SCHEMES

LIST OF ABBREVIATIONS

NIPAm	*N*-isopropylacrylamide
BIS	*N,N'*-Methylene(bisacrylamide)
AAc	Acrylic Acid
pNIPAm	Poly(*N*-isopropylacrylamide)
VPT	Volume Phase Transition
LCST	Lower Critical Solution Temperature
pNIPAm-co-AAc	Poly(*N*-isopropylacrylamide-*co*-acrylic acid)
VPTT	Volume Phase Transition Temperature
SDS	Sodium Dodecyl Sulfate
APS	Ammonium Persulfate
RI	Refractive Index
APTMS	3-Aminopropyltrimethoxysilane
AFA	4-Aminofluorescein
ABP	aminobenzophenone
PAH	poly(allylamine hydrochloride)
DIC	Differential Interference Contrast
FL	Fluorescence microscopy image
PEG	Poly(ethylene glycol)
CMC	Critical Micelle Concentration
DMSO	Dimethyl sulfoxide
MWCO	Molecular Weight Cut Off

MES	2-[*N*-morpholino]ethanesulfonic acid
EDC	1-ethyl-3-(3-dimethylaminopropyl)carbodiimide
DCC	Dicyclohexyl-carbodiimide
PBS	Phosphate Buffered Saline
SEM	Scanning Electron Microscope
TEM	Transmission Electron Microscopy
EtOH	Ethanol
Ag	Antigen
Ab	Antibody
K_d	Dissociation Constant
FPS	Frame per Second
CCD	Charge Coupled Device
N.A.	Numerical Aperture

SUMMARY

This dissertation is aimed towards using stimuli-responsive pNIPAm-co-AAc microgels synthesized via free-radical precipitation polymerization to prepare stimuli-responsive hydrogel microlenses. Chapter 1 gives a detailed background of hydrogels, and their applications using responsive hydrogels. Chapter 2 describes the use of colloidal hydrogel microparticles as microlens elements and the fabrication method to form the hydrogel microlens arrays via Coulombic interactions. Chapter 3 shows the demonstration of tunable microlenses prepared by the method used in Chapter 2. In this chapter the microlenses are subjected to various pH and temperature in aqueous solutions. Chapter 4 shows that microlens arrays constructed on Au nanoparticle-functionalized glass substrates display dramatic changes in lensing power as a function of an impingent frequency-doubled Nd:YAG laser. The microlens photoswitching is highly reversible, with sub-millisecond lens switching times. Chapter 5 describes the development of bioresponsive hydrogel microlenses as a new protein detection technology. The microlens method is shown to be very specific for the target protein, with no detectable interference from nonspecific protein binding. Chapter 6 describes the use of bioresponsive hydrogel microlenses as a label-free biosensing scaffolding. These microstructures simultaneously act as the biosensor's scaffolding/immobilization architecture, transducer, amplifier, and also allow for broad tunability of the analyte concentration to which the microlens is sensitive.

CHAPTER 1

INTRODUCTION TO HYDROGELS AS RESPONSIVE MATERIALS

This Chapter is intended to introduce a general background to hydrogel materials and their broad applications with the focus on the behavior of responsive hydrogels. First, hydrogel basics and classifications will be described in terms of the types of cross-links and monomers used. Then, some important examples of responsive hydrogels will be illustrated by classifying response types and applications. Finally, some of the recent advances in bioresponsive hydrogel materials will be extensively discussed in this Chapter.

1.1 Hydrogels

Hydrogels are difficult to define because they contain both fluidic and solid properties. For instance, they have structural integrity when displaced from their container. However, small molecules can transport through the hydrogel network as they move in a fluid. Here, hydrogels will be defined as physically/chemically cross-linked polymeric materials that swell strongly in aqueous phase.[1-4] Hydrogels are further characterized as a cross-linked network that exhibits visco-elastic or pure elastic behavior, which provides dimensional stability to the soft material. The swelling of hydrogels is another characteristic because they can absorb aqueous media about thousand times more than their dry weight.[4-6] This water-absorbing property of the hydrogels can be controlled not only by cross-links but also by the monomer identity, which makes them enable to

respond to various stimuli via the volume phase transtion[3] Most of recent advances in responsive hydrogels sophisticate this classic property for useful applications in tunable optical elements,[7-11] micro-fluidic flow control,[12-17] surface patterning,[18-20] sensing transducers,[21-28] catalysis,[29-32] drug delivery,[33-52] protein separation,[53-56] cellular/tissue engineering[5,57-63] and bio-assay/sensing.[2,21,64-75]

1.1.1 Cross-links in Hydrogels

Cross-links play an important role in sustaining the structural stability of the hydrogels. Based on the type of cross-links, hydrogels can be classified as physically or chemically cross-linked.[3] In the class of physically cross-linked hydrogels, their networks are formed by noncovalent interactions such as hydrophobic interactions, ionic interactions, hydrogen bonds, coordination bonds, and protein-ligand associations.[1,3,6,76-81] The motivations in the preparation of this class of hydrogels is often to accomplish reversible or degradable hydrogels that exhibit a transition from dimensionally stable polymer to a polymer solution. Such a transition behavior can be achieved mainly due to the weak binding strength of noncovalent interactions. These hydrogels have been studied for encapsulation of proteins, drugs, or cells and then, their release from the dissolved hydrogels.[33,59,82,83] For chemically cross-linked hydrogels, the cross-links are often formed by polymerizing monomers with cross-linking agents such as *N,N'* methylene(bisacrylamide) (BIS), which provides stable hydrogel structures due to the higher binding strength of covalent bonds.[1,3,15]

1.1.2 Monomers in Hydrogels

Hydrogels are polymeric gels that can be formed by polymerization of monomers with or without cross-linking agents as previously described in this Chapter. Thus, the characteristic behaviors of the polymeric hydrogels are mostly originated from the monomers used for the polymerization. Based on the type of the monomers, the hydrogels are enable to show significant transition behaviors in response to external stimuli such as temperature, pH, photon flux, ionic strength, and electric currents.[7,10,84-102] These thermoresponsive hydrogels undergo a reversible phase separation at the lower critical solution temperature (LCST) or upper critical solution temperature (UCST) of the polymer as the hydrogel goes from a swollen (or deswollen) state to a deswollen (or swollen) state.[84,86,96,103,104] For instance, *N*-isopropylacrylamide (NIPAm) is one of the extensively studied monomers for hydrogel polymerizations due to the polymer's thermal behavior in aqueous solutions. Thermoresponsive poly(*N*-isopropylacrylamide) pNIPAm hydrogels can be prepared via a number of polymerization routes.[92,96,105-111] By simply adding Acrylic acid (AAc) as a comonomer during the polymerization, a thermoresponsive hydrogel can be endowed with pH responsivity,.[87,112,113] The same methodology can be used to make hydrogels attractive for a number of applications as responsive materials.

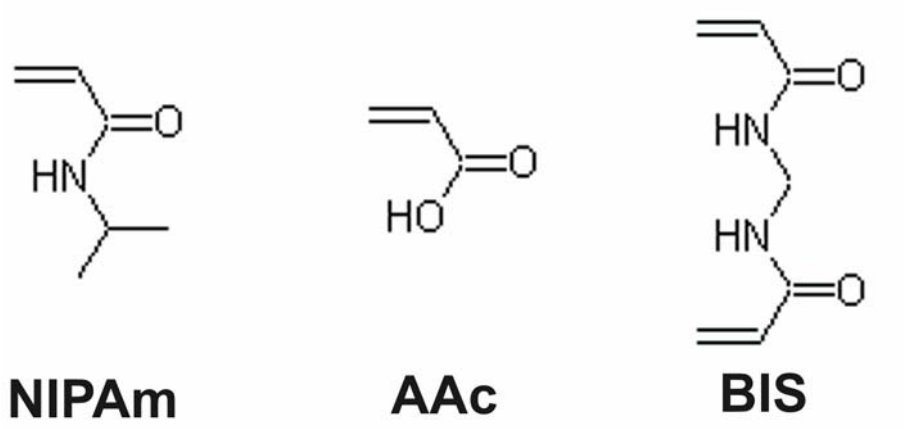

Figure 1-1. Common monomers used in the synthesis of thermo/pH responsive microgels.
NIPAm – *N*-isopropylacrylamide
AAc – Acrylic acid
BIS – *N,N'*- methylenebisacrylamide

1.1.3 Microgel Synthesis

Responsive microgels, colloidally stable particles, are characterized by the fast response time for the volume phase transition in sub-second range as well as by their smaller size, higher surface area, and high diffusivity than those of their macrogel counterparts.[114] These microgels can be synthesized by the precipitation polymerization technique, which is the most common method to prepare thermoresponsive microgels. In this procedure, thermoresponsive pNIPAm hydrogel particles have been prepared with narrow size distribution. The volume phase transition temperature (VPTT) of the

microgel is affected by cross-linking density, solvents and comonomer in similar fashion as their macrogel counterpart does.[112,113,115]

Responsive pNIPAm microgels can be synthesized via a number of routes such as precipitation polymerization, miniemulsion polymerization and microemulsion polymerization.[96,111,116-125] Here, standard temperature induced precipitation polymerization method for pNIPAm-*co*-AAc microgel formation will be described because all studies on this dissertation used such microgels as a basic template. This method takes advantage of the water solubility of the precursor monomers and the temperature dependent solubility of the polymerized form of the monomers. Precipitation polymerization is carried out in a three-neck round bottom flask containing water that is rigorously purged with N_2. The purge is required to remove any dissolved O_2 from the reaction mixture, which acts as a free radical scavenger capable of preventing the polymerization reaction from occurring. The solution of main monomer NIPAm and the cross-linker BIS are allowed to stir and heat above the LCST of the NIPAm. A number of comonomers can be added to the solution, which provides various functionalities to hydrogel dependant on monomers. Note that some concentration of the surfactant, such as sodium dodecyl sulfate (SDS), at a concentration below the critical micelle concentration (CMC) can be used as a microgel stabilizer in these reactions. For all studies contained in this dissertation AAc was used as a comonomer. The chemical structures for the common monomers used in this dissertation are shown in Figure 1-1. The reaction can be initiated by adding the free-radical initiator ammonium persulfate (APS). Addition of APS results in its cleavage producing free radical fragments in solution, which are able to react with the solubilized monomer and cross-linker. Upon

addition of initiator, pNIPAm chains form and grow and upon reaching a certain critical chain length, collapse upon themselves forming precursor particles. Precursor particles serve as nuclei for microgel growth eventually reaching a stable structure with a diameter which can be also modulated by the amount of surfactant SDS when present in the reaction mixture.[106,126-128] For example, high SDS concentrations result in small microgels while low SDS concentrations result in large microgels. Figure 1-2 shows a schematic of the various stages of microgel growth. As discussed previously, numerous comonomers are available that can be added to the reaction mixture to add multiple functionalities to microgels.

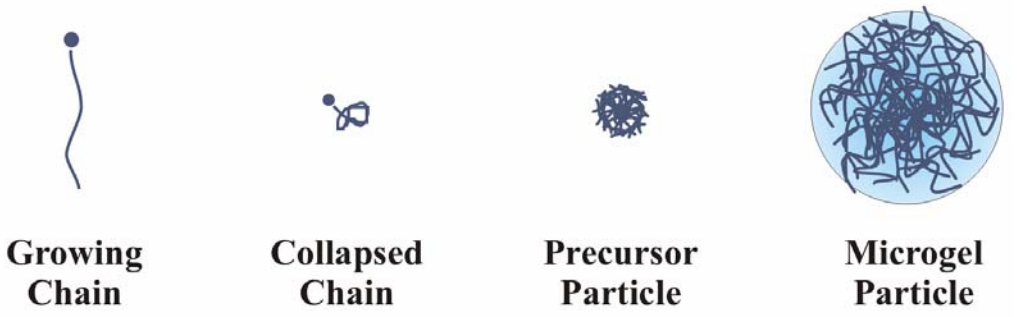

Figure 1-2. Schematic of the various stages of microgel growth during precipitation polymerization involving pNIPAm chain growth, which collapse upon reaching a critical chain length. The collapsed chains then serve as precursor particles for growth resulting in a stable microgel.

1.2 Responsive Hydrogels

Responsive hydrogels are classified as responsive materials for their stimuli responsive properties and also distinguished from non-responsive hydrogels that are simply swollen in aqueous phase.[85,96,103] Extensive efforts in the field of responsive hydrogels have been focused on the design of structures that respond to specific stimuli.[2,21,32,49,59,65,72,129,130] An equilibrium degree of hydrogel swelling can be modified by adjusting polymer hydrophilicity, network elasticity, and charge density.[86,87,103,131]

One of the earliest studies on the transitional swelling of polymer networks was reported by Dusek and Patterson.[103] In their theoretical calculations, they expected that the critical conditions for the phase transition of free swelling gel can be achieved by adjusting cross-linking of polymeric gel and dissolved solvent quality. In contrast to free swelling gel, they also suggested that the phase transition of polymer network under the tensional condition can be achieved.

In other pioneering work, the Tanaka group showed that thermoresponsive ionic gels exhibit a discontinuous transition in contrast to a continuous transition exhibited by non-ionic gels. They also reported that deswelling rate of the ionic gels is inversely proportional to the square of the smallest dimension of the material.[86-88,90,91] In addition to this contribution, Yan and Hoffman reported that polymerization of NIPAm gels at higher temperatures than the LCST of the polymer results in formation of the gels that have a large pore size.[108] By their methodology, the pNIPAm gels with faster swelling rate were successfully synthesized.

Early responsive hydrogel studies were focused on the development of new materials that responded to various stimuli such as pH, temperature, light, and electric

field that eventually cause the phase separation of the polymeric materials.[33,84,87,88,94] For instance, when gels are formed by polymerizing the thermoresponsive main monomer, NIPAm, and the light-sensitive chromophore chlorophyllin, in presence of cross-link agent, the phase transition of the gels are induced by illumination.[94] Another interesting study on responsive gels was performed by applying electric fields to polyacrylamide gels. In this study, some portion of acrylamide group was converted into acrylic acid group by hydrolysis, and then the volume phase transition of the ionic gels was induced under electric fields, which provide pH gradient and Coulombic interaction between electrods.[88]

Based on these pioneering works, responsive polymeric gels have been extensively studied for useful application in the field of controlled drug release. In early studies, ionic polymer gels composed of poly(ethyloxazoline) (PEOx) and either poly(methacrylic acid) (PMMA) or poly(acrylic acid) were used to load insulin into the gel matrix. By applying electric current to the insulin-loaded matrix, the loaded insulin was released from the matrix by disrupting hydrogen bonding in the responsive gels.[33] Although this study was far from practical applications, the concept of erodible gels which response to external stimuli has since been widely investigated in the field of drug release.[35,36,63,132-135]

In other fields of responsive hydrogels, the phase transition of the responsive gels was used for the formation of chemical sensing materials in combination with non-responsive materials.[18,21,24,27,54,66-69,75,136,137] For chemical sensing, a crystalline colloidal array is prepared from non-responsive polymer spheres which were then polymerized in a responsive hydrogel. The hydrogel matrix also contains molecular recognition moieties

for metal ions, which results in the hydrogel swelling in the presence of the metal ions due to an increased osmotic pressure. Eventually, the swelling of the hydrogel matrix shifts the distance between non-responsive colloidal spheres and thus the Bragg peak shifts in wavelength.[21] They also reported that the crystalline colloidal array can be modified with different molecular recognition moieties, which results in various types of sensing platforms for the detection of glucose, organophosphorus compounds, and creatinine.

Some interesting studies using responsive hydrogels was reported by Beebe group.[12] In their work, responsive hydrogels are used to create functional compartment for flow control within microfluidic channels via photo-polymerization. By fabricating gate components with different types of responsive hydrogels, they have shown that the microfluidic system can be controlled autonomously when the hydrogel gate undergoes a swelling or deswelling transition in response to a fluid stream. More importantly, they mentioned that the fast response times of responsive gels can be attained in micron scale mainly due to the short diffusion paths, while their responsive hydrogel construct are actually macro-scale with slow response rate about a few seconds.

Responsive microgels formed by precipitation polymerization have been widely used not only for the alternative of responsive macrogels but also for development of the novel responsive materials in advanced applications. In the case of new applications using the microgels, microgel colloidal crystalline assemblies have been prepared by using thermoresponsive hydrogel microparticles, which results in the unusual phase behavior due to the microgel thermoresponsivity and the inherent softness of their interaction potentials.[138-140] In these studies, the thermoresponsivity of the microgel

particles makes the crystalline assemblies rapidly and widely tunable in the structures by local environment changes such as temperature and irradiation. Since the hydrogel particles can be formed in a true micrometer scale and also they undergo swelling or deswelling of the particle volumes in response to external stimuli, the microgels have been utilized to fabricate responsive hydrogel microlenses via simple Coulombic interactions without complex fabrication steps.[7,10,64,65] These studies will be extensively described in the later chapters of this dissertation.

1.3 Bioresponsive Hydrogels

Bioresponsive soft materials, which undergo structural and/or morphological changes in response to a biological stimulus, have been investigated for numerous applications in drug delivery, tissue regeneration, bioassays/biosensors, and biomimetic systems.[5,21,33-52,57-75] In contrast to simple stimuli-sensitive hydrogels as described in previous section, more sophisticated hydrogels that are coupled to bioresponsive moieties have been engineered by varying the polymer composition, polymeric structure, and the display of specific functional groups. Here, recent efforts in the field of bioresponsive materials will be described by the response types of the structures to biological stimuli.

First, bioresponsive hydrogels can be designed in a degradable form in response to external stimuli such as enzymes. This type of hydrogel has been widely studied for development of intelligent drug delivery systems and tissue regeneration agents.[42,59,60,141,142] The second type is biologically decorated gels that exhibit an association or repulsion to biological stimuli. Such materials have been applied in the fields of targeting cells, protein sieving, and development of the functional substrates to

prevent or enhance cell adhesion.[49,53,58,143] Reversibly bio-responsive materials have also been developed, wherein they display a change in their volume and/or optical properties in response to the stimulus. One potential application of such bioresponsive materials is in biomolecular sensing, where a physicochemical change of a material is monitored and related to a protein, oligonucleotide, or ligand binding event.[2,21,64,65,72,144]

One of the recent studies on biodegradable materials was reported by Kim and Healy.[145] In this effort, pNIPAm-*co*-AAc hydrogels are prepared by photo-polymerization with the peptide cross-linker that provides enzyme degradable capability of the hydrogels. In the presence of the specific enzyme, collagenase, the peptide cross-linked hydrogels were successfully degraded in dependence on the concentration of the enzyme and the initial cross-linking density. Similarly, the preparation of poly(acrylamide) hydrogels with peptide cross-linker was reported by Moore group.[141] These hydrogels are also dissolved when exposed to a solution of α-chymotrypsin.

One potential application of such biodegradable hydrogels was reported by the Hubbell group in the field of tissue regeneration.[59,60] In their studies, hydrogels were prepared by engineering the network with integrin binding sites and substrate for matrix metalloproteinase (MMP), which allows degradable network and invasive structure by cells. When the engineered hydrogels were subjected to primary human fibroblasts, the cell adhesion and invasion into the network were observed via integrin binding and MMP mediation of the cells, respectively. This result suggests that novel functional hydrogels can be used for fundamental studies on cell-matrix interactions and furthermore as biocompatible materials for tissue regeneration. In a similar concept, drug delivery devices by applying the biodegradable hydrogels have been explored wherein drug

release is coupled to a change in the hydrogel conformation.[42] In this research, the hydrogel matrix polymerized with peptide cross-links is loaded with chemotherapy agents and then releases them via enzymatic cleavage of hydrogel cross-links in the presence of MMP.

Another type of bioresponsive hydrogel was demonstrated by conjugating a bio-affinity pair to the hydrogels. In this model, the hydrogels have been used as a convenient construct for post-functionalization that allows specific capabilities such as protein:ligand binding. One interesting example of such kinds of the hydrogels is in targeting cell as a potential drug carrier, where pNIPAm core-shell hydrogel nanoparticles are conjugated with the folic acid that is a ligand for targeting cancer cells.[49] In this work, when the folic acid labeled hydrogel particles are incubated with cancer cells that overexpress the folate receptors, the hydrogel particles are incorporated into the cancer cells via receptor-mediated endocytosis.

In similar fashion, more sophisticated hydrogel nanoparticles have been proposed for protein sieving in combination with the degradable concept as previously discussed. In this study, core-shell hydrogel nanoparticles are synthesized by "seed and feed" polymerization route, in which the shell is composed of chemically degradable cross-links and the core is coupled with a ligand. Then, the protein sieving through the degradable shell to the ligand labeled core is controlled by adjusting the pore size of the shell via the cleavage of the cross-links.[53] These results suggest that by manipulating the cross-linking density of the hydrogel shell, one can simply sieve a particular size of proteins, which also eliminates the concern about nonspecific binding of macromolecules such as larger proteins in some applications.

One of the advanced types of bioresponsive hydrogels is in biomolecular sensing/assays, where a physicochemical change of a hydrogel is monitored and related to a protein, oligonucleotide, or ligand binding event. Some important studies on the reversibly bioresponsive hydrogel platform were reported by the Miyata group.[2,71,72,144] In their work, reversibly bioresponsive hydrogels were formed by grafting the antigen and the antibody counterpart into hydrogel network, which provides reversible non-covalent cross-links via antigen-antibody binding. In the presence of free antigen, the bound antigen-antibody cross-links are disrupted via competitive binding of the free antigen, which results in swelling of the hydrogels mainly due to decrease of the cross-link degree. In addition, the hydrogels undergo reversible volume change, when they exposed to free antigen solution or buffer solution via disruption or formation of the cross-link, respectively. More recently, they reported that bioresponsive gel can be used to recognize tumor-specific glycoprotein marker (α-fetoprotein, AFP), where the gel is prepared by biomolecular imprinting using lectin-AFP-antibody complex.[2] In this study, the biomolecular imprinted gel shows tumor marker responsive behavior by changing volume in presence of the AFP. These both studies have shown that the cross-link of the gel can be dynamically tuned by using biomolecular binding pairs as a cross-link, resulting in the volume change. However, there are still challenging issues that the response time of the bioresponsive gels are slow about ~1h, and the volume change in response to stimuli is about 5% with respect to the original volume. These issues are mainly due to the fact that the reported hydrogels are bulk gels which have a slower phase transition than that of microgels.

Ulijn group has shown that the molecular accessibility of enzyme responsive hydrogel beads can be controlled by the presence of a specific enzyme.[146] In this study, hydrogel beads that consist of acrylamide and PEG are incorporated with enzyme cleavable peptide linkers containing cationic arginine residues. The charged residues result in the swelling of the hydrogels via Columbic repulsion and in turn the increase of the pore size. When the enzyme responsive hydrogels are exposed to a target enzyme, the incorporated peptide linkers are cleaved from the hydrogel network, which results in deswelling of the hydrogel via the decrease of Coulombic repulsion. Another interesting study on bioresponsive hydrogels have been shown by Daunert group.[147] In their research, the conformational change of a protein is used to prepare bioresponsive hydrogels since certain proteins show the conformational change and then different binding affinities via allostery. The bioresponsive hydrogels prepared by calmodulin (protein) and phenothiazine (ligand) are responsive to Ca^{+} (stimulus or allosteric enhancer). In the presence of Ca^{+}, the hydrogels are deswollen by the conformational change of the protein and thus protein-ligand binding in the hydrogel network.

These so-called bioresponsive materials may in the future allow for the design of systems that can be triggered to perform a task or set of tasks in response to a biological event. While these materials have been successfully employed for various bio-applications such as controlled drug delivery systems, bio-sensing/assay and in tissue engineering, they are still of enormous interest for developing more sophisticated materials that display more complex responsivities.

1.4 References

(1) Hoffman, A. S., Hydrogels for biomedical applications. *Adv. Drug Deliv. Rev.* **2002**, *54*, 3-12.

(2) Miyata, T.; Jige, M.; Nakaminami, T.; Uragami, T., Tumor marker-responsive behavior of gels prepared by biomolecular imprinting. *Proc. Natl. Acad. Sci. USA* **2006**, *103*, 1190-1193.

(3) Hennink, W. E.; van Nostrum, C. F., Novel crosslinking methods to design hydrogels. *Adv. Drug Deliv. Rev.* **2002**, *54*, 13-36.

(4) Yeomans, K., Hydrogels - very versatile materials. *Chem. Rev.* **2000**, *10*, 2-5.

(5) Drury, J. L.; Mooney, D. J., Hydrogels for tissue engineering: scaffold design variables and applications. *Biomaterials* **2003**, *24*, 4337-4351.

(6) DeRossi, D.; Kajiwara, K.; Osada, Y.; Yamauchi, A. *Polymer Gels. Fundamentals and Biomedical Applications*; Plenum Press: New York, 1991.

(7) Kim, J.; Serpe, M. J.; Lyon, L. A., Photoswitchable Microlens Arrays. *Angew. Chem. Intl. Ed.* **2005**, *44*, 1333-1336.

(8) Dong, L.; Agarwal Abhishek, K.; Beebe David, J.; Jiang, H., Adaptive liquid microlenses activated by stimuli-responsive hydrogels. *Nature* **2006**, *442*, 551-554.

(9) Serpe, M. J.; Kim, J.; Lyon, L. A., Colloidal hydrogel microlenses. *Adv. Mater.* **2004**, *16*, 184-187.

(10) Kim, J.; Serpe, M. J.; Lyon, L. A., Hydrogel Microparticles as Dynamically Tunable Microlenses. *J. Am. Chem. Soc.* **2004**, *126*, 9512-9513.

(11) Reese, C. E.; Mikhonin, A. V.; Kamenjicki, M.; Tikhonov, A.; Asher, S. A., Nanogel Nanosecond Photonic Crystal Optical Switching. *J. Am. Chem. Soc.* **2004**, *126*, 1493-1496.

(12) Beebe, D. J.; Moore, J. S.; Bauer, J. M.; Yu, Q.; Liu, R. H.; Devadoss, C.; Jo, B.-H., Functional hydrogel structures for autonomous flow control inside microfluidic channels. *Nature* **2000**, *404*, 588-590.

(13) Atencia, J.; Beebe, D. J., Controlled microfluidic interfaces. *Nature* **2005**, *437*, 648-655.

(14) Yu, Q.; Bauer, J. M.; Moore, J. S.; Beebe, D. J., Responsive biomimetic hydrogel valve for microfluidics. *Appl. Phys. Lett.* **2001**, *78*, 2589-2591.

(15) Eddington, D. T.; Beebe, D. J., Flow control with hydrogels. *Adv. Drug Deliv. Rev.* **2004**, *56*, 199-210.

(16) Zhao, B.; Moore, J. S., Fast pH- and Ionic Strength-Responsive Hydrogels in Microchannels. *Langmuir* **2001**, *17*, 4758-4763.

(17) Arndt, K. F.; Kuckling, D.; Richter, A., Application of sensitive hydrogels in flow control. *Polym. Adv. Technol.* **2000**, *11*, 496-505.

(18) Hu, Z.; Chen, Y.; Wang, C.; Zheng, Y.; Li, Y., Polymer gels with engineered environmentally responsive surface patterns. *Nature* **1998**, *393*, 149-152.

(19) Galindo, F.; Lima, J. C.; Luis, S. V.; Parola, A. J.; Pina, F., Write-read-erase molecular-switching system trapped in a polymer hydrogel matrix. *Adv. Funct. Mater.* **2005**, *15*, 541-545.

(20) Suh, K. Y.; Langer, R.; Lahann, J., A novel photoderinable reactive polymer coating and its use for microfabrication of hydrogel elements. *Adv. Mater.* **2004**, *16*, 1401-1405.

(21) Holtz, J. H.; Asher, S. A., Polymerized colloidal crystal hydrogel films as intelligent chemical sensing materials. *Nature* **1997**, *389*, 829-832.

(22) Yoshimura, I.; Miyahara, Y.; Kasagi, N.; Yamane, H.; Ojida, A.; Hamachi, I., Molecular recognition in a supramolecular hydrogel to afford a semi-wet sensor chip. *J. Am. Chem. Soc.* **2004**, *126*, 12204-12205.

(23) Lee, M.-C.; Kabilan, S.; Hussain, A.; Yang, X.; Blyth, J.; Lowe, C. R., Glucose-Sensitive Holographic Sensors for Monitoring Bacterial Growth. *Analytical Chemistry* **2004**, *76*, 5748-5755.

(24) Holtz, J. H.; Holtz, J. S. W.; Munro, C. H.; Asher, S. A., Intelligent Polymerized Crystalline Colloidal Arrays: Novel Chemical Sensor Materials. *Analytical Chemistry* **1998**, *70*, 780-791.

(25) Liu, L.; Li, P.; Asher, S. A., Entropic trapping of macromolecules by mesoscopic periodic voids in a polymer hydrogel. *Nature* **1999**, *397*, 141-144.

(26) Lee, K.; Asher, S. A., Photonic Crystal Chemical Sensors: pH and Ionic Strength. *J. Am. Chem. Soc.* **2000**, *122*, 9534-9537.

(27) Asher, S. A.; Sharma, A. C.; Goponenko, A. V.; Ward, M. M., Photonic Crystal Aqueous Metal Cation Sensing Materials. *Analytical Chemistry* **2003**, *75*, 1676-1683.

(28) Alvarez-Lorenzo, C.; Guney, O.; Oya, T.; Sakai, Y.; Kobayashi, M.; Enoki, T.; Takeoka, Y.; Ishibashi, T.; Kuroda, K.; Tanaka, K.; Wang, G.; Grosberg, A. Y.; Masamune, S.; Tanaka, T., Reversible adsorption of calcium ions by imprinted temperature sensitive gels. *J. Chem. Phys.* **2001**, *114*, 2812-2816.

(29) Bergbreiter, D. E.; Liu, Y.-S.; Osburn, P. L., Thermomorphic Rhodium(I) and Palladium(0) Catalysts. *J. Am. Chem. Soc.* **1998**, *120*, 4250-4251.

(30) Bergbreiter, D. E.; Case, B. L.; Liu, Y.-S.; Caraway, J. W., Poly(N-isopropylacrylamide) soluble polymer supports in catalysis and synthesis. *Macromolecules* **1998**, *31*, 6053-6062.

(31) Nagayama, H.; Maeda, Y.; Shimasaki, C.; Kitano, H., Catalytic Properties of Enzymes Modified With Temperature- Responsive Polymer-Chains. *Macromol. Chem. Phys.* **1995**, *196*, 611-620.

(32) Shimoboji, T.; Larenas, E.; Fowler, T.; Kulkarni, S.; Hoffman, A. S.; Stayton, P. S., Photoresponsive polymer-enzyme switches. *Proc. Natl. Acad. Sci. USA* **2002**, *99*, 16592-16596.

(33) Kwon, I. C.; Bae, Y. H.; Kim, S. W., Electrically erodible polymer gel for controlled release of drugs. *Nature* **1991**, *354*, 291-293.

(34) Kim, S. W.; Bae, Y. H.; Okano, T., Hydrogels: swelling, drug loading, and release. *Pharm. Res.* **1992**, *9*, 283-90.

(35) Jeong, B.; Bae, Y. H.; Lee, D. S.; Kim, S. W., Biodegradable block copolymers as injectable drug-delivery systems. *Nature* **1997**, *388*, 860-862.

(36) Peppas, N. A., Hydrogels and drug delivery. *Current Opinion in Colloid & Interface Science* **1997**, *2*, 531-537.

(37) Langer, R., Drug delivery and targeting. *Nature* **1998**, *392*, 5-10.

(38) Park, T. G., Temperature modulated protein release from pH/temperature-sensitive hydrogels. *Biomaterials* **1999**, *20*, 517-521.

(39) Kikuchi, A.; Okano, T., Pulsatile drug release control using hydrogels. *Adv. Drug Delivery Rev.* **2002**, *54*, 53-77.

(40) Nolan, C. M.; Serpe, M. J.; Lyon, L. A., Thermally modulated insulin release from microgel thin films. *Biomacromolecules* **2004**, *5*, 1940-1946.

(41) Serpe, M. J.; Yarmey, K. A.; Nolan, C. M.; Lyon, L. A., Doxorubicin Uptake and Release from Microgel Thin Films. *Biomacromolecules* **2005**, *6*, 408-413.

(42) Tauro, J. R.; Gemeinhart, R. A., Matrix Metalloprotease Triggered Delivery of Cancer Chemotherapeutics from Hydrogel Matrixes. *Bioconjugate Chem.* **2005**, *16*, 1133-1139.

(43) Cheng, J.; Teply, B. A.; Jeong, S. Y.; Yim, C. H.; Ho, D.; Sherifi, I.; Jon, S.; Farokhzad, O. C.; Khademhosseini, A.; Langer, R. S., Magnetically Responsive Polymeric Microparticles for Oral Delivery of Protein Drugs. *Pharmaceutical Research* **2006**, *23*, 557-564.

(44) LaVan, D. A.; McGuire, T.; Langer, R., Small-scale systems for in vivo drug delivery. *Nature Biotechnology* **2003**, *21*, 1184-1191.

(45) Murthy, N.; Thng, Y. X.; Schuck, S.; Xu, M. C.; Frechet, J. M. J., A novel strategy for encapsulation and release of proteins: Hydrogels and microgels with acid-labile acetal cross-linkers. *J. Am. Chem. Soc.* **2002**, *124*, 12398-12399.

(46) Gupta, P.; Vermani, K.; Garg, S., Hydrogels: from controlled release to pH-responsive drug delivery. *Drug Discovery Today* **2002**, *7*, 569-579.

(47) Qiu, Y.; Park, K., Environment-sensitive hydrogels for drug delivery. *Adv. Drug Deliv. Rev.* **2001**, *53*, 321-339.

(48) Moselhy, J.; Wu, X. Y.; Nicholov, R.; Kodaria, K., In vitro studies of the interaction of poly(NIPAm/MAA) nanoparticles with proteins and cells. *J. Biomater. Sci., Polym. Ed.* **2000**, *11*, 123-147.

(49) Nayak, S.; Lee, H.; Chmielewski, J.; Lyon, L. A., Folate-Mediated Cell Targeting and Cytotoxicity Using Thermoresponsive Microgels. *J. Am. Chem. Soc.* **2004**, *126*, 10258-10259.

(50) Uhrich, K. E.; Cannizzaro, S. M.; Langer, R. S.; Shakesheff, K. M., Polymeric Systems for Controlled Drug Release. *Chemical Reviews* **1999**, *99*, 3181-3198.

(51) Kiser, P. F.; Wilson, G.; Needham, D., A synthetic mimic of the secretory granule for drug delivery. *Nature* **1998**, *394*, 459-462.

(52) Sato, K.; Kodama, D.; Naka, Y.; Anzai, J.-i., Electrochemically Induced Disintegration of Layer-by-Layer-Assembled Thin Films Composed of 2-Iminobiotin-Labeled Poly(ethyleneimine) and Avidin. *Biomacromolecules* **2006**, *7*, 3302-3305.

(53) Nayak, S.; Lyon, L. A., Ligand-functionalized core/shell microgels with permselective shells. *Angew. Chem. Intl. Ed.* **2004**, *43*, 6706-6709.

(54) Liu, L.; Li, P.; Asher, S. A., Entropic trapping of macromolecules by mesoscopic periodic voids in a polymer hydrogel. *Nature* **1999**, *397*, 141-144.

(55) Kim, J. J.; Park, K., Smart hydrogels for bioseparation. *Bioseparation* **1998**, *7*, 177-84.

(56) Kawaguchi, H.; Fujimoto, K., Smart latexes for bioseparation. *Bioseparation* **1998**, *7*, 253-258.

(57) Yaszemski, M. J.; Payne, R. G.; Hayes, W. C.; Langer, R. S.; Aufdemorte, T. B.; Mikos, A. G., The ingrowth of new bone tissue and initial mechanical properties of a degrading polymeric composite scaffold. *Tissue Engineering* **1995**, *1*, 41-52.

(58) Luo, Y.; Shoichet, M. S., A photolabile hydrogel for guided three-dimensional cell growth and migration. *Nature Materials* **2004**, *3*, 249-253.

(59) Lutolf, M. P.; Raeber, G. P.; Zisch, A. H.; Tirelli, N.; Hubbell, J. A., Cell-responsive synthetic hydrogels. *Adv. Mater.* **2003**, *15*, 888-892.

(60) Lutolf, M. P.; Lauer-Fields, J. L.; Schmoekel, H. G.; Metters, A. T.; Weber, F. E.; Fields, G. B.; Hubbell, J. A., Synthetic matrix metalloproteinase-sensitive hydrogels for the conduction of tissue regeneration: Engineering cell-invasion characteristics. *Proc. Natl. Acad. Sci. USA* **2003**, *100*, 5413-5418.

(61) Choi, S. H.; Yoon, J. J.; Park, T. G., Galactosylated poly(N-isopropylacrylamide) hydrogel submicrometer particles for specific cellular uptake within hepatocytes. *J. Colloid Interf. Sci.* **2002**, *251*, 57-63.

(62) Jen, A. C.; Wake, M. C.; Mikos, A. G., Review: Hydrogels for cell immobilization. *Biotechnol. Bioeng.* **1996**, *50*, 357-364.

(63) Lee, K. Y.; Peters, M. C.; Anderson, K. W.; Mooney, D. J., Controlled growth factor release from synthetic extracellular matrices. *Nature* **2000**, *408*, 998-1000.

(64) Kim, J.; Singh, N.; Lyon, L. A., Label-free biosensing with hydrogel microlenses. *Angew. Chem. Intl. Ed.* **2006**, *45*, 1446-1449.

(65) Kim, J.; Nayak, S.; Lyon, L. A., Bioresponsive Hydrogel Microlenses. *J. Am. Chem. Soc.* **2005**, *127*, 9588-9592.

(66) Asher, S. A.; Alexeev, V. L.; Goponenko, A. V.; Sharma, A. C.; Lednev, I. K.; Wilcox, C. S.; Finegold, D. N., Photonic crystal carbohydrate sensors: Low ionic strength sugar sensing. *J. Am. Chem. Soc.* **2003**, *125*, 3322-3329.

(67) Alexeev, V. L.; Sharma, A. C.; Goponenko, A. V.; Das, S.; Lednev, I. K.; Wilcox, C. S.; Finegold, D. N.; Asher, S. A., High ionic strength glucose-sensing photonic crystal. *Analytical Chemistry* **2003**, *75*, 2316-2323.

(68) Walker, J. P.; Asher, S. A., Acetylcholinesterase-Based Organophosphate Nerve Agent Sensing Photonic Crystal. *Analytical Chemistry* **2005**, *77*, 1596-1600.

(69) Ben-Moshe, M.; Alexeev, V. L.; Asher, S. A., Fast Responsive Crystalline Colloidal Array Photonic Crystal Glucose Sensors. *Analytical Chemistry* **2006**, *78*, 5149-5157.

(70) Lu, Z.-R.; Kopeckova, P.; Kopecek, J., Antigen responsive hydrogels based on polymerizable antibody Fab' fragment. *Macromolecular Bioscience* **2003**, *3*, 296-300.

(71) Miyata, T.; Uragami, T.; Nakamae, K., Biomolecule-sensitive hydrogels. *Adv. Drug Deliv. Rev.* **2002**, *54*, 79-98.

(72) Miyata, T.; Asami, N.; Uragami, T., A reversibly antigen-responsive hydrogel. *Nature* **1999**, *399*, 766-769.

(73) Kataoka, K.; Miyazaki, H.; Bunya, M.; Okano, T.; Sakurai, Y., Totally synthetic polymer gels responding to external glucose concentration: Their preparation and application to on-off regulation of insulin release. *J. Am. Chem. Soc.* **1998**, *120*, 12694-12695.

(74) Hassan, C. M.; III, F. J. D.; Peppas, N. A., Dynamic Behavior of Glucose-Responsive Poly(methacrylic acid-g-ethylene glycol) Hydrogels. *Macromolecules* **1997**, *30*, 6166-6173.

(75) Sharma, A. C.; Jana, T.; Kesavamoorthy, R.; Shi, L.; Virji, M. A.; Finegold, D. N.; Asher, S. A., A general photonic crystal sensing motif: Creatinine in bodily fluids. *J. Am. Chem. Soc.* **2004**, *126*, 2971-2977.

(76) Akiyoshi, K.; Kang, E.-C.; Kurumada, S.; Sunamoto, J.; Principi, T.; Winnik, F. M., Controlled Association of Amphiphilic Polymers in Water: Thermosensitive Nanoparticles Formed by Self-Assembly of Hydrophobically Modified Pullulans and Poly(N-isopropylacrylamides). *Macromolecules* **2000**, *33*, 3244-3249.

(77) Collier, J. H.; Hu, B.-H.; Ruberti, J. W.; Zhang, J.; Shum, P.; Thompson, D. H.; Messersmith, P. B., Thermally and Photochemically Triggered Self-Assembly of Peptide Hydrogels. *J. Am. Chem. Soc.* **2001**, *123*, 9463-9464.

(78) Eagland, D.; Crowther, N. J.; Butler, C. J., Complexation between polyoxyethylene and poly(methacrylic acid). The importance of the molar mass of polyoxyethylene. *Eur. Polym. J.* **1994**, *30*, 767-73.

(79) Mathur, A. M.; Hammonds, K. F.; Klier, J.; Scranton, A. B., Equilibrium swelling of poly(methacrylic acid-g-ethylene glycol) hydrogels Effect of swelling medium and synthesis conditions. *J. Control. Release* **1998**, *54*, 177-184.

(80) Watanabe, T.; Ohtsuka, A.; Murase, N.; Barth, P.; Gersonde, K., NMR studies on water and polymer diffusion in dextran gels. Influence of potassium ions on microstructure formation and gelation mechanism. *Magnet. Reson. Med.* **1996**, *35*, 697-705.

(81) Gacesa, P., Alginates. *Carbohyd. Polym.* **1988**, *8*, 161-82.

(82) Gombotz, W. R.; Wee, S., Protein release from alginate matrixes. *Adv. Drug Deliv. Rev.* **1998**, *31*, 267-285.

(83) Goosen, M. F. A.; O'Shea, G. M.; Gharapetian, H. M.; Chou, S.; Sun, A. M., Optimization of microencapsulation parameters: semipermeable microcapsules as a bioartificial pancreas. *Biotechnol. Bioeng.* **1985**, *27*, 146-50.

(84) Heskins, M.; Guillet, J. E., Solution properties of poly(N-isopropylacrylamide). *J. Macromol. Sci. Chem.* **1968**, *A2*, 1441-1455.

(85) Tanaka, T., Collapse of Gels and the Critical Endpoint. *Phys. Rev. Lett.* **1978**, *40*, 820-823.

(86) Tanaka, T.; Fillmore, D. J., Kinetics of Swelling of Gels. *J. Chem. Phys.* **1979**, *70*, 1214 - 1218.

(87) Tanaka, T.; Fillmore, D. J.; Sun, S.-T.; Nishio, I.; Swislow, G.; Shah, A., Phase Transition in Ionic Gels. *Phys. Rev. Lett.* **1980**, *45*, 1636-1639.

(88) Tanaka, T.; Nishio, I.; Sun, S. T.; Uenonishio, S., Collapse of Gels in an Electric-Field. *Science* **1982**, *218*, 467-469.

(89) Tanaka, T.; Sato, E.; Hirokawa, Y.; Hirotsu, S.; Peetermans, J., Critical Kinetics of Volume Phase Transition of Gels. *Phys. Rev. Lett.* **1985**, *55*, 2455-2458.

(90) Tanaka, T., Kinetics of phase transition in polymer gels. *Physica A* **1986**, *140A*, 261-268.

(91) Matsuo, E. S.; Tanaka, T., Kinetics of discontinuous volume-phase transition of gels. *J. Chem. Phys.* **1988**, *89*, 1695-1703.

(92) Inomata, H.; Goto, S.; Saito, S., Phase transition of N-substituted acrylamide gels. *Macromolecules* **1990**, *23*, 4887-8.

(93) Li, Y.; Tanaka, T., Kinetics of Swelling and Shrinking of Gels. *J. Chem. Phys.* **1990**, *92*, 1365-1371.

(94) Suzuki, A.; Tanaka, T., Phase-Transition in Polymer Gels Induced by Visible-Light. *Nature* **1990**, *346*, 345-347.

(95) Wu, C.; Zhou, S., Laser Light Scattering Study of the Phase Transition of Poly(N-isopropylacrylamide) in Water. 1. Single Chain. *Macromolecules* **1995**, *28*, 8381-8387.

(96) Pelton, R., Temperature-sensitive aqueous microgels. *Adv. Colloid. Interface Sci.* **2000**, *85*, 1-33.

(97) Wang, J. P.; Gan, D. J.; Lyon, L. A.; El-Sayed, M. A., Temperature-jump investigations of the kinetics of hydrogel nanoparticle volume phase transitions. *J. Am. Chem. Soc.* **2001**, *123*, 11284-11289.

(98) Jones, C. D.; Lyon, L. A., Photothermal patterning of microgel/gold nanoparticle composite colloidal crystals. *J. Am. Chem. Soc.* **2003**, *125*, 460-465.

(99) Jones, C. D.; Serpe, M. J.; Schroeder, L.; Lyon, L. A., Microlens formation in microgel/gold colloid composite materials via photothermal patterning. *J. Am. Chem. Soc.* **2003**, *125*, 5292-5293.

(100) Nayak, S.; Debord, S. B.; Lyon, L. A., Investigations into the deswelling dynamics and thermodynamics of thermoresponsive microgel composite films. *Langmuir* **2003**, *19*, 7374-7379.

(101) Nayak, S.; Lyon, L. A., Photoinduced Phase Transitions in Poly(N-isopropylacrylamide) Microgels. *Chem. Mater.* **2004**, *16*, 2623-2627.

(102) Nayak, S.; Lyon, L. A., Soft nanotechnology with soft nanoparticles. *Angew. Chem. Intl. Ed.* **2005**, *44*, 7686-7708.

(103) Dusek, K.; Patterson, K., Transition on swollen polymer networks induced by intramolecular condensation. *Journal of Polymer Science, Polymer Physics Edition* **1968**, *6*, 1209-16.

(104) Arotcarena, M.; Heise, B.; Ishaya, S.; Laschewsky, A., Switching the inside and the outside of aggregates of water-soluble block copolymers with double thermoresponsivity. *J. Am. Chem. Soc.* **2002**, *124*, 3787-3793.

(105) Zhou, G.; Elaissari, A.; Delair, T.; Pichot, C., Synthesis and characterization of surface-cyanofunctionalized poly(N-isopropylacrylamide) latexes. *Colloid Polym. Sci.* **1998**, *276*, 1131-1139.

(106) McPhee, W.; Tam, K. C.; Pelton, R., Poly(N-isopropylacrylamide) latexes prepared with sodium dodecyl sulfate. *J. Colloid Interface Sci.* **1993**, *156*, 24-30.

(107) Park, T. G.; Hoffman, A. S., Deswelling Characteristics of Poly(N-Isopropylacrylamide) Hydrogel. *J. Appl. Polym. Sci.* **1994**, *52*, 85-89.

(108) Yan, Q.; Hoffman, A. S., Synthesis of macroporous hydrogels with rapid swelling and deswelling properties for delivery of macromolecules. *Poly. Commun.* **1995**, *36*, 887-889.

(109) Varga, I.; Gilanyi, T.; Meszaros, R.; Filipcsei, G.; Zrinyi, M., Effect of Cross-Link Density on the Internal Structure of Poly(N-isopropylacrylamide) Microgels. *J. Phys. Chem. B* **2001**, *105*, 9071-9076.

(110) Hu, T. J.; You, Y. Z.; Pan, C. Y.; Wu, C., The coil-to-globule-to-brush transition of linear thermally sensitive poly(N-isopropylacrylamide) chains grafted on a spherical microgel. *J. Phys. Chem. B* **2002**, *106*, 6659-6662.

(111) Guo, Z. L.; Wang, J. T.; Zhu, H. J., Preparation of temperature sensitive ultrafine particles of poly(N-isopropyl acrylamide) by microemulsion polymerization. *Acta Polym. Sin.* **2001**, 489-493.

(112) Jones, C. D.; Lyon, L. A., Synthesis and Characterization of Multiresponsive Core-Shell Microgels. *Macromolecules* **2000**, *33*, 8301-8306.

(113) Jones, C. D.; Lyon, L. A., Shell-Restricted Swelling and Core Compression in Poly(N-Isopropylacrylamide) Core-Shell Microgels. *Macromolecules* **2003**, *36*, 1988-1993.

(114) Kawaguchi, H., Functional polymer microspheres. *Prog. Polym. Sci.* **2000**, *25*, 1171-1210.

(115) Pelton, R.; Richardson, R.; Cosgrove, T.; Ivkov, R., The Effects of Temperature and Methanol Concentration on the Properties of Poly(N-isopropylacrylamide) at the Air/Solution Interface. *Langmuir* **2001**, *17*, 5118-5120.

(116) Neyret, S.; Vincent, B., The properties of polyampholyte microgel particles prepared by microemulsion polymerization. *Polymer* **1997**, *38*, 6129-6134.

(117) Braun, O.; Selb, J.; Candau, F., Synthesis in microemulsion and characterization of stimuli- responsive polyelectrolytes and polyampholytes based on N-isopropylacrylamide. *Polymer* **2001**, *42*, 8499-8510.

(118) Dowding, P. J.; Vincent, B.; Williams, E., Preparation and swelling properties of poly(NIPAM) "minigel" particles prepared by inverse suspension polymerization. *J. Colloid Interf. Sci.* **2000**, *221*, 268-272.

(119) HernandezBarajas, J.; Hunkeler, D., Heterophase water-in-oil polymerization of acrylamide by a hybrid inverse-emulsion/inverse-microemulsion process. *Polymer* **1997**, *38*, 5623-5641.

(120) Landfester, K.; Willert, M.; Antonietti, M., Preparation of polymer particles in nonaqueous direct and inverse miniemulsions. *Macromolecules* **2000**, *33*, 2370-2376.

(121) Ming, W. H.; Zhao, Y. Q.; Cui, J.; Fu, S. K.; Jones, F. N., Formation of irreversible nearly transparent physical polymeric hydrogels during a modified microemulsion polymerization. *Macromolecules* **1999**, *32*, 528-530.

(122) Platkowski, K.; Pross, A.; Reichert, K. H., The inverse emulsion polymerization of acrylamide with pentaerythritolmyristate as emulsifier. 2. Mathematical modelling. *Polym. Int.* **1998**, *45*, 229-238.

(123) Pross, A.; Platkowski, K.; Reichert, K. H., The inverse emulsion polymerization of acrylamide with pentaerythritolmyristate as emulsifier - .1. Experimental studies. *Polym. Int.* **1998**, *45*, 22-26.

(124) Wu, C.; Zhou, S. Q., Light scattering study of spherical poly(N-isopropylacrylamide) microgels. *J. Macromol. Sci. Phys.* **1997**, *B36*, 345-355.

(125) Glukhikh, V.; Graillat, C.; Pichot, C., Inverse Emulsion Polymerization of Acrylamide .2. Synthesis and Characterization of Copolymers with Methacrylic-Acid. *J. Polym. Sci. Pol. Chem.* **1987**, *25*, 1127-1161.

(126) Sayil, C.; Okay, O., *J. Appl. Polym. Sci.* **2002**, *83*, 1228-1232.

(127) Woodward, N. C.; Chowdhry, B. Z.; Leharne, S. A.; Snowden, M. J., *European Polymer Journal* **2000**, *36*, 1355-1364.

(128) Gilanyi, T.; Varga, I.; Meszaros, R.; Filipcsei, G.; Zrinyi, M., Interaction of Monodisperse Poly(N-isopropylacrylamide) Microgel Particles with Sodium Dodecyl Sulfate in Aqueous Solution. *Langmuir* **2001**, *17*, 4764-4769.

(129) Martin, B. D.; Ampofo, S. A.; Linhardt, R. J.; Dordick, J. S., Biocatalytic Synthesis of Sugar-Containing Poly(Acrylate)-Based Hydrogels. *Macromolecules* **1992**, *25*, 7081-7085.

(130) Aggeli, A.; Bell, M.; Boden, N.; Keen, J. N.; Knowles, P. F.; McLeish, T. C.; Pitkeathly, M.; Radford, S. E., Responsive gels formed by the spontaneous self-assembly of peptides into polymeric beta-sheet tapes. *Nature* **1997**, *386*, 259-262.

(131) Jones, C. D.; Lyon, L. A., Dependence of shell thickness on core compression in acrylic acid modified poly(N-isopropylacrylamide) core/shell microgels. *Langmuir* **2003**, *19*, 4544-4547.

(132) Ghandehari, H.; Kopeckova, P.; Yeh, P. Y.; Kopecek, J., Biodegradable and pH sensitive hydrogels: Synthesis by a polymer-polymer reaction. *Macromol. Chem. Phys.* **1996**, *197*, 965-980.

(133) Jeong, S. H.; Huh, K. M.; Park, K., Hydrogel drug delivery systems. *Polymers in Drug Delivery* **2006**, 49-62.

(134) Boulmedais, F.; Tang, C. S.; Keller, B.; Voros, J., Controlled electrodissolution of polyelectrolyte multilayers: a platform technology towards the surface-initiated delivery of drugs. *Adv. Funct. Mater.* **2006**, *16*, 63-70.

(135) Grayson, A. C. R.; Choi, I. S.; Tyler, B. M.; Wang, P. P.; Brem, H.; Cima, M. J.; Langer, R., Multi-pulse drug delivery from a resorbable polymeric microchip device. *Nature Materials* **2003**, *2*, 767-772.

(136) Lee, K.; Asher, S. A., Photonic Crystal Chemical Sensors: pH and Ionic Strength. *J. Am. Chem. Soc.* **2000**, *122*, 9534-9537.

(137) Goponenko, A. V.; Asher, S. A., Modeling of Stimulated Hydrogel Volume Changes in Photonic Crystal Pb2+ Sensing Materials. *J. Am. Chem. Soc.* **2005**, *127*, 10753-10759.

(138) Debord, J. D.; Lyon, L. A., Thermoresponsive photonic crystals. *J. Phys. Chem. B* **2000**, *104*, 6327-6331.

(139) Debord, S. B. L., L. A., Influence of Particle Volume Fraction on Packing in Responsive Hydrogel Colloidal Crystals. *J. Phys. Chem. B* **2003**, *107*, 2927-2932.

(140) Lyon, L. A.; Debord, J. D.; Debord, S. B.; Jones, C. D.; McGrath, J. G.; Serpe, M. J., Microgel Colloidal Crystals. *J. Phys. Chem. B* **2004**, *108*, 19099-19108.

(141) Plunkett, K. N.; Berkowski, K. L.; Moore, J. S., Chymotrypsin Responsive Hydrogel: Application of a Disulfide Exchange Protocol for the Preparation of Methacrylamide Containing Peptides. *Biomacromolecules* **2005**, *6*, 632-637.

(142) Kim, S.; Chung, E. H.; Gilbert, M.; Healy, K. E., Synthetic MMP-13 degradable ECMs based on poly(N-isopropylacrylamide-co-acrylic acid) semi-interpenetrating polymer networks. I. Degradation and cell migration. *Journal of Biomedical Materials Research, Part A* **2005**, *75A*, 73-88.

(143) Nolan, C. M.; Reyes, C. D.; Debord, J. D.; Garcia, A. J.; Lyon, L. A., Phase transition behavior, protein adsorption, and cell adhesion resistance of poly(ethylene glycol) crosslinked microgel particles. *Biomacromolecules* **2005**, *6*, 2032-2039.

(144) Miyata, T.; Asami, N.; Uragami, T., Preparation of an Antigen-Sensitive Hydrogel Using Antigen-Antibody Bindings. *Macromolecules* **1999**, *32*, 2082-2084.

(145) Kim, S.; Healy, K. E., Synthesis and Characterization of Injectable Poly(N-isopropylacrylamide-co-acrylic acid) Hydrogels with Proteolytically Degradable Cross-Links. *Biomacromolecules* **2003**, *4*, 1214-1223.

(146) Thornton, P. D.; McConnell, G.; Ulijn, R. V., Enzyme responsive polymer hydrogel beads. *Chem. Commun.* **2005**, 5913-5915.

(147) Ehrick, J. D.; Deo, S. K.; Browning, T. W.; Bachas, L. G.; Madou, M. J.; Daunert, S., Genetically engineered protein in hydrogels tailors stimuli-responsive characteristics. *Nature Materials* **2005**, *4*, 298-302.

CHAPTER 2

COLLOIDAL HYDROGEL MICROLENSES

This chapter describes the use of colloidal hydrogel microparticles as microlens elements and the fabrication method to form the hydrogel microlens arrays. The fabrication of substrate supported microgels is achieved by using electrostatic interactions between aminopropyltrimethoxysilane (APTMS) modified glass substrates and the microgels acrylic acid (AAc) groups. The lensing ability was confirmed using an inverted light microscope by imaging a photomask through each of the microgels present on the surface producing individually addressable images.

2.1 Introduction

Micro-optical structures have been of recent interest to both industrial and academic pursuits regarding the miniaturization of optical elements and the development of novel functional materials.[1-7] Microlenses in particular have been applied to such fields as telecommunications, image analysis, and photolithography.[8-18] Microlenses and microlens arrays are well known and can be made by a number of routes such as photolithography,[10-12,19] photothermal patterning,[20,21] photopolymerization/photo-curing,[22-25] and polymeric particle self-assembly/melting.[26,27] These systems have been studied in detail but often have the limitation of requiring multiple fabrication steps resulting in lenses with fixed focal lengths, relatively large diameters and/or slow focal length switching speeds. A self-assembly approach, in which the microlens precursors are

synthesized by traditional solution polymerization routes and are then directly assembled on a substrate, would be extremely beneficial with respect to the speed of fabrication and the ultimate size limitations of such arrays. Accomplishment of the above goals would also enable one to investigate diverse, complex hydrogel responses by simply monitoring optical properties of the hydrogel microlenses rather than in measuring size changes of hydrogels.

For the studies presented in this chapter, poly(*N*-isopropylacrylamide-*co*-acrylic acid) (pNIPAm-*co*-AAc) microgels were immobilized on glass substrates via Coulombic interactions to form supported hydrogel microlens arrays. Because pNIPAm-*co*-AAc microgels are mechanically soft, it is possible for the attractive forces between the positively charged substrate and the anionic microgel to cause the microgel to deform upon attachment and subsequent drying to produce a monolayer-microgel substrate where the particles are deformed in an anisotropic fashion. As previously reported in the literature,[28-30] pNIPAm-*co*-AAc microgels are also responsive to external stimuli, allowing the possibility of dynamically tuning the microgel curvature in response to solution temperature and pH changes. The responsive behavior of the hydrogel microlenses will be discussed in Chapter 3.[31]

2.2 Experimental Section

Materials

All reagents were purchased from Sigma-Aldrich unless otherwise specified. *N*-Isopropylacrylamide (NIPAm) was re-crystallized from hexanes (J.T. Baker) and dried under vacuum prior to use. Acrylic acid (AAc) was distilled under reduced pressure. *N*,*N*'-Methylene(bisacrylamide) (BIS) and ammonium persulfate (APS) were used as received. 3-Aminopropyltrimethoxysilane (APTMS) was purchased from United Chemical Technologies Inc. and was kept in a desiccator for storage. The glass substrates used were 24 x 50 mm Fisher Finest brand cover glass obtained from Fisher Scientific. Sulfuric acid and 30% hydrogen peroxide (J.T. Baker) were used to make Piranha cleaning solutions. 95% and absolute ethanol was used for various purposes in this investigation. All water used throughout this investigation was first house distilled and then deionized to a resistance of at least 18 MΩ (Barnstead Thermolyne E-Pure system) and then filtered through a 0.2 μm filter to remove particulate matter. 3M transparency film for laser printers and a Hewlett Packard LaserJet 4000N printer was used for pattern printing.

Glass Substrate Preparation

APTMS functionalized glass cover slips were used throughout this section as positively charged substrates for microgel deposition. Prior to functionalization the glass substrates were cleaned as previously outlined.[32] Glass cover slips were first wiped clean of any dust using a Kimwipe (Kimberly-Clark). Following this step the substrates were immersed in hot Piranha solution, 4:1 H_2SO_4 : H_2O_2, (~70 °C) to remove any organics from the substrate surface. Next, the substrates were rinsed copiously with H_2O then

copiously with 95% ethanol. Following this rinsing procedure the substrates were immersed in an ethanolic (absolute ethanol) 1% APTMS solution for ~2 hrs. After 2 hrs the substrates were removed from the APTMS solution and again rinsed copiously with 95% ethanol. These substrates were stored in 95% ethanol for no longer than 5 days prior to use. Prior to particle deposition, these substrates were rinsed with H_2O and dried under a stream of nitrogen gas.

Microgel Synthesis

The same batch of microgels was used throughout all the experiments presented in this chapter and all other chapters. Responsive microgels were prepared by free-radical precipitation polymerization of NIPAm. Acrylic acid was used as a comonomer to incorporate carboxyl functional groups for multi responsiveness (temperature, pH, and further bio-functionalization in Chapter 5 and 6). For the synthesis, reactant mixture composed of a total monomer concentration of 300 mM with a molar composition of 89.4% NIPAm, 0.5% BIS (crosslinker), was made by dissolving the monomers in 100 mL deionized water. The reactant mixture was filtered through a 0.8 μm filter and then transferred into a 250 mL three-neck round bottom flask. During 60 minutes of N_2 purge, the mixture was heated to 70 °C and maintained at the same temperature throughout the synthesis. Comonomers, AAc (10%) and 4-acrylamido-fluorescein (0.1%), was added to the reaction mixture. After the addition of the comonomers, 1 mL of 6.13 mM APS was added to initiate the polymerization process. The copolymerization was allowed to proceed for 4 hours at 70 °C under N_2. The resultant colloidal dispersion was dialyzed against water for ~2 weeks with the water being changed twice per day, using 10000 MW cut-off dialysis tubing (VWR).

Microscopy

Optical and electron microscopies were used throughout these studies to confirm microgel shape, size and lensing ability. A Hitachi S800 scanning electron microscope (SEM) was used to determine the shape of microgels attached to the glass substrate. Images were obtained by attaching a dry microgel decorated glass substrate to a SEM peg at a 45˚ angle and placed in the SEM chamber. The substrate was then imaged with an accelerating voltage of 4 kV and the sample tilted relative to the incoming electrons in order to obtain profile images of the microgels, as previously described.[33] Brightfield transmission, polarized light, and differential interference contrast (DIC) optical microscopies were used to confirm the lensing abilities of the microgels attached to the substrate as well as to determine the microgel size. An Olympus IX 70 inverted microscope equipped with a high numerical aperture, oil immersion 100X objective (N.A.=1.30) was used to obtain images of the microgels adsorbed to the glass substrate as well as imaging a mask through the microgel to prove the lensing abilities of the microgels. Images were captured using a black and white CCD camera (PixelFly, Cooke Corporation). The experimental setup is shown in Scheme 2-1.

Scheme 2-1. Inverted light microscopy setup used for imaging experiments in this Chapter.

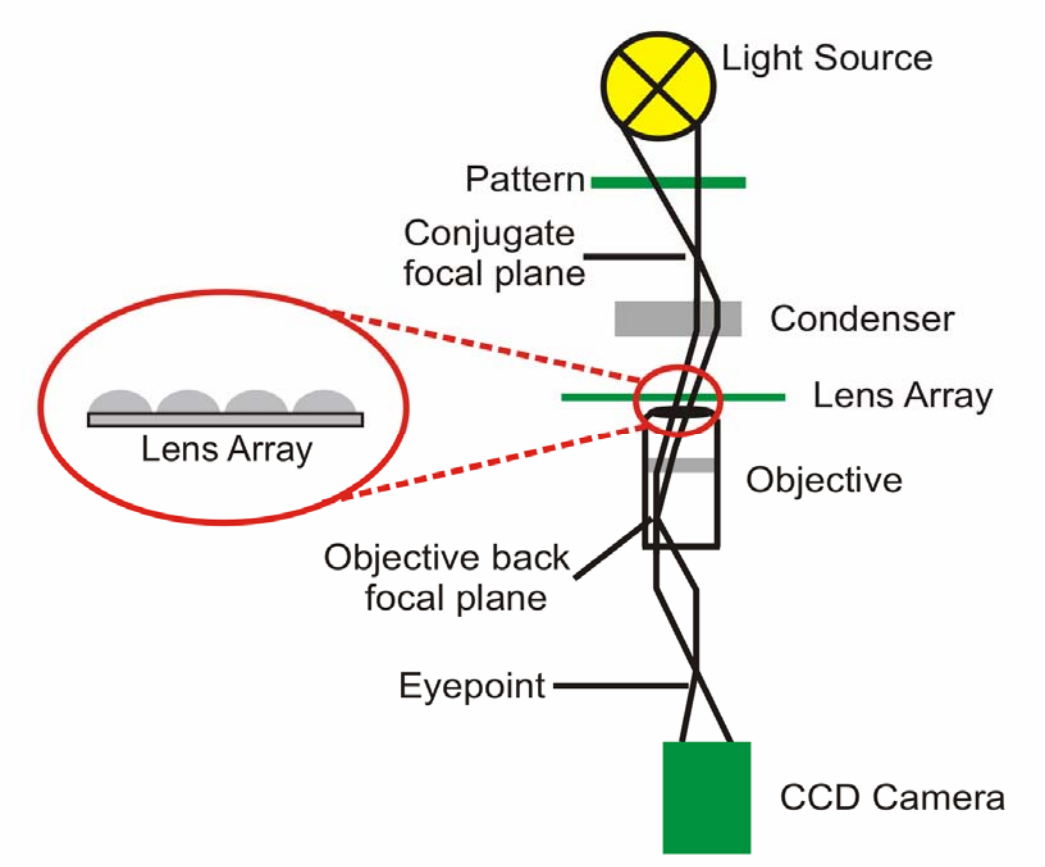

2.3 Results and Discussion

Microgels that are approximately 2 μm in diameter in their water-swollen state were used to fabricate microlenses. A differential image contrast (DIC) microscope image of the microgels adsorbed to a glass substrate is shown in Figure 2-1(a). Microgels were adsorbed to an APTMS functionalized glass substrate by exposing the glass substrate to a 10% (v/v) aqueous microgel solution for approximately 1 hr. The substrate was then rinsed with deionized H_2O and air dried for approximately 1 day prior to imaging. Because these microgels are soft/deformable materials it should be the case that when the microgel dries on a surface it does so in an anisotropic fashion (one dimension deswells more than the other) under conditions where the surface/microgel adhesion is strong. This anisotropic drying behavior is seen in the SEM image of the microgels in Figure 2-1(b) where it is observed that the microgels de-swell in the z-dimension more than they do in the x-y dimension. This type of microgel behavior has been reported previously by other investigators.[33] From Figure 2-1(b) it is apparent that the microgels do resemble traditional plano-convex lenses but it is not intuitive that this type of material can actually be used as an optical element. To evaluate the optical properties of the deformed microgels, an inverted optical microscope was used and the particles were imaged through crossed polarizers.

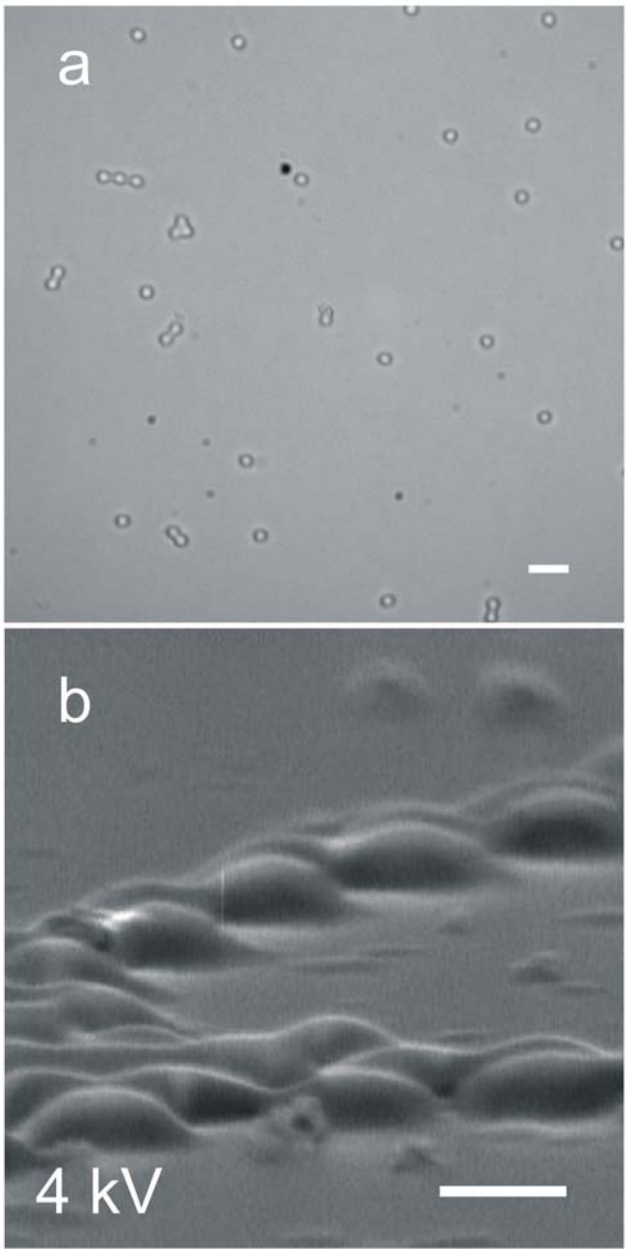

Figure 2-1. (a) DIC image of microgels used throughout this section, scale bar is 5 μm. (b) SEM image of the microgels imaged at a grazing angle relative to the substrate. As can be seen from the image, the microgels have a plano-convex shape. Scale bar for the SEM is 1 μm.

When a microscope is set up in crossed polar, where the polarization directions for the polarizer and analyzer are perpendicular, a characteristic “cross” pattern arising from optical interference is visible in the objective back focal plane. This cross pattern can be seen by looking down the eyepiece tube of the microscope after the eyepiece has been removed or if an optical element, such as a long focal length Bertrand lens is inserted into the imaging system. To determine if microgels can act as microlenses we inserted the substrate containing dried microgels onto the microscope and imaged in a standard brightfield transmission configuration, Figure 2-1(a). The polarizer/analyzer pair was then inserted into the microscope such that their polarization directions were perpendicular, as determined by observing the characteristic cross pattern upon removal of the microscope eyepiece. The eyepiece was then replaced and the microgels were observed under crossed polars with slight defocusing of the objective. Upon defocusing, characteristic cross patterns, as seen in the top right inset of Figure 2-2, could be observed through each microgel attached to the substrate. Normally, if a Bertrand lens was inserted into a microscope under crossed polars, the observer would see one large cross pattern through the eyepiece. The fact that a cross pattern is visible through each microgel is indicative of the microgels all acting as independent lenses.

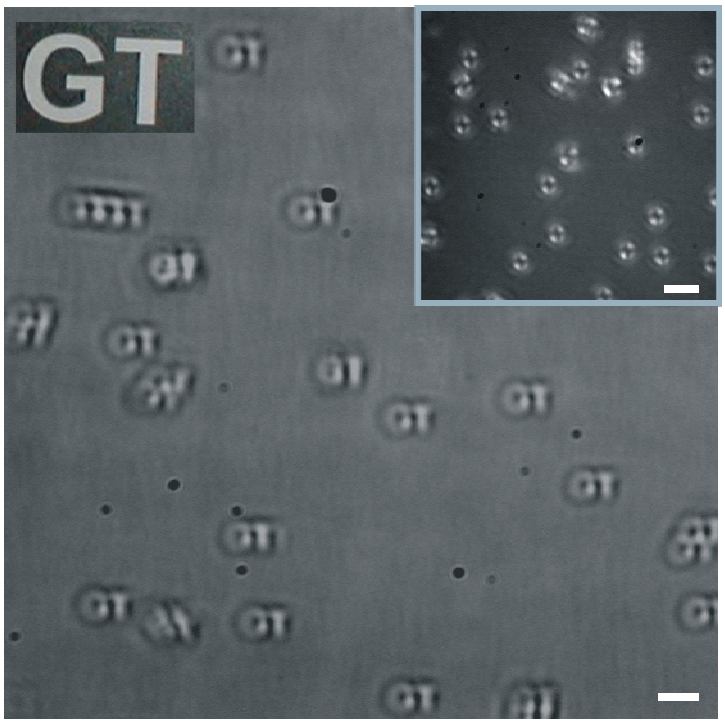

Figure 2-2. Microscope image of the substrate supported microgels from Figure 2-1(a) illustrating the microgels' ability to project a pattern that has been placed at the illumination aperture stop. The scale bar is 5 μm. Top left inset shows the photomask used for the GT projection onto the microgel array. Top right inset shows that each microgel on the substrate is displaying the characteristic cross pattern, which is visible under crossed polars when a Bertrand lens is inserted into the microscope, through every microgel attached to the substrate. The scale bar is 10 μm.

From this observation it seems that the microgels are acting as independent microlenses. To test their ability to reconstruct and project a real-space image, a photomask made by printing a GT pattern on a standard transparency slide using a standard laser printer, was inserted near a conjugate plane to the back focal plane of the objective. The mask is shown in the top left inset of Figure 2-2. The appropriate conjugate plane lies at or near the filament of the halogen bulb used for bright field illumination. The pattern was inserted into the microscope as close to the bulb as possible (at the aperture stop) so that the light passed through the GT pattern before being projected upon the lenses. The same substrate used to show the cross pattern was used here as well. If the microgels were indeed acting as microlenses the microgels should be able to independently project the GT pattern upon defocusing of the objective. Slight defocusing is necessary since it is impossible to place the pattern exactly at the true conjugate focal plane. Shown in Figure 2-2 is an image of the microgels with the pattern GT projected through each microgel attached to the substrate. The interesting feature of these microlenses is their ability to project the GT pattern with high pattern integrity, despite the fact that these optical elements were prepared by simple solution polymer chemistry. Another interesting observation was the fact that not every microgel brings the GT into focus at the same exact point, which illustrates that our microgels have a variety of different focal lengths (i.e. curvature). Altering the surface chemistry or the softness of the microgels by varying their crosslink density presumably can control this.

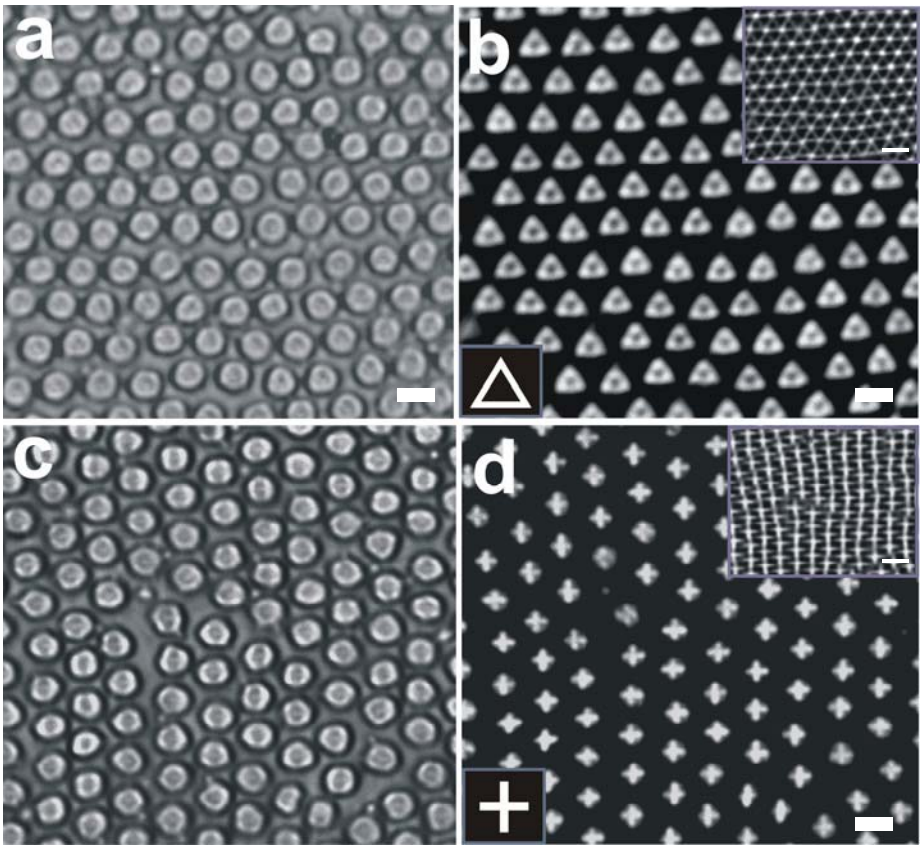

Figure 2-3. Microscope image of a portion (~25 μm x 25 μm) of the substrate supported microgels in an ordered array. Panels (a, c) show the microscope image of the microgels dried on the substrate while panels (b, d) show the image projection of the pattern, shown in the bottom left insets of panels (b, d). The scale bar is 2 μm. The above images show that the microgels exhibit the ability to project patterns in an ordered array. Shown in the top right insets of panels (b, d) are projections of the patterns in a defocused state illustrating the ability of the array to form connected features, which allows for the formation of more complex patterns. The scale bar is 5 μm.

Thus far we have demonstrated the construction of microlenses from soft colloidal precursors arranged on a substrate in a random fashion. To further illustrate the usefulness of this microlens fabrication process ordered microlens arrays were assembled following the same procedure as outlined above but instead of rinsing the substrate with H_2O after one hour the microgel solution was allowed to completely dry on the substrate without rinsing, which took about 4-5 hours on average. Light microscopy images of a select region of the arrays are shown in Figure 2-3 (a, c). The images show that the microgels self-assemble into ordered arrays spontaneously upon drying which results in very few defects. Next, we showed that these arrays were useful for pattern projection as shown in Figure 2-3 (b, d) for a triangle pattern and a cross pattern, respectively. It was also shown that more complex patterns could be obtained from the simple patterns used by defocusing the patterns to the point that the images overlap, as seen in the top right insets of Figure 2-3 (b, d).

2.4 Conclusions

This Chapter has demonstrated the ability of pNIPAm-co-AAc microgels to act as microlenses. This was accomplished by assembling the microgels onto substrates through electrostatic interactions, which restricts the dimensional changes of the particles in the x-y plane, thus causing the particle to adopt a plano-convex shape following drying. The lensing ability of these particles has been illustrated by observing their ability to bring an image present in the back focal plane of an optical microscope into the image plane. This effect indicates that the substrate-supported microgels are capable of acting as independent optical elements. It was also illustrated that ordered microlens arrays could be easily obtained by following a simple drying procedure. The next section describes the use of the above microlens arrays in solution, which show focal length tunability dependent on solution conditions.

2.5 References

(1) Xia, Y. N.; Whitesides, G. M., Soft lithography. *Angew. Chem. Int. Ed.* **1998**, *37*, 551-575.

(2) Yang, P. D.; Wirnsberger, G.; Huang, H. C.; Cordero, S. R.; McGehee, M. D.; Scott, B.; Deng, T.; Whitesides, G. M.; Chmelka, B. F.; Buratto, S. K.; Stucky, G. D., Mirrorless lasing from mesostructured waveguides patterned by soft lithography. *Science* **2000**, *287*, 465-467.

(3) Qi, M. H.; Lidorikis, E.; Rakich, P. T.; Johnson, S. G.; Joannopoulos, J. D.; Ippen, E. P.; Smith, H. I., A three-dimensional optical photonic crystal with designed point defects. *Nature* **2004**, *429*, 538-542.

(4) Kim, J.; Serpe, M. J.; Lyon, L. A., Photoswitchable Microlens Arrays. *Angew. Chem. Intl. Ed.* **2005**, *44*, 1333-1336.

(5) Shogenji, R.; Kitamura, Y.; Yamada, K.; Miyatake, S.; Tanida, J., Bimodal fingerprint capturing system based on compound-eye imaging module. *Appl. Optics* **2004**, *43*, 1355-1359.

(6) Pan, C. T.; Shen, S. C., Design and fabrication of polymeric microoptical components using excimer laser ablation. *Mater. Sci. Technol.* **2004**, *20*, 270-274.

(7) Dong, L.; Agarwal Abhishek, K.; Beebe David, J.; Jiang, H., Adaptive liquid microlenses activated by stimuli-responsive hydrogels. *Nature* **2006**, *442*, 551-554.

(8) Chen, S. H.; Yi, X. J.; Kong, L. B.; He, M.; Wang, H. C., Monolithic integration technique for microlens arrays with infrared focal plane arrays. *Infrared Phys. Technol.* **2002**, *43*, 109-112.

(9) Motamedi, M. E.; Tennant, W. E.; Sankur, H. O.; Melendes, R.; Gluck, N. S.; Park, S.; Arias, J. M.; Bajaj, J.; Pasko, J. G.; McLevige, W. V.; Zandian, M.; Hall, R. L.; Richardson, P. D., Micro-optic integration with focal plane arrays. *Opt. Eng.* **1997**, *36*, 1374-1381.

(10) Wu, H. K.; Odom, T. W.; Whitesides, G. M., Connectivity of features in microlens array reduction photolithography: Generation of various patterns with a single photomask. *J. Am. Chem. Soc.* **2002**, *124*, 7288-7289.

(11) Wu, M. H.; Park, C.; Whitesides, G. M., Fabrication of arrays of microlenses with controlled profiles using gray-scale microlens projection photolithography. *Langmuir* **2002**, *18*, 9312-9318.

(12) Wu, M. H.; Whitesides, G. M., Fabrication of diffractive and micro-optical elements using microlens projection lithography. *Adv. Mater.* **2002**, *14*, 1502-1506.

(13) Wu, M. H.; Paul, K. E.; Yang, J.; Whitesides, G. M., Fabrication of frequency-selective surfaces using microlens projection photolithography. *Appl. Phys. Lett.* **2002**, *80*, 3500-3502.

(14) Wu, H. K.; Odom, T. W.; Whitesides, G. M., Reduction photolithography using microlens arrays: Applications in gray scale photolithography. *Analytical Chemistry* **2002**, *74*, 3267-3273.

(15) Wu, H.; Odom, T. W.; Whitesides, G. M., Generation of chrome masks with micrometer-scale features using microlens lithography. *Adv. Mater.* **2002**, *14*, 1213-1216.

(16) Wu, M. H.; Park, C.; Whitesides, G. M., Generation of submicrometer structures by photolithography using arrays of spherical microlenses. *J. Colloid Interface Sci.* **2003**, *265*, 304-309.

(17) Wu, M. H.; Paul, K. E.; Whitesides, G. M., Patterning flood illumination with microlens arrays. *Appl. Optics* **2002**, *41*, 2575-2585.

(18) Wu, M. H.; Whitesides, G. M., Fabrication of two-dimensional arrays of microlenses and their applications in photolithography. *J. Micromech. Microeng.* **2002**, *12*, 747-758.

(19) Karkkainen, A. H. O.; Tamkin, J. M.; Rogers, J. D.; Neal, D. R.; Hormi, O. E.; Jabbour, G. E.; Rantala, J. T.; Descour, M. R., Direct photolithographic deforming of organomodified siloxane films for micro-optics fabrication. *Appl. Optics* **2002**, *41*, 3988-3998.

(20) Jones, C. D.; Lyon, L. A., Photothermal patterning of microgel/gold nanoparticle composite colloidal crystals. *J. Am. Chem. Soc.* **2003**, *125*, 460-465.

(21) Jones, C. D.; Serpe, M. J.; Schroeder, L.; Lyon, L. A., Microlens formation in microgel/gold colloid composite materials via photothermal patterning. *J. Am. Chem. Soc.* **2003**, *125*, 5292-5293.

(22) Croutxe-Barghorn, C.; Soppera, O.; Lougnot, D. J., Fabrication of refractive microlens arrays by visible irradiation of acrylic monomers: influence of photonic parameters. *Eur. Phys. J.-Appl. Phys* **2001**, *13*, 31-37.

(23) Croutxe-Barghorn, C.; Soppera, O.; Lougnot, D. J., Fabrication of microlenses by direct. *Appl. Surf. Sci.* **2000**, *168*, 89-91.

(24) Okamoto, T.; Mori, M.; Karasawa, T.; Hayakawa, S.; Seo, I.; Sato, H., Ultraviolet-cured polymer microlens arrays. *Appl. Optics* **1999**, *38*, 2991-2996.

(25) Yang, S.; Krupenkin, T. N.; Mach, P.; Chandross, E. A., Tunable and latchable liquid microlens with photopolymerizable components. *Adv. Mater.* **2003**, *15*, 940-943.

(26) Lu, Y.; Yin, Y. D.; Xia, Y. N., A self-assembly approach to the fabrication of patterned, two- dimensional arrays of microlenses of organic polymers. *Adv. Mater.* **2001**, *13*, 34-37.

(27) Hirai, T.; Hayashi, S., Lens functions of polymer microparticle arrays. *Colloid Surf. A-Physicochem. Eng. Asp.* **1999**, *153*, 503-513.

(28) Jones, C. D.; Lyon, L. A., Synthesis and Characterization of Multiresponsive Core-Shell Microgels. *Macromolecules* **2000**, *33*, 8301-8306.

(29) Gan, D.; Lyon, L. A., Tunable Swelling Kinetics in Core-Shell Hydrogel Nanoparticles. *J. Am. Chem. Soc.* **2001**, *123*, 7511-7517.

(30) Serpe, M. J.; Lyon, L. A., Optical and Acoustic Studies of pH-Dependent Swelling in Microgel Thin Films. *Chem. Mater.* **2004**, *16*, 4373-4380.

(31) Kim, J.; Serpe, M. J.; Lyon, L. A., Hydrogel Microparticles as Dynamically Tunable Microlenses. *J. Am. Chem. Soc.* **2004**, *126*, 9512-9513.

(32) Goss, C. A.; Charych, D. H.; Majda, M., Application of (3-Mercaptopropyl)Trimethoxysilane as a Molecular Adhesive in the Fabrication of Vapor-Deposited Gold Electrodes on Glass Substrates. *Analytical Chemistry* **1991**, *63*, 85-88.

(33) Crowther, H. M.; Vincent, B., Swelling behavior of poly N-isopropylacrylamide microgel particles in alcoholic solutions. *Colloid Polym. Sci.* **1998**, *276*, 46-51.

CHAPTER 3

DINAMICALLY TUNABLE HYDROGEL MICROLENSES

This Chapter describes the demonstration of tunable microlenses prepared by combining responsive polymers, self-assembly, and microscopic analysis methods. The construct presented here is highly versatile and can be expanded upon through simple water-based polymer chemistry. Tunable micro-optical elements were prepared by aqueous free-radical polymerization and electrostatic self-assembly techniques. Stimuli-responsive poly(N-isopropylacrylamide-co-acrylic acid) (pNIPAm-AAc) microgels were used as lenses to generate dynamically tunable optical elements. By using optical microscopy to investigate the micron scale dynamics of the self-assembled microlenses, this Chapter demonstrates focal length tuning through modulation of the solution pH and/or temperature.

3.1 Introduction

Poly(*N*-isopropylacrylamide)-based hydrogels are materials that can be made to respond to external stimuli.[1-6] It has been shown by our group[7,8] and others[9-12] that stimuli responsive particles (100 nm-2 μm diameter) composed of this material and copolymers thereof can be easily synthesized. The Chapter 2 has shown that microlens array technology has gained in interest for applications in the various fields[13-23] and the microlens arrays has been fabricated via a number of routes.[18,19,24-29] However, the fabrication of dynamically tunable microlens arrays is challenging, and has only been

realized in few limited cases. Therefore, the fact that these materials are stimuli responsive makes them perfect candidates for use in dynamically tunable microlens structures. As discussed in Chapter 2, ordered microlens arrays can be fabricated by assembling pNIPAm-co-AAc microgels onto an aminopropyltrimethoxysilane (APTMS) functionalized glass substrate through common electrostatic interactions. An example of such an ordered microlens array is shown in the SEM image in Figure 3-1.

Plano-convex lens formation is presumably due to deformation of the microgels in an anisotropic fashion during substrate attachment due to the mechanical softness of microgels. The lens-like structure has been shown to effectively focus images in air due to the particle shape and the high refractive index (RI) contrast between in microgel polymer (~1.4) in air (~1.0). This chapter demonstrates that such microlens arrays are able to project images in aqueous environments despite the decreased RI contrast of the water-swollen microgels. Also, since the microgels can still act as lenses in aqueous media, the responsivity of the microgels with respect to temperature and pH can be exploited to dynamically tune the microlens optical properties.

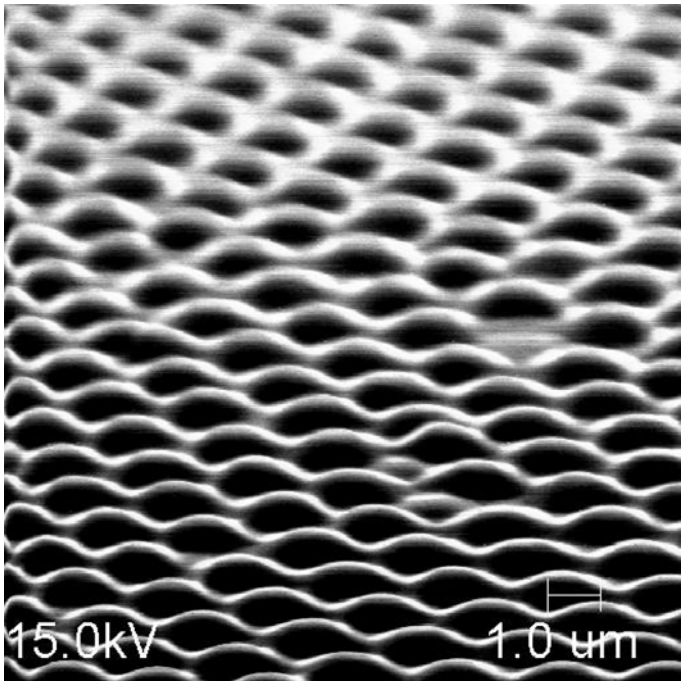

Figure 3-1. SEM image of a microlens array imaged at a grazing angle with respect to the substrate. The microgels have formed an ordered array of plano-convex shapes.

3.2 Experimental Section

Materials

All reagents, materials, and water were purchased and/or prepared as previously described in the Chapter 2 unless otherwise specified.

Microgel Synthesis

The same batch of microgels was used throughout this investigation and was the exact same microgels used in the Chapter 2.

Microlens Substrate Preparation

Glass substrates were cleaned by exposing the slides to an Ar plasma (Harrick Scientific) for 30 min to remove any organics from the substrate surface. The substrates were functionalized in an ethanolic (absolute ethanol) 1% APTMS solution as previously described in the Chapter 2. The substrate was then exposed to an aqueous 10% (v/v) microgel solution at pH 6.5 (~0.001 M ionic strength) and allowed to completely dry on the substrate (~24 hrs). The substrate was subsequently immersed in DI water for 2 hrs, then rinsed with DI water, and dried with nitrogen gas to leave behind only microgels strongly attached to the substrate by electrostatic interaction. Different pH solutions (~0.001 M ionic strength) were introduced into the void space of a microlens array/silicone gasket/coverslip sandwich assembly to facilitate optical measurements for exploration into the tunable microlens arrays in response to pH and temperature. This experimental setup is illustrated in Scheme 3-1.

Scheme 3-1. Inverted light microscopy setup used for aqueous phase imaging experiments. This setup is slightly modified from Scheme 2-1 in Chapter 2.

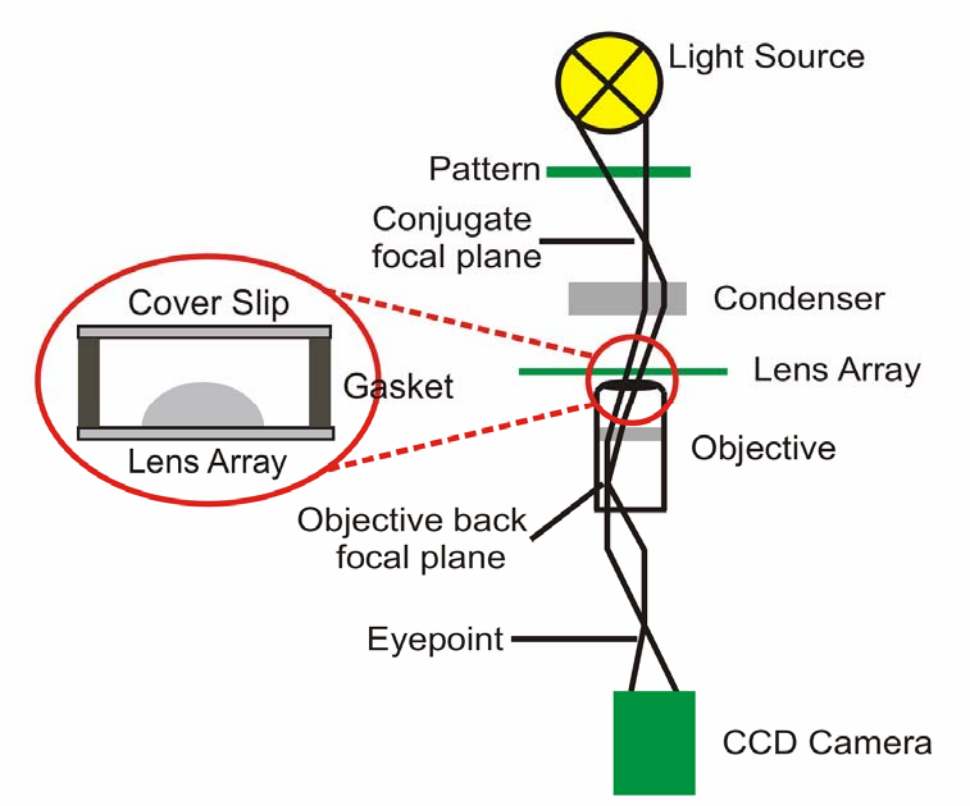

Microscopy

Optical and electron microscopies were used throughout this investigation to confirm microgel shape, size and lensing ability. A Hitachi S800 scanning electron microscope (SEM) was used to determine the shape of microgels attached to the glass substrate. SEM images were obtained by attaching a dry microgel decorated glass substrate to a SEM peg and placed in the SEM chamber. The substrate was then imaged

with an accelerating voltage of 15 kV with the sample tilted relative to the incoming electrons in order to obtain profile images of the microgels. Brightfield transmission and differential image contrast (DIC) optical microscopies were used to confirm the lensing abilities of the microgels attached to the substrate. An Olympus IX 70 inverted microscope equipped with a high numerical aperture, oil immersion 100X objective (N.A.=1.30), a microscope objective heater and a Peltier-based temperature stage was used for imaging the pattern under various conditions. Images were captured using a black and white CCD camera (PixelFly, Cooke Corporation) as a function of pH and temperature.

3.3 Results and Discussion

Figure 3-2 shows the focal length tunability of a microlens in response to pH at 25 °C. The differential interference contrast (DIC) images in panels (a) and (b) show that the substrate bound microgel is compact at pH 3.0 and swollen at pH 6.5, respectively. This behavior is due to the AAc groups within the microgel network becoming negatively charged (pK_a~4.25) at pH 6.5, which in turn causes gel swelling due to Coulombic repulsion and osmotic effects.[9,10] Since the diameter, refractive index, and presumably the curvature of the substrate-bound microgels are tunable in response to pH, the lens power should be similarly tunable. This lens power tunability is illustrated in Figure 3-2 (c) and (d) at pH 3.0 and 6.5, respectively. This figure is made by zooming in on a single particle from an array, as seen in Figure 3-3. Panel (c) in Figure 3-2 shows that the microgel at pH 3.0 is able to bring into focus a cross pattern placed conjugate to the objective back focal plane,[30] while Panel (d) shows that the same microgel at pH 6.5 is not able to focus

the cross pattern at the same focal point. This focal length tunability can be understood by considering the microgels to be more optically dense at pH 3.0 than they are in their highly water swollen state at pH 6.5. Taking into account the fact that focal lengths are dependent upon the ratio of the RI between the lens material and the surrounding medium, where a higher RI difference results in a lens with a shorter focal length (higher lensing power), it can be understood why the cross pattern is visible through the microlens at pH 3.0 and is not clearly focused at pH 6.5.

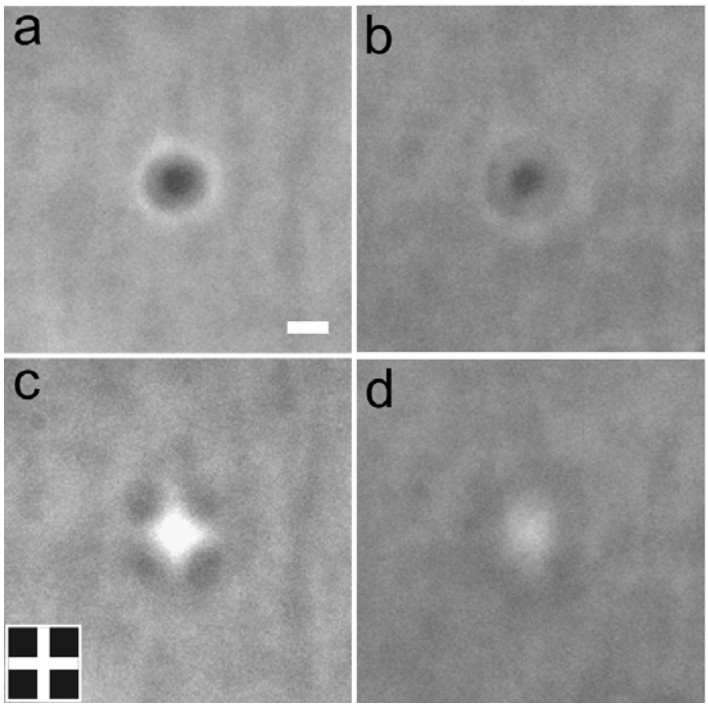

Figure 3-2. Panels (a) and (b) show the DIC microscopy images of a substrate-bound microgel at pH 3.0 and 6.5, respectively. Panels (c) and (d) show the projection of the cross pattern (inset bottom left) through the microgel at the respective pH values. The more compact structure present at pH 3.0 is able to focus a cross pattern with a higher fidelity than the same microlens at pH 6.5. The scale bar is 1 μm.

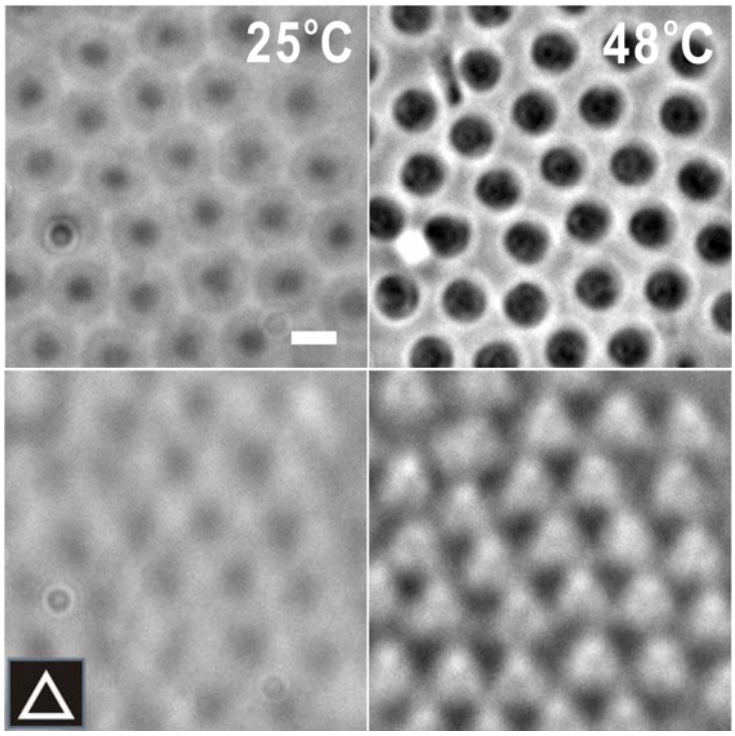

Figure 3-3. DIC and pattern projection images of particle arrays in water at pH 6.5 showing homogeneous image quality from lens to lens. The scale bar is 1 μm and the triangle pattern used is shown in the inset.

Since pNIPAm-co-AAc microgels are thermoresponsive at pH 3.0 but significantly less so at pH 6.5, the microlenses should display a pH dependent thermal tunability. Figures 3-4 and 3-5 show the responsivity of the substrate bound microgels and their resulting lensing ability as a function of temperature at pH 3.0 and 6.5, respectively. The DIC microscopy images in Figure 3-4 (top) show that the substrate bound microgels respond to increases in temperature by decreasing in size. This decrease

in swelling results in an increase in RI contrast with respect to water, which should result in an improved microlens focusing. Figure 3-4 (bottom), illustrates that this is the case. As the temperature is increased from 25 °C to 40 °C the microlens structure is able to focus a cross pattern with higher fidelity. It is also interesting to note that the microlens undergoes a sharp size transition at ~ 31 °C[7,8,31] which is the same point at which the microlens drastically changes its lensing ability.

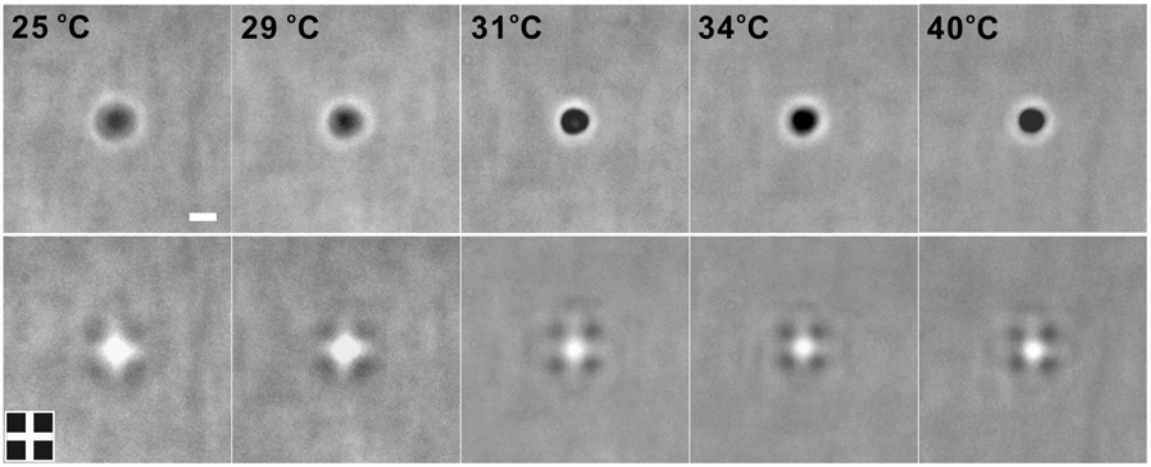

Figure 3-4. (Top) DIC microscopy images of a substrate bound microgel in pH 3.0 solution as a function of temperature. (Bottom) Projection of the cross pattern (inset bottom left) through the microgel at the indicated temperatures. As the microgel size decreases, the focusing ability of the microlens increases. The scale bar is 1 μm.

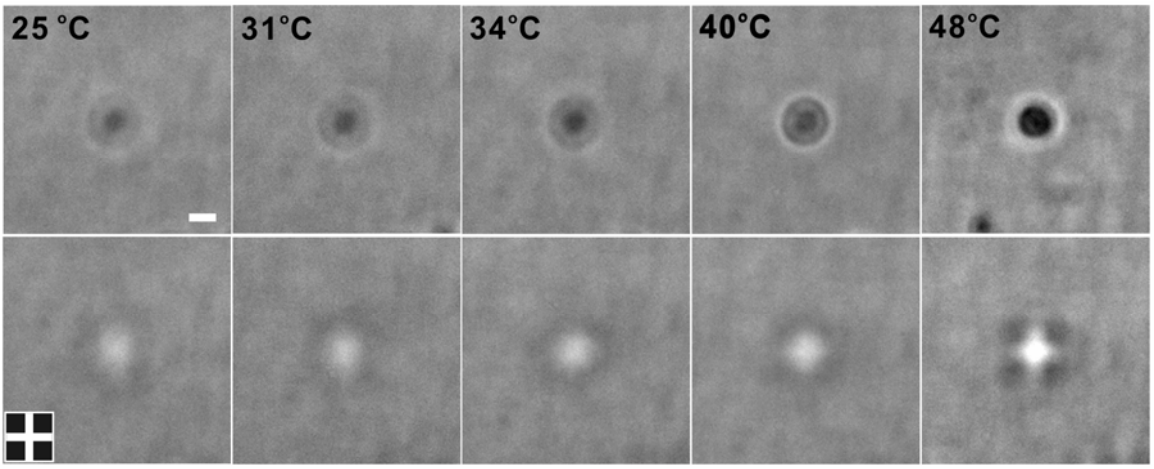

Figure 3-5. (Top) DIC microscopy images of a substrate bound microgel in pH 6.5 solution as a function of temperature. (Bottom) Projection of the cross pattern (inset bottom left) through the microgel at the indicated temperatures. The microgel lensing ability is invariant with temperature over a wide range due to Coulombic repulsion and osmotic pressure in the microgel network as a result of AAc deprotonation. Only upon reaching 48 °C does the microlens bring the pattern into focus. Note however that the image is still inferior to the pattern projected by the same microlens at pH 3.0. The scale bar is 1 μm.

Figure 3-5(top) shows the DIC images of the substrate bound microgel at pH 6.5 as a function of temperature. In contrast to the behavior at pH 3.0, the higher pH results in a microgel that is not responsive to heating over the same temperature range. It is not until 48 °C that the microgel undergoes a transition, which is consistent with previous studies.[7] As expected, the lensing ability of the microlens, which is shown in Figure 3-5(bottom), is unaffected by temperature up until the transition temperature of 48 °C, at which point the optical properties drastically change.

3.4 Conclusions

This chapter discusses that substrate supported, stimuli-responsive pNIPAm-co-AAc microgels form dynamically tunable microlenses and their tunable properties in microlens formation are visualized by employing optical microscopy. The lenses are produced via simple aqueous phase polymerization and the arrays are fabricated without the need for photolithographic or micromolding processes. These characteristics make this system attractive for the rapid construction of lens arrays with wet chemical methods. Furthermore, these structures have been shown to be tunable as a function of temperature and pH, where the water content of the microgel has a profound effect on lensing ability due to changes in refractive index contrast with the medium. Various and detailed investigations into the changes in substrate supported microlens deswelling and swelling will be discussed in Chapter 4, 5, and 6.

3.5 References

(1) Kikuchi, A.; Okano, T., Pulsatile drug release control using hydrogels. *Adv. Drug Deliv. Rev.* **2002**, *54*, 53-77.

(2) Qiu, Y.; Park, K., Environment-sensitive hydrogels for drug delivery. *Adv. Drug Deliv. Rev.* **2001**, *53*, 321-339.

(3) Miyata, T.; Asami, N.; Uragami, T., A reversibly antigen-responsive hydrogel. *Nature* **1999**, *399*, 766-769.

(4) Kim, J.; Singh, N.; Lyon, L. A., Label-free biosensing with hydrogel microlenses. *Angew. Chem. Intl. Ed.* **2006**, *45*, 1446-1449.

(5) Kim, J.; Nayak, S.; Lyon, L. A., Bioresponsive Hydrogel Microlenses. *J. Am. Chem. Soc.* **2005**, *127*, 9588-9592.

(6) Kim, J.; Serpe, M. J.; Lyon, L. A., Hydrogel Microparticles as Dynamically Tunable Microlenses. *J. Am. Chem. Soc.* **2004**, *126*, 9512-9513.

(7) Jones, C. D.; Lyon, L. A., Synthesis and Characterization of Multiresponsive Core-Shell Microgels. *Macromolecules* **2000**, *33*, 8301-8306.

(8) Gan, D.; Lyon, L. A., Tunable Swelling Kinetics in Core-Shell Hydrogel Nanoparticles. *J. Am. Chem. Soc.* **2001**, *123*, 7511-7517.

(9) Pelton, R., Temperature-sensitive aqueous microgels. *Adv. Colloid. Interface Sci.* **2000**, *85*, 1-33.

(10) Saunders, B. R.; Vincent, B., Microgel particles as model colloids: theory, properties and applications. *Adv. Colloid Interface Sci.* **1999**, *80*, 1-25.

(11) Heskins, M.; Guillet, J. E., Solution properties of poly(N-isopropylacrylamide). *J. Macromol. Sci. Chem.* **1968**, *A2*, 1441-1455.

(12) Dusek, K.; Patterson, K., Transition on swollen polymer networks induced by intramolecular condensation. *Journal of Polymer Science, Polymer Physics Edition* **1968**, *6*, 1209-16.

(13) Shogenji, R.; Kitamura, Y.; Yamada, K.; Miyatake, S.; Tanida, J., Bimodal fingerprint capturing system based on compound-eye imaging module. *Appl. Optics* **2004**, *43*, 1355-1359.

(14) Arimoto, H.; Javidi, B., Integral three-dimensional imaging with digital reconstruction. *Opt. Lett.* **2001**, *26*, 157-159.

(15) Motamedi, M. E.; Tennant, W. E.; Sankur, H. O.; Melendes, R.; Gluck, N. S.; Park, S.; Arias, J. M.; Bajaj, J.; Pasko, J. G.; McLevige, W. V.; Zandian, M.; Hall, R. L.; Richardson, P. D., Micro-optic integration with focal plane arrays. *Opt. Eng.* **1997**, *36*, 1374-1381.

(16) Chen, S. H.; Yi, X. J.; Kong, L. B.; He, M.; Wang, H. C., Monolithic integration technique for microlens arrays with infrared focal plane arrays. *Infrared Phys. Technol.* **2002**, *43*, 109-112.

(17) Quan, C.; Wang, S. H.; Tay, C. J.; Reading, I.; Fang, Z. P., Integrated optical inspection on surface geometry and refractive index distribution of a microlens array. *Opt. Commun.* **2003**, *225*, 223-231.

(18) Wu, H. K.; Odom, T. W.; Whitesides, G. M., Connectivity of features in microlens array reduction photolithography: Generation of various patterns with a single photomask. *J. Am. Chem. Soc.* **2002**, *124*, 7288-7289.

(19) Wu, M. H.; Park, C.; Whitesides, G. M., Fabrication of arrays of microlenses with controlled profiles using gray-scale microlens projection photolithography. *Langmuir* **2002**, *18*, 9312-9318.

(20) Wu, M. H.; Whitesides, G. M., Fabrication of diffractive and micro-optical elements using microlens projection lithography. *Adv. Mater.* **2002**, *14*, 1502-1506.

(21) Wu, M. H.; Paul, K. E.; Yang, J.; Whitesides, G. M., Fabrication of frequency-selective surfaces using microlens projection photolithography. *Appl. Phys. Lett.* **2002**, *80*, 3500-3502.

(22) Wu, M. H.; Paul, K. E.; Whitesides, G. M., Patterning flood illumination with microlens arrays. *Appl. Optics* **2002**, *41*, 2575-2585.

(23) Wu, H.; Odom, T. W.; Whitesides, G. M., Generation of chrome masks with micrometer-scale features using microlens lithography. *Adv. Mater.* **2002**, *14*, 1213-1216.

(24) Karkkainen, A. H. O.; Rantala, J. T.; Maaninen, A.; Jabbour, G. E.; Descour, M. R., Siloxane-based hybrid glass materials for binary and grayscale mask photoimaging. *Adv. Mater.* **2002**, *14*, 535-540.

(25) Karkkainen, A. H. O.; Tamkin, J. M.; Rogers, J. D.; Neal, D. R.; Hormi, O. E.; Jabbour, G. E.; Rantala, J. T.; Descour, M. R., Direct photolithographic deforming of organomodified siloxane films for micro-optics fabrication. *Appl. Optics* **2002**, *41*, 3988-3998.

(26) Sakurai, Y.; Okuda, S.; Nagayama, N.; Yokoyama, M., Novel microlens array fabrication utilizing UV-photodecomposition of polysilane. *J. Mater. Chem.* **2001**, *11*, 1077-1080.

(27) Jones, C. D.; Lyon, L. A., Photothermal patterning of microgel/gold nanoparticle composite colloidal crystals. *J. Am. Chem. Soc.* **2003**, *125*, 460-465.

(28) Jones, C. D.; Serpe, M. J.; Schroeder, L.; Lyon, L. A., Microlens formation in microgel/gold colloid composite materials via photothermal patterning. *J. Am. Chem. Soc.* **2003**, *125*, 5292-5293.

(29) Lu, Y.; Yin, Y. D.; Xia, Y. N., A self-assembly approach to the fabrication of patterned, two- dimensional arrays of microlenses of organic polymers. *Adv. Mater.* **2001**, *13*, 34-37.

(30) Serpe, M. J.; Kim, J.; Lyon, L. A., Colloidal hydrogel microlenses. *Adv. Mater.* **2004**, *16*, 184-187.

(31) Tanaka, T.; Fillmore, D. J.; Sun, S.-T.; Nishio, I.; Swislow, G.; Shah, A., Phase Transition in Ionic Gels. *Phys. Rev. Lett.* **1980**, *45*, 1636-1639.

CHAPTER 4

PHOTO-SWITCHABLE MICROLENS ARRAYS

This Chapter describes work on 2-D microlens arrays composed of temperature/pH responsive pNIPAm-co-AAc microgels. The arrays are constructed on Au nanoparticle-functionalized glass substrates by self-assembly of responsive microgel particles. The microlens array is composed of discrete optical elements that display dramatic changes in lensing power in response to an impingent frequency-doubled Nd:YAG laser. This wavelength is resonant with the plasmon absorption of the underlying Au nanoparticles, which thereby re-radiate the absorbed energy as heat into the thermoresponsive microlenses. Microlens photoswitching is highly reversible, with sub-millisecond lens switching times.

4.1 Introduction

As discussed in Chapter 2 and Chapter 3, using an electrostatic self-assembly approach, ordered microlens arrays can be fabricated on glass substrates, and furthermore, they effectively function as optical elements capable of focusing images in air and water.[1,2] The lensing ability of the hydrogel microlenses is mainly due to the hemispherical particle shape that results from immobilization on the solid support, and the refractive index (RI) contrast between the deswollen microgel polymer (~1.4) and the medium. Microlens array focal length tunability in water has also been demonstrated based on the thermoresponsivity of pNIPAm-co-AAc microgels in aqueous solution. As

the temperature of a pNIPAm microgel in solution is increased to that polymer's intrinsic lower critical solution temperature (LCST), the microgels undergo a phase transition from a solvent swollen state to a deswollen state.[3-9] Accordingly, the thermoresponsive optical properties of the microlens arrays can be understood not only by considering the microgels to be more optically dense above the LCST, but also by considering the fact that lensing power is dependent upon the ratio of the refractive index (RI) between the lens material and the surrounding medium, where a higher RI difference results in a shorter focal length lens.

This chapter describes the demonstration of microlens arrays comprised of fast-responding, reversible, photo-tunable lens elements, which are prepared using simple wet chemical methods. These arrays are fabricated by exposing 3-aminopropyltrimethoxysilane (APTMS) functionalized glass substrates to citrate stabilized Au nanoparticles (16±1.6 nm), which attach to the glass substrate via electrostatic interactions.[10] The presence of Au nanoparticles on the surface allows for local heating of the sample through excitation of surface plasmon modes on the Au nanoparticles with a frequency-doubled Nd:YAG laser (λ=532 nm).[11,12] Plasmon excitation results in energy transfer to the environment in the form of thermal dissipation through electron-phonon and phonon-phonon coupling.[13] This Au nanoparticle-coated substrate is subsequently rendered positively charged by exposure to the cationic polyelectrolyte poly(allylamine hydrochloride) (PAH). In this fashion, the PNIPAm-co-AAc microgel particles coat the APTMS/Au/PAH modified glass substrate *via* electrostatic self-assembly. Figure 4-1 shows a schematic depiction and a scanning electron microscopy (SEM) image of this structure. In this arrangement, one takes

advantage of the conjugate focal planes in the microscope by placing a pattern near a plane conjugate to the back focal plane of the objective. When the microgels act as lens elements as a function of incident laser power, they change the effective focal length of the microscope, bringing the back focal plane of the objective near the eyepoint. This is observed as a projection of the pattern through each active element in the lens array.

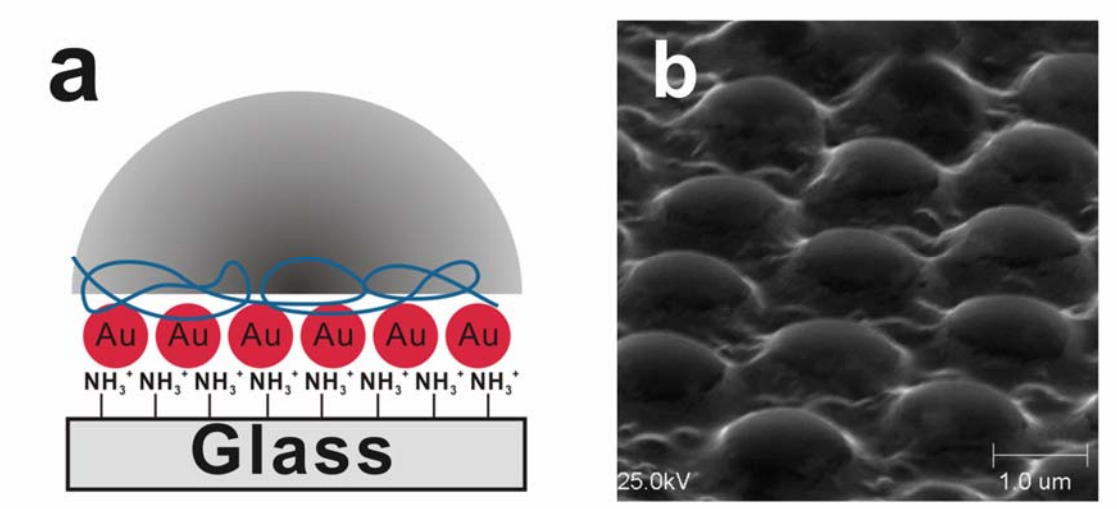

Figure 4-1. (a) Schematic depiction of the multicomponent film used to create photoswitchable microlens arrays. (b) SEM image of the constructed microlens array at grazing angle.

4.2 Experimental Section

Materials

All reagents, materials, and water were purchased and/or prepared as previously described in the Chapter 2 unless otherwise specified. Poly(allylamine hydrochloride) (PAH), MW 70 000, was purchased from Sigma-Aldrich and used as received.

Microgel Synthesis

The same batch of microgels was used throughout this investigation and was the exact same microgels used in the Chapter 2.

Au Nanoparticle Synthesis

250 mL of 1.0 mM $HAuCl_4$ solution was stirred while heating to a vigorous boil. 25 mL of a 38.8 mM sodium citrate was then rapidly added to the above solution producing a pale yellow solution, which quickly became a deep burgundy. The solution was allowed boil for an additional 10 min following the color change. The heat source was then removed and stirring was allowed to proceed for 15 min. The particle diameter determined by transmission electron microscopy (TEM, JEOL 1210 Analytical TEM) was 16±1.6 nm.[12]

Microlens Array Substrate Preparation

Glass substrates were cleaned by exposing the slides to an Ar plasma (Harrick Scientific) for at least 30 min for removal of organics from the substrate surface and functionalized in an ethanolic (absolute ethanol) 1% APTMS solution as previously described in the Chapter 2. Prior to assembly, each substrate was rinsed with DI H_2O and dried under a stream of nitrogen gas. A concentrated solution of 16±1.6 nm gold nanoparticles was allowed to electrostatically assemble onto the APTMS functionalized glass substrate for 30 min. This substrate was then exposed to a 0.0053 monoM (moles/L

monomer) solution of the linear polyelectrolyte PAH, MW 70 000, for 30 min, thereby allowing for electrostatic adsorption of a monolayer of the polymer. After each deposition step, the substrate was rinsed copiously with DI water and dried under a stream of nitrogen gas. The substrate was then exposed to an aqueous 10% (v/v) microgel solution at pH ~6.5, which was allowed to completely dry on the substrate (~24 hrs). At this pH, the microgels are anionic, resulting in good adhesion to the cationic substrate, as well as a high surface coverage. The substrate was subsequently immersed in DI water for 2 hrs, rinsed with DI water, and dried with nitrogen gas to leave behind microgels that are strongly attached to the substrate by electrostatic interactions.

Microscopy

The same optical and electron microscopies as described in the Chapter 2 were used to confirm microgel shape, size and the tunability of the micro-optical elements attached to the substrate. An Olympus IX 70 inverted microscope equipped with a high numerical aperture, oil immersion 100X objective (N.A.=1.30), a microscope objective heater and a Peltier-based temperature stage as previously shown in the Chapter 2 was used for imaging the pattern under various conditions. The experimental setup is shown in Scheme 4-1. Images were captured using a black and white CCD camera (PixelFly, Cooke Corporation) as a function of laser intensity, which was adjusted by neutral density filters, (10.22 mW/μm^2 ~ 184.97 mW/μm^2). An Itronx Imaging Technologies FASTCAM DVR CCD camera[*] was used to determine the time scale of the laser induced optical switching at a rate of 2000 frames per second (FPS).

[*] We thank Prof. M. Srinivasarao for the fast frame rate CCD camera used in this study.

Scheme 4-1. Inverted light microscopy setup used for detection of the photoswichable behavior of microlens arrays in the liquid phase.

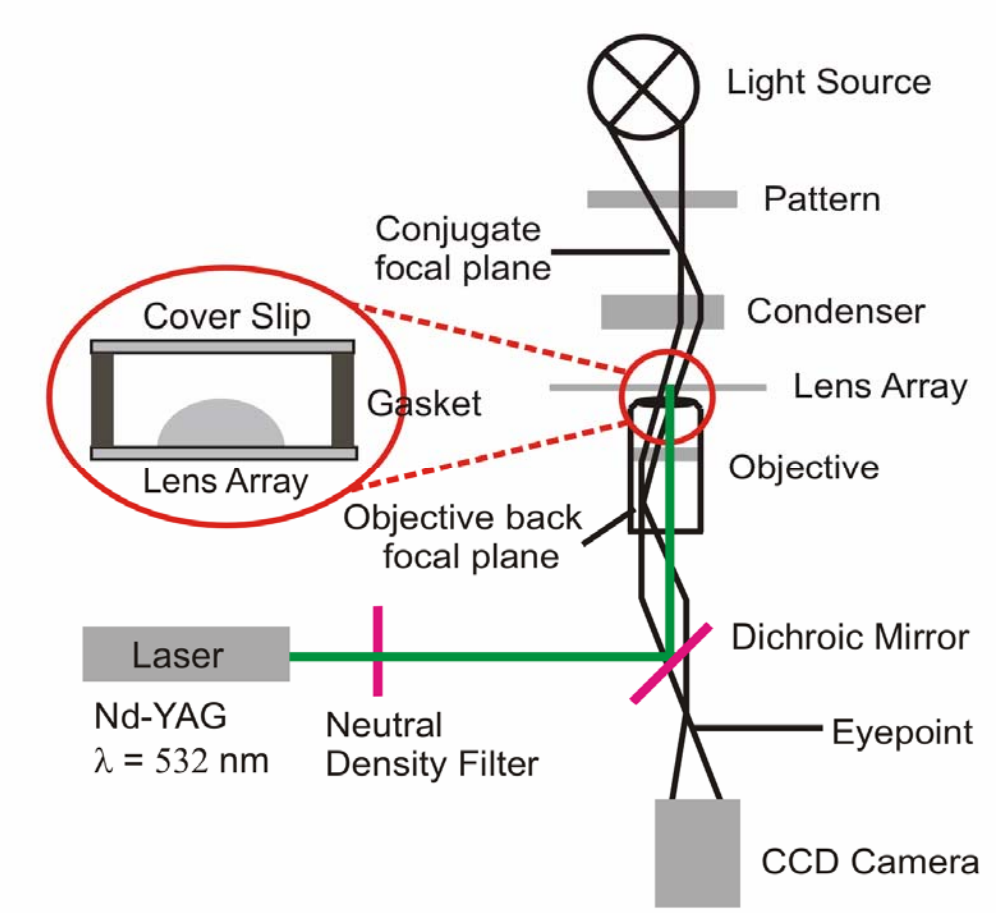

4.3 Results and Discussion

For photo-switchable microlens tuning study, hydrogel microlens arrays assembled to APTMS/Au/PAH modified glass substrate as described in experimental section were used. The key characteristics of this construct with respect to photo-tuning relate to the optical properties of the colloidal Au array, and the thermoresponsivity of the microgel lens elements. UV-vis spectroscopy was used to confirm the presence of Au nanoparticles on the glass substrate following assembly.

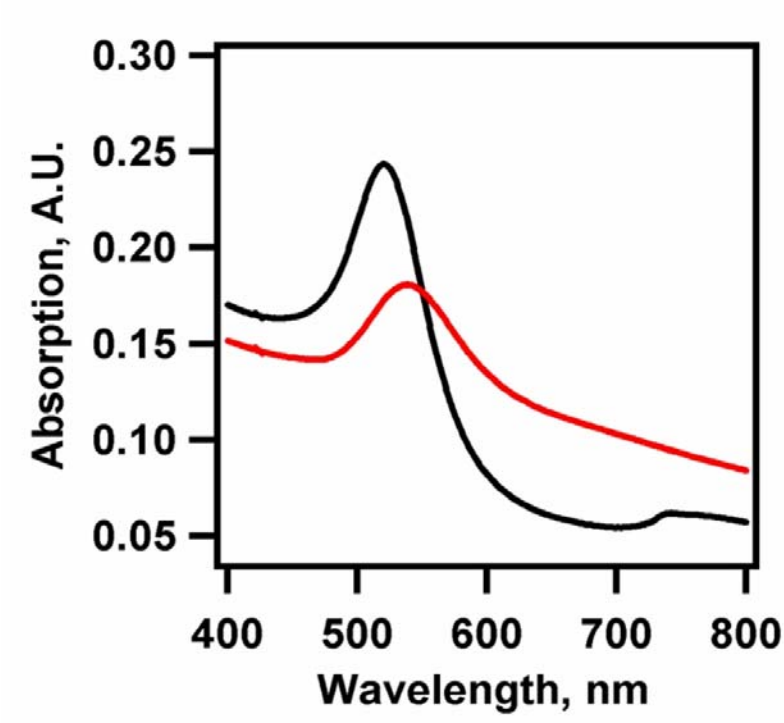

Figure 4-2. UV-vis spectra for Au nanoparticles in solution (black) and a bound to substrate (red).

Figure 4-2 shows the spectra for Au nanoparticles in aqueous solution and an Au nanoparticle functionalized substrate coated with a microlens array. The absorption spectrum for the substrate-bound Au nanoparticles is shifted to slightly higher wavelengths than that of the Au nanoparticle solution. A long-wavelength shoulder is also apparent in the spectrum of the lens array. The long-wavelength shoulder is most likely due to slight Au nanoparticle aggregation on the substrate during assembly, while the plasmon resonance shift results from the microlens array. The deswollen microlenses present a higher local refractive index to the Au nanoparticles surface, thereby shifting the plasmon resonance to lower energy.

The photoresponsivity of the microlens arrays was initially investigated by monitoring the projection of a triangle pattern through the lenses while exposed to a pH 3.0 solution, in response to various laser powers and bath temperatures in Figure 4-3. Panels (a) and (b) show the focal length tunability of the microlens arrays at a bath temperature of 25 °C upon laser exposure. Each lens is capable of projecting the triangle image only in the region of laser light excitation, where the effective temperature is higher than the microgel LCST. The number of lenses that display a high quality image is also tunable by varying the laser power (see Figure 4-4). Similarly, panels (c) and (d) show the focal length tunability of the microlens arrays at a bath temperature of 10 °C upon laser exposure. A smaller area of the array is switched under these conditions, as the bath temperature is further from the 31 °C LCST of pNIPAm. Note that the same laser power is impingent on the array in panels (b) and (c). Since a fixed laser power induces a fixed temperature jump, moving the bath temperature far below the LCST results in photo-induced temperature excursion that is now below the polymer LCST in Figure 4-

3(c). It is also theoretically possible to control single lens elements of the array by this method. Since the laser spot is essentially diffraction limited in size (~266 nm diameter) under these illumination conditions, it is in fact smaller than an individual lens. By controlling the bath temperature and the laser intensity one can therefore interrogate a single lens element.

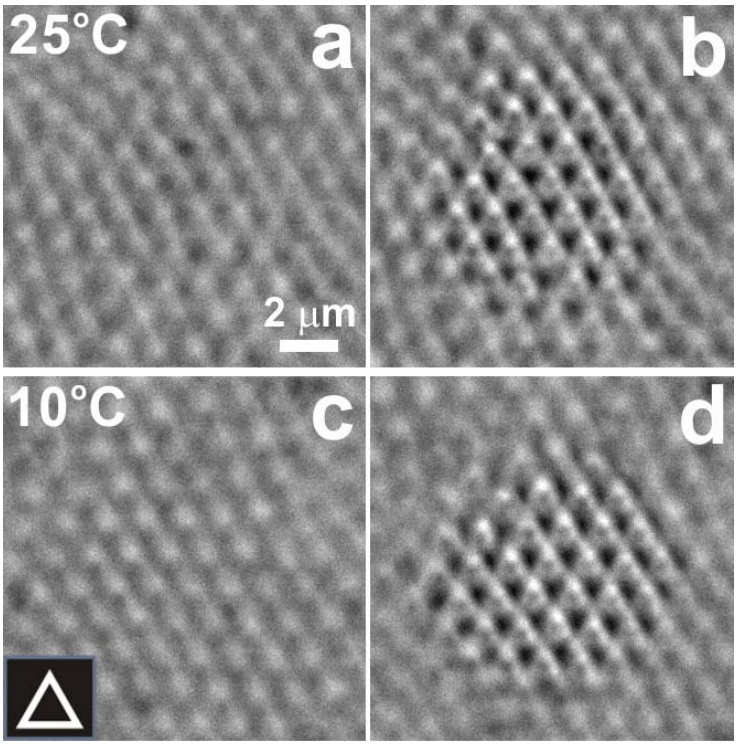

Figure 4-3. Photo-switching of microlens arrays as a function of laser power and solution temperature at pH 3.0. Arrays at 25 °C (a, b) and 10 °C (c, d) show laser power dependent optical properties by projecting a triangle pattern (bottom left) only when the laser power is sufficient to produce the necessary temperature jump to above the microgel LCST. Laser powers are 10.22 mW/μm^2 (a), 38.45 mW/μm^2 (b, c), and 88.90 mW/μm^2 (d). From the figure it can also be seen that each lens is capable of projecting an image only in the region surrounding the incident laser light excitation.

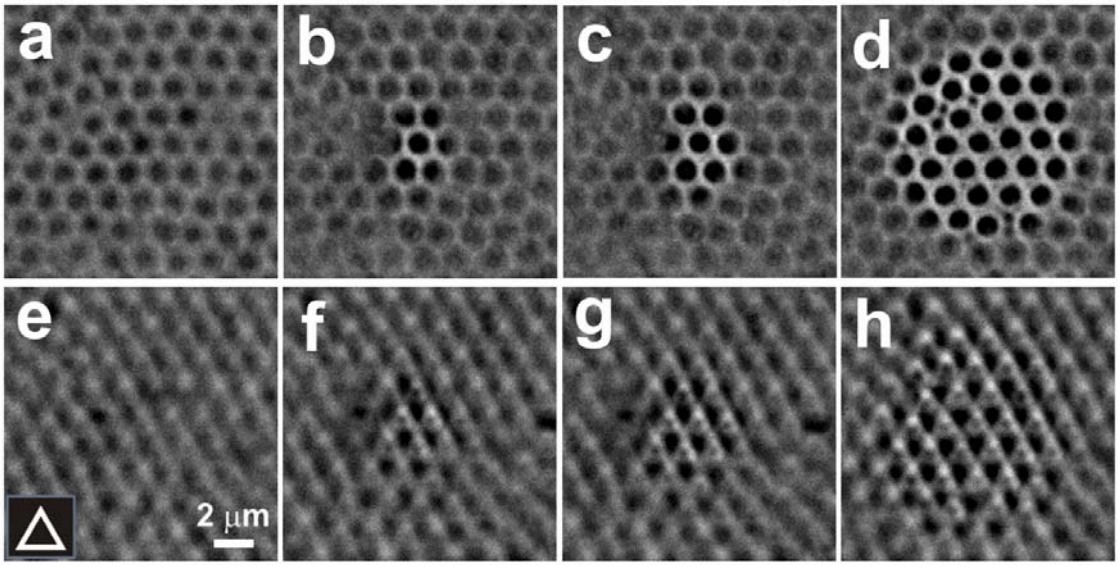

Figure 4-4. (Top) DIC microscopy images of substrate bound microgels in pH 3.0 solution at 25 °C as a function of laser power. (Bottom) Projection of a triangle pattern (inset bottom left) through the microgel at different laser powers. As the laser power increases, the modulated region of the microlens array increases. The laser intensities at the microlens array surface are 10.22 mW/μm^2 (a,e), 20.14 mW/μm^2 (b,f), 24.66 mW/μm^2 (c,g), 38.45 mW/μm^2 (d,h).

Figures 4-5(a) and (b) show images projected through the microlens array at 25 °C and pH 6.5 as a function of laser power. Comparing Figures 4-3(b) and 4-5(a), where the laser powers are identical, suggests that the microlens array at pH 6.5 is less sensitive to laser irradiation than at pH 3.0. This behavior is due to the higher LCST of the microgels at this pH, caused by AAc deprotonation within the microgel network at pH values above the pKa (pK_a~4.25).[4] As expected, the lensing ability of the microlens is unaffected by temperature up to the transition temperature of ~48 °C as observed by the bulk heating experiments (see Figure 4-6). Figure 4-5(b) and (d) illustrates that the microlens array is again extremely sensitive to the bath temperature, as indicated by a decrease in the area of the modulated region at low temperature. This effect can also be confirmed by comparing the modulated area in Figure 4-3(d) to Figure 4-5(d). This effect is due to the lower LCST of the microgels at pH 3.0, which are therefore able to respond to smaller temperature jumps than the microgels at pH 6.5. Note that similar behavior is also observed with different pattern (a square pattern) in Figure 4-7.

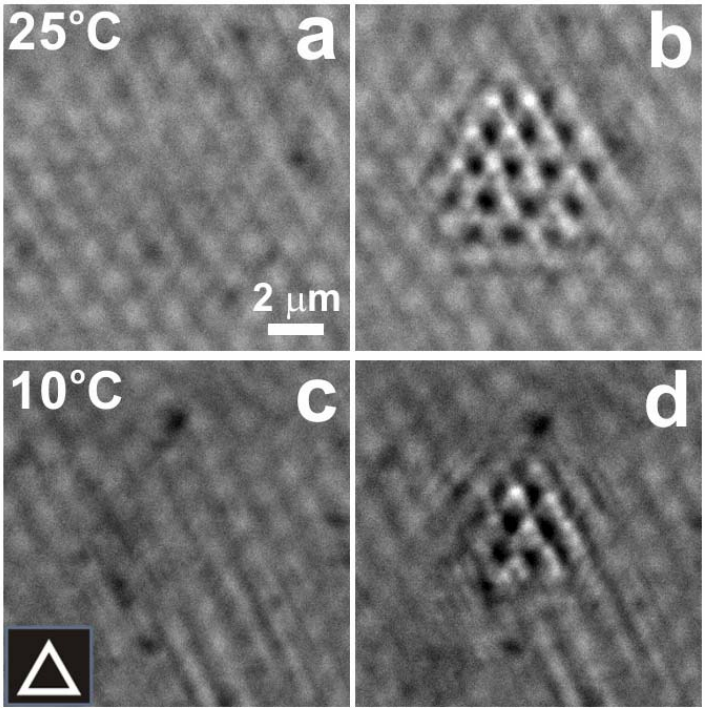

Figure 4-5. Photo-switching of microlens arrays as a function of laser power and solution temperature at pH 6.5. Again it can be seen that the arrays at 25 °C (a, b) and 10 °C (c, d) show laser power dependent optical properties by projecting a triangle pattern (bottom left) only when the laser power is sufficient to produce the necessary temperature jump to above the microgel LCST. Laser powers are 38.45 mW/μm^2 (a), 88.90 mW/μm^2 (b, d), and 48.56 mW/μm^2 (c). By comparison to Figure 2 it can be seen that more laser power is required to modulate the micro-optical array at this pH.

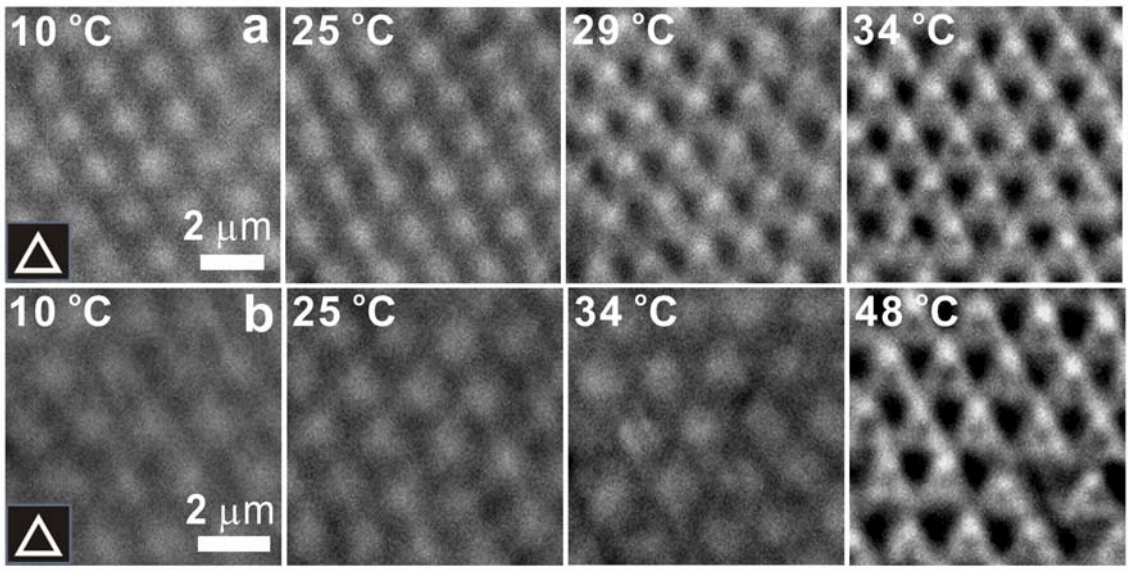

Figure 4-6. Projection of a triangle pattern (inset left) through the microlens array at pH 3.0 (a) and at pH 6.5 (b) as a function of bath temperature.

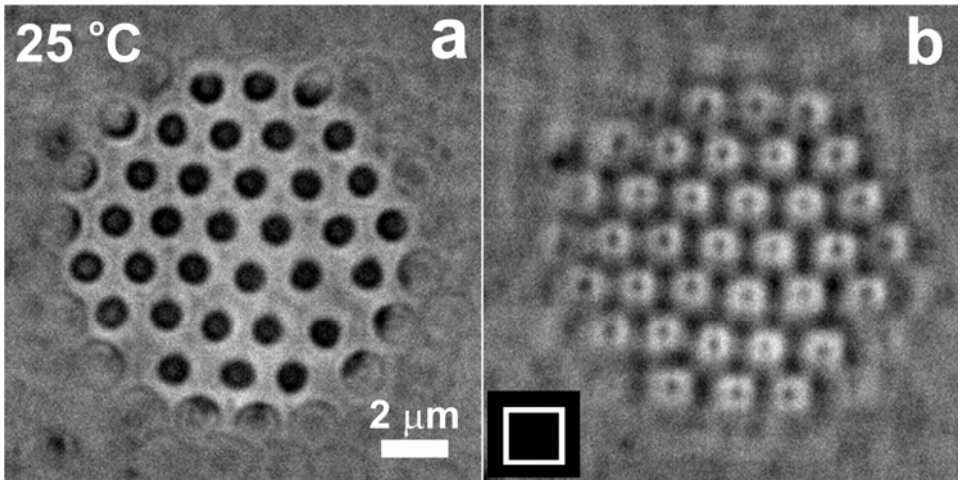

Figure 4-7. (a) DIC microscopy images of substrate bound microgels in pH 6.5 solution at 25 °C. (b) Projection of a square pattern (inset bottom left) through the microgel. The laser intensities at the microlens array surface are 221.83 mW/μm^2.

The reversibility and response rate of the microlens array are shown in Figure 4-8. The laser modulation frequency was controlled by passing it through an optical chopper. Row (a) shows that the optical properties of the microlens array can be fully modulated, in a completely reversible fashion, using 10 ms laser pulses. This experiment was performed without the projection of a pattern through the array, as the camera was not sensitive enough to detect the projected image while acquiring images at 2000 frames per second. It should be pointed out that the apparent response time of microlenses in the array was measured at <500 μs, as we cannot resolve intermediate stages of microgel deswelling at 2000 frames per second under the conditions presented in Figure 4-8 (see Figure 4-9). In other words, individual lens elements go from a non-lensing to a lensing state within one frame at this image capture rate. Literature reports place microgel deswelling rates on the timescale of tens to hundreds of microseconds, depending on the network density and particle size.[14] Figure 4-8 (b) and (c) also shows that this reversibility is diminished upon increasing the laser repetition frequency from 200 to 500 Hz. This is due to the fact that while microgel *deswelling* is caused by fast thermal dissipation from the laser-excited Au nanoparticles to the microlenses, the *reswelling* of the microgel is limited by the slow dissipation of heat away from the substrate. Thus, the microlens array appears totally deswollen at 500 Hz, as the pulsing frequency is faster than the microgel reswelling rate.

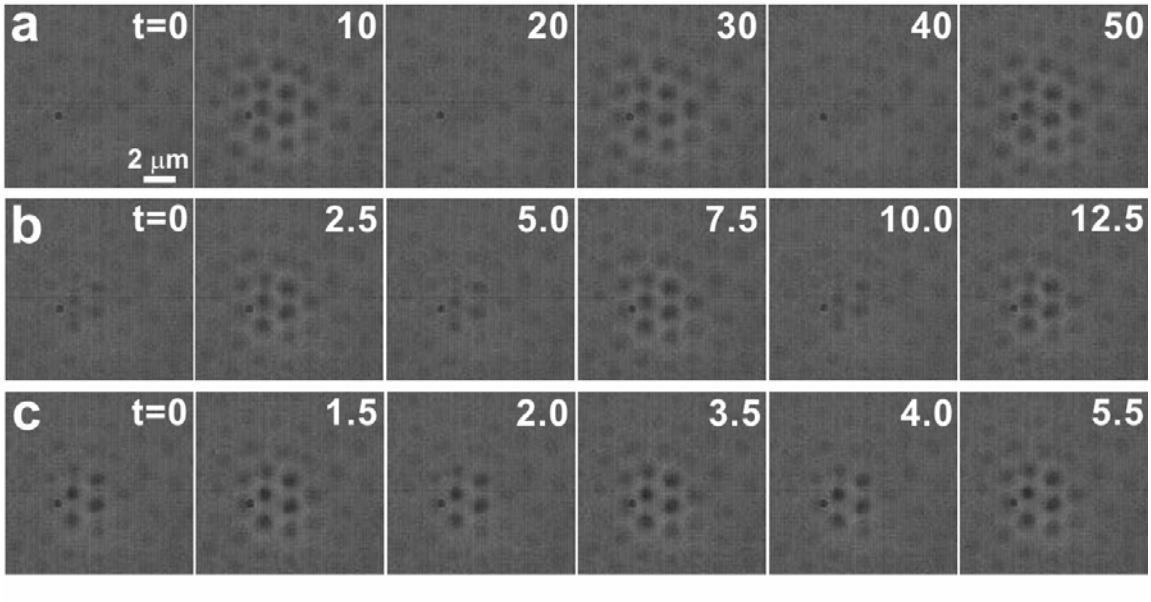

Figure 4-8. Images captured with a fastcam DVR CCD camera at 2000 FPS while chopping the Nd:YAG laser source at 50 Hz (a), 200 Hz (b), and 500 Hz (c) in pH 6.5 solution at 15 °C. The optical properties of the array can be reversibly modulated in phase with laser pulses of 50 Hz (a). However, once the laser modulation frequency exceeds the rate of thermal diffusion from the microgels, the modulation of the microlens array diminishes (b,c). The laser intensity at the array surface is 184.97 mW/μm^2. The numbers at the top right of each image indicate the Δt in milliseconds.

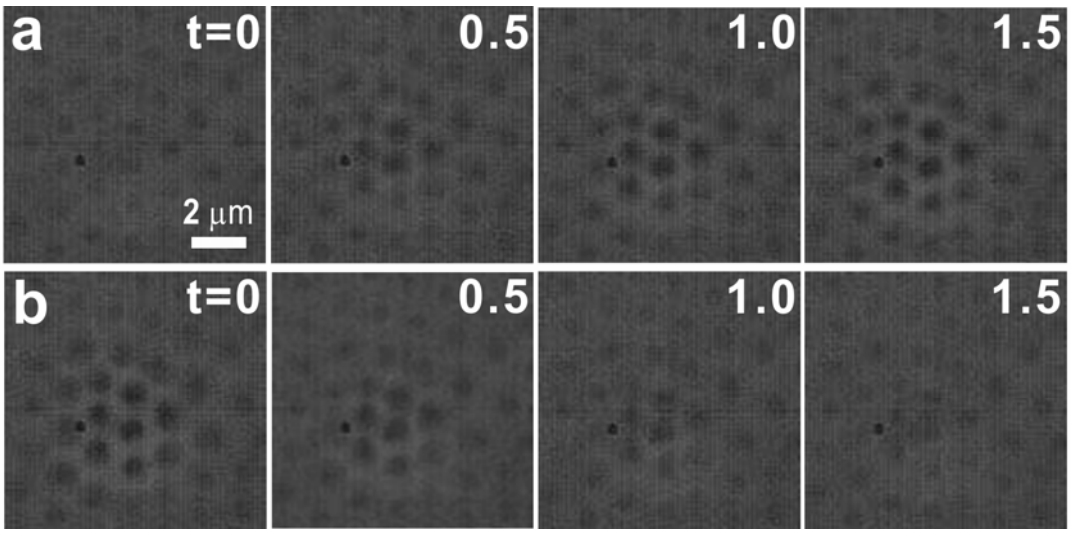

Figure 4-9. Images captured with a fastcam DVR CCD camera at 2000 FPS while chopping a Nd:YAG laser source at a frequency of 50 Hz in pH 6.5 solution at 15 °C. The on (a) and off (b) time is on the order of ~1.5 msec. The laser intensity at the microlens array surface is 184.97 mW/μm^2. The numbers at the top right indicate Δt in milliseconds.

4-4 Conclusions

This chapter has shown that a high-density microlens array can be fabricated by using simple wet-chemical methods and, also, the microlens array can be tuned or switched by an external laser source. The fabrication technology is inexpensive, scalable, and rapid, in contrast to traditional micromolding or photolithographic approaches. The unique characteristics of the micro optics include the ability to confine the tunable region to the single microlens scale, fast response rate (~10-fold faster than video rate), and highly reversible behavior under pulsed laser control. These characteristics make this system an attractive enabling technology for the future development of agile micro-optical components.

REFERENCES

(1) Serpe, M. J.; Kim, J.; Lyon, L. A., Colloidal hydrogel microlenses. *Adv. Mater.* **2004**, *16*, 184-187.

(2) Kim, J.; Serpe, M. J.; Lyon, L. A., Hydrogel Microparticles as Dynamically Tunable Microlenses. *J. Am. Chem. Soc.* **2004**, *126*, 9512-9513.

(3) Gan, D.; Lyon, L. A., Tunable Swelling Kinetics in Core-Shell Hydrogel Nanoparticles. *J. Am. Chem. Soc.* **2001**, *123*, 7511-7517.

(4) Jones, C. D.; Lyon, L. A., Synthesis and Characterization of Multiresponsive Core-Shell Microgels. *Macromolecules* **2000**, *33*, 8301-8306.

(5) Pelton, R., Temperature-sensitive aqueous microgels. *Adv. Colloid. Interface Sci.* **2000**, *85*, 1-33.

(6) Dusek, K.; Patterson, K., Transition on swollen polymer networks induced by intramolecular condensation. *Journal of Polymer Science, Polymer Physics Edition* **1968**, *6*, 1209-16.

(7) Tanaka, T.; Fillmore, D. J.; Sun, S.-T.; Nishio, I.; Swislow, G.; Shah, A., Phase Transition in Ionic Gels. *Phys. Rev. Lett.* **1980**, *45*, 1636-1639.

(8) Tanaka, T.; Fillmore, D. J., Kinetics of Swelling of Gels. *J. Chem. Phys.* **1979**, *70*, 1214 - 1218.

(9) Arotcarena, M.; Heise, B.; Ishaya, S.; Laschewsky, A., Switching the inside and the outside of aggregates of water-soluble block copolymers with double thermoresponsivity. *J. Am. Chem. Soc.* **2002**, *124*, 3787-3793.

(10) Freeman, R. G.; Grabar, K. C.; Allison, K. J.; Bright, R. M.; Davis, J. A.; Guthrie, A. P.; Hommer, M. B.; Jackson, M. A.; Smith, P. C.; Walter, D. G.; Natan, M. J., Self-Assembled Metal Colloid Monolayers - an Approach to Sers Substrates. *Science* **1995**, *267*, 1629-1632.

(11) Jones, C. D.; Serpe, M. J.; Schroeder, L.; Lyon, L. A., Microlens formation in microgel/gold colloid composite materials via photothermal patterning. *J. Am. Chem. Soc.* **2003**, *125*, 5292-5293.

(12) Jones, C. D.; Lyon, L. A., Photothermal patterning of microgel/gold nanoparticle composite colloidal crystals. *J. Am. Chem. Soc.* **2003**, *125*, 460-465.

(13) Link, S.; El-Sayed, M. A., Shape and size dependence of radiative, non-radiative and photothermal properties of gold nanocrystals. *International Reviews in Physical Chemistry* **2000**, *19*, 409-453.

(14) Wang, J. P.; Gan, D. J.; Lyon, L. A.; El-Sayed, M. A., Temperature-jump investigations of the kinetics of hydrogel nanoparticle volume phase transitions. *J. Am. Chem. Soc.* **2001**, *123*, 11284-11289.

CHAPTER 5

BIORESPONSIVE HYDROGEL MICROLENSES

This Chapter describes the development of bioresponsive hydrogel microlenses as a new protein detection technology. Stimuli-responsive poly(*N*-isopropylacrylamide-*co*-acrylic acid) (pNIPAm-co-AAc) microgels have been synthesized via free-radical precipitation polymerization. These hydrogel microparticles were then functionalized with biotin via EDC coupling. Hydrogel microlenses were prepared from the particles via Coulombic assembly onto a silane-modified glass substrate. Arrays containing both pNIPAm-co-AAc microgels (as an internal control) and biotinylated pNIPAm-co-AAc microgels were then used to detect multivalent binding of both avidin and polyclonal anti-biotin. Protein binding was determined by monitoring the optical properties of the microlenses using a brightfield optical microscopy technique. The microlens method is shown to be very specific for the target protein, with no detectable interference from nonspecific protein binding. Finally, the reversibility of the hydrogel microlens assay has been studied in the case of anti-biotin to determine the potential application of the microlens assay technology in a displacement-type assay. These results suggest that the microlens method may be an appropriate one for label-free detection of proteins or small molecules via displacement of tethered protein-ligand pairs.

5.1 Introduction

Over the past decade, a number of applications involving stimuli-sensitive hydrogels have arisen due to the great potential for hydrogels as matrices, actuators, and transducers.[1-13] Many of these hydrogels have been thermoresponsive, which undergo a reversible phase separation at the lower critical solution temperature (LCST) or upper critical solution temperature (UCST) of the polymer.[14-18] It has been reported that specifically engineering such hydrogels with additional functionalities, can result in hydrogels responsive to stimuli such as pH, ionic strength, photon flux, and biomolecular binding events.[8,9,19-28] These additional stimuli-responsive characteristics make them useful for numerous applications, such as controlled drug release,[11,25,29-31] tissue regeneration,[1,32] surface patterning,[3,33] microfluidic flow control,[12,34-37] tunable optics,[4,10,26,38] molecular switches,[2] and sensing transducers.[4,39,40]

Previous Chapters described that poly(*N*-isopropylacrylamide-*co*-acrylic acid) (pNIPAm-*co*-AAc) microgels can be used to fabricate dynamically tunable microlens arrays. Such tunable microlens arrays are easily assembled on an aminopropyltrimethoxysilane (APTMS) functionalized glass substrate *via* common electrostatic interactions. The optical properties of these hydrogel-based microlenses can be tuned by different stimuli, such as temperature, pH, and photons, as a result of the responsivity of the network to those stimuli.[26,38] Furthermore, the lens-like structure enables us to visualize subtle changes in gel swelling at the micro-scale using a simple optical microscope setup. This Chapter will describe the use of this microlensing methodology to visualize the modulation of gel swelling via protein-ligand interactions.

This construct represents a new method of visualizing protein assays wherein the gel substrate itself is also the transducer element.

The particular issue in developing a biological assay is not only achieving high selectivity to the target molecules but also simplicity in fabrication. An inexpensive assay technique that is generalizable to a wide range of different affinity pairs with high selectivity would increase the potential for the use of the technique in many applications such as protein assays, drug screening, chemical sensing, and the detection of genetic defects such as single nucleotide polymorphisms. Chapter 5 will show development of a new protein assay method by utilizing ligand functionalized hydrogels, which simultaneously associate with the protein of interest and report on the binding event. In particular, the technique described here is free from false signals due to non-specific binding and could be used for very complex mixtures by employing the inherent advantage of a displacement-type assay scheme.

5.2 Experimental Section

Materials

All reagents, materials, and water were purchased and/or prepared as previously described in the Chapter 2 unless otherwise specified. Dimethyl sulfoxide (DMSO) was obtained from J.T. Baker. 1-ethyl-3-(3-dimethylaminopropyl) carbodiimide (EDC) and biotin hydrazide were purchased from Pierce. Unlabled avidin and fluorescent avidin conjugate (texas red) were obtained from Molecular Probes. Polyclonal anti-avidin (raised in rabbit) and polyclonal anti-biotin (raised in goat) were purchased from Sigma-Aldrich.

Microgel Synthesis

The same batch of microgels was used throughout this investigation and was the exact same microgels used in the Chapter 2.

Microgel Biotinylation

1 mL of the synthesized microgel solution was cleaned *via* centrifugation to remove unreacted materials and was then resuspended in 2-[*N*-morpholino]ehtanesulfonic acid (MES) buffer pH 4.7. The microgel solution was then diluted 10-fold with the MES buffer to reduce the concentration of the particles. This diluted solution was used for biotinylation. Separately, 3.8 mg of biotin hydrazide was dissolved in 0.5 mL of DMSO and was added to the diluted microgel solution. The amount of biotin hydrazide used is 50 % of the total amount of acrylic acid in the microgel solution. 15 mg of EDC was added to the microgel and biotin solution to activate the coupling reaction.[41] The solution was stirred overnight at 4 °C. The unreacted biotin hydrazide was removed by several cycles of centrifugation and resuspension in pH 7.5 Phosphate buffered saline (PBS) buffer.

Hydrogel Microlens Substrate Preparation

Glass cover slips were cleaned in an Ar plasma (Harrick Scientific) and functionalized in an ethanolic (absolute ethanol) 1% APTMS solution as previously described in the Chapter 2. The substrate was then exposed to an aqueous 10% (v/v dilution of initial concentration following synthesis) microgel solution at pH 6.5 (~0.001 M ionic strength) for 5 min. The substrate was subsequently rinsed with DI water and dried with nitrogen gas, and then exposed to a biotinylated microgel solution buffered by 10 mM PBS buffer pH 7.5. After 5 min, the substrate was immersed in DI water for 2 hrs,

rinsed with DI water, and dried with nitrogen gas to leave behind microgels that are strongly attached to the substrate by Coulombic interactions. For microscopic investigations of microlens response to protein binding, 150 μL of various avidin, biotin, anti-avidin, and anti-biotin solutions buffered in 10 mM PBS were introduced into the void space of a microlens array/silicone gasket/coverslip sandwich assembly.

Scheme 5-1. Inverted light microscopy setup used for bioresponsive hydrogel microlens imaging experiments.

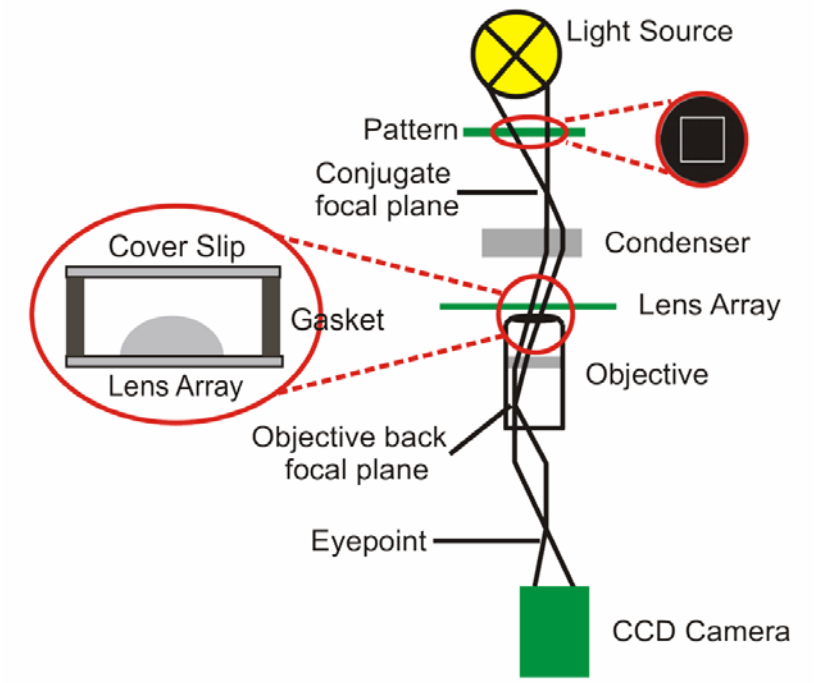

Microscopy

Brightfield and fluorescence optical microscopies were used to observe the hydrogel microlenses. Brightfield transmission and differential interference contrast (DIC) optical microscopies were used to study the changes in the optical properties of the hydrogel microlens attached to the substrate, while epi-fluorescence microscopy was used to visualize the binding of fluorescently labeled proteins to the fluorescently labeled microlenses. An Olympus IX70 inverted microscope equipped with a high numerical aperture, oil immersion 100X objective (NA=1.30) was used for all microscopies reported here. Images were captured using either a black/white or a color CCD camera (PixelFly, Cooke Corporation).

5.3 Results and Discussion

The main strategy in this work is to utilize the biotinylated pNIPAm-*co*-AAc hydrogel microparticles as both the protein recognizing and transducing material (Scheme 5-2). In this strategy, a portion (~50%) of the acid groups of the microgels are conjugated to the biotin ligand *via* EDC coupling. These biotinylated microgels then interact with multivalent proteins (avidin and anti-biotin), which form additional cross-links between polymer chains in the network. Such a cross-linking event results in the change in the equilibrium swelling volume of the microgel and hence an increase in the local refractive index (RI) of the microgel. Chapters 3 and 4 have shown that the optical properties of the hydrogel microlenses are dependent on the refractive index (RI) contrast between the hydrogel and the surrounding medium.[26,38] Also, microlenses formed from

pH and temperature responsive gels are able to project images of different fidelities in response to pH and temperature changes, respectively.

Scheme 5-2. Conceptual representation of the hydrogel microlens assay. (a) pNIPAm-co-AAc hydrogel microparticles synthesized by aqueous free-radical precipitation polymerization method. (b) Biotinylation of pNIPAm-co-AAc hydrogel microparticles via EDC coupling. (c) Formation of cross-links in the hydrogels by multivalent binding of avidin to biotin on the hydrogel microlenses. (d) Cross-link formation in the hydrogel microlens by multivalent binding of anti-biotin to biotin on the hydrogel microlenses.

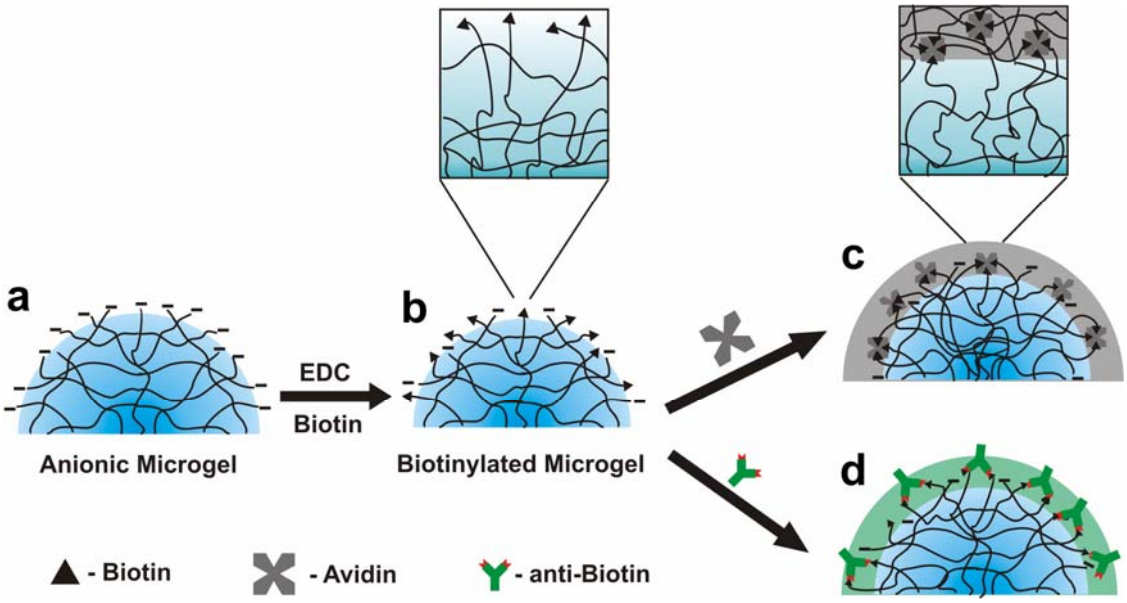

To investigate the potential utility of hydrogel microlenses in this protein assay system, we prepared substrates containing a random, binary distribution of microlenses, where both pNIPAm-*co*-AAc microlenses and biotinylated pNIPAm-*co*-AAc microlenses are present in approximately equal number densities. Under the deposition conditions used, a sub-monolayer coverage of microlenses is obtained, which allows for imaging of individual microlens optical properties without interference from adjacent particles. Both modified and unmodified microlenses were used to prepare these samples such that the unmodified microlens can act as an internal control and reference state. The microlenses were then exposed to various concentrations of avidin solutions by introduction of 150 μL the proper solution into the void space of a microlens array/silicone gasket/coverslip sandwich assembly. The effects of avidin concentration on the optical properties of the microlenses are shown in Figure 5-1. It is interesting to note that only the biotinylated hydrogel microlenses (left elements in each panel) show a difference in appearance in the differential interference contrast (DIC)[42] images as the avidin concentration is increased, with the most marked difference being the formation of the dark circle at the particle periphery (Figure 5-1(a)). The non-biotinylated microlenses (right elements in each panel) do not show any apparent change at different concentrations of avidin. In Figure 5-1(b), the biotinylated microlenses exhibit a large change in image formation (white square) at 100 nM avidin (equivalent to 15 pmoles of protein), while the non-biotinylated hydrogel microlenses show a weak, poorly focused image over the entire range of the avidin concentrations. The change in lens projection observed for the biotinylated lenses appears to be the formation of a double image, where the periphery of the particle appears bright, while a small, more tightly focused square appears at the center of the microlens.

These phenomena are due to the local RI change of the biotinylated hydrogels caused by the formation of biotin-avidin networking on the surface at a critical avidin concentration. The higher RI decreases the effective focal length of the microlens, hence creating a smaller, more tightly focused image of the white square pattern. It may also be the case that the higher refractive index at the microlens surface causes an increase in light scattering, which may be the origin of the bright appearance of the particle periphery. Regardless of the detailed origins of the image formation, it is clear that the ligand-modified lenses are sensitive to protein binding, and directly report on that binding through a change in both microlens appearance (Figure 5-1(a)) and microlens performance (Figure 5-1(b)). Also, note that the biotinylated hydrogel microlenses have very different optical properties (focal lengths) than the non-biotinylated microlenses before introduction of the protein (e.g. in PBS only). This arises from the decrease in the number of acidic sites in the biotinylated microgels, which decreases the equilibrium swelling volume and hence increases the RI of the microlens.

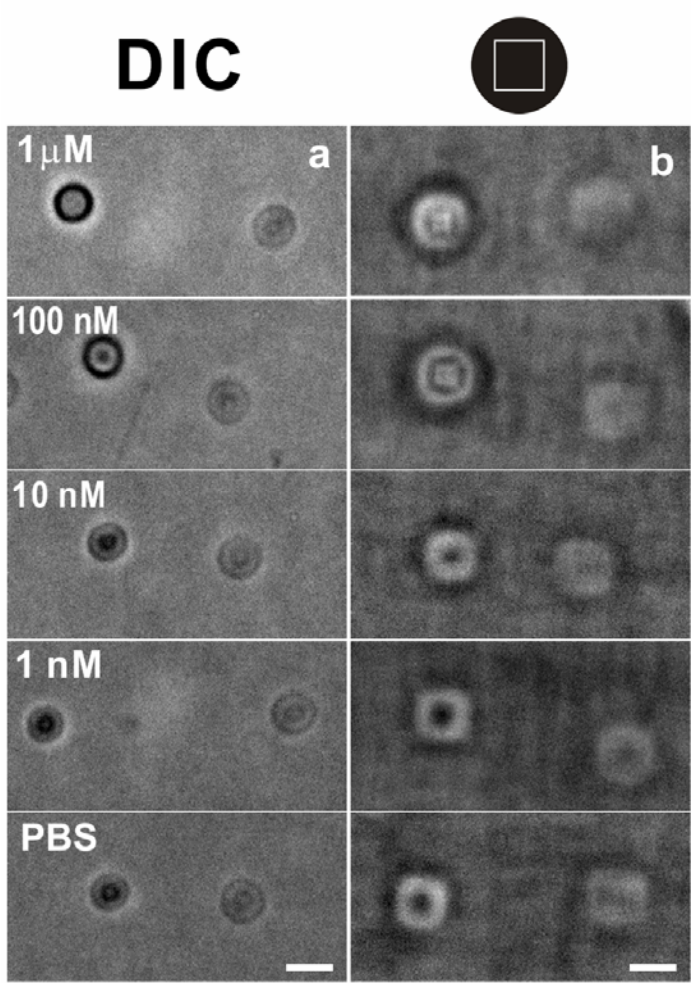

Figure 5-1. Dependence of microlens swelling in 10 mM PBS buffer solution as a function of avidin concentration at room temperature. (a) DIC microscopy images of a substrate bound pNIPAm-co-AAc hydrogels (right element in each panel) and biotinylated pNIPAm-co-AAc hydrogels (left element in each panel) at the indicated avidin concentrations. (b) Projection of the single square pattern (top right) through the hydrogel microlenses under the same conditions as described for column a. As the avidin concentration increases, only the biotinylated hydrogel microlenses form dark circles in DIC images (a) and show modulation of the square images in projection mode (b). Note that a 150 μL of each solution was used for this experiment (100 nM is equivalent to 15 pmoles of avidin). The scale bar is 2 μm.

In designing any affinity-based assay system, mediation of non-specific adsorption and enhancement of selectivity are two of the key figures of merit. Thus, fluorescence microscopy was used to investigate specific biotin-avidin binding to the hydrogel microlenses (Figure 5-2(a) and (b)). Note that the avidin and hydrogels are labeled by fluorescent chromophores with red (texas red) and green (fluorescein) emission spectra, respectively. The appearance of the red fluorescence at the periphery of the left element in panel (a) confirms that the avidin only binds to the surface of the biotinylated hydrogel microlens. Interestingly, there is no discernable non-specific adsorption to the non-biotinylated hydrogel microlens at the same solution avidin concentration (right element in panel (a)). Non-biotinylated microlenses also do not show any non-specific adsorption when they are present alone on the substrate (data not shown). This observance in wider view area is also shown in Figure 5-3. Note that in PBS buffer, both microlenses display only green fluorescence due to fluorescein, although the biotinylated microlens appears to have weaker fluorescence intensity than that of the non-biotinylated one. This may be due to a difference in the photobleaching rate between the two particles, or it may be that biotin acts as a quencher when placed in close proximity to fluorescein. Finally, brightfield transmission microscopy was used to scrutinize the selectivity of these assay system by exposing the biotinylated microlenses to a solution of anti-avidin (panel (c, d)). The DIC images of the hydrogel microlenses are unchanged by the presence of anti-avidin at a solution concentration of 730 nM (equivalent to 110 pmoles) as compared to images acquired in PBS buffer solution.

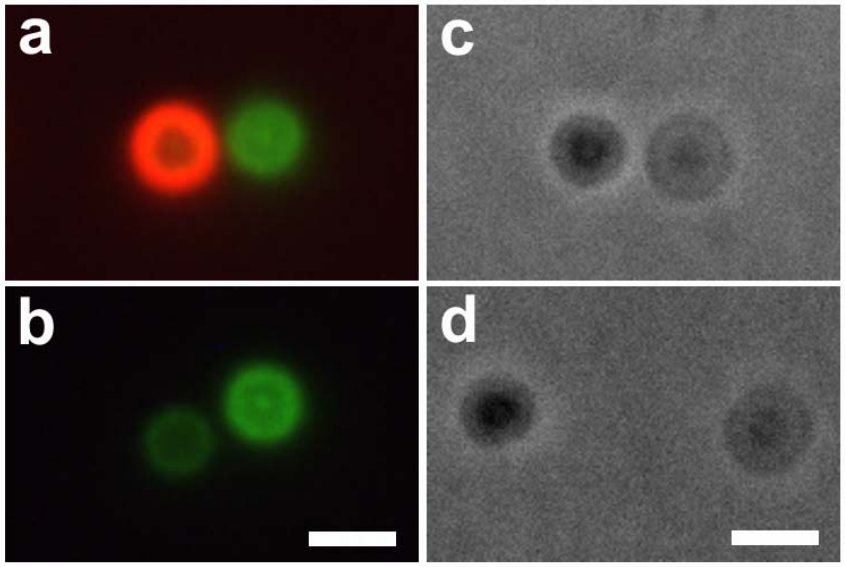

Figure 5-2. Fluorescence microscopy images of hydrogel microlenses in (a) 1 μM avidin in 10 mM PBS and (b) a 10 mM PBS buffer solution. Note that the microgel is labeled with 4-acrylamidofluorescein (green) and avidin (red) is conjugated with Texas red. Biotin-avidin binding is observed only on the biotinylated microgel (left element in each panel) and not on the non-biotinylated microgel (right element in each panel) at the tested avidin concentration. (c) DIC microscopy image of the bare microgels (right element in each panel) and the biotinylated microgels (left element in each panel) in 730 nM anti-avidin in 10 mM PBS and (d) 10 mM PBS buffer solution. There is no discernable change on DIC images due to the nonspecific adsorption of anti-avidin. Note that 150 μL of each solution was used for this experiment (1 μM is equivalent to 150 pmoles). The scale bar is 2 μm.

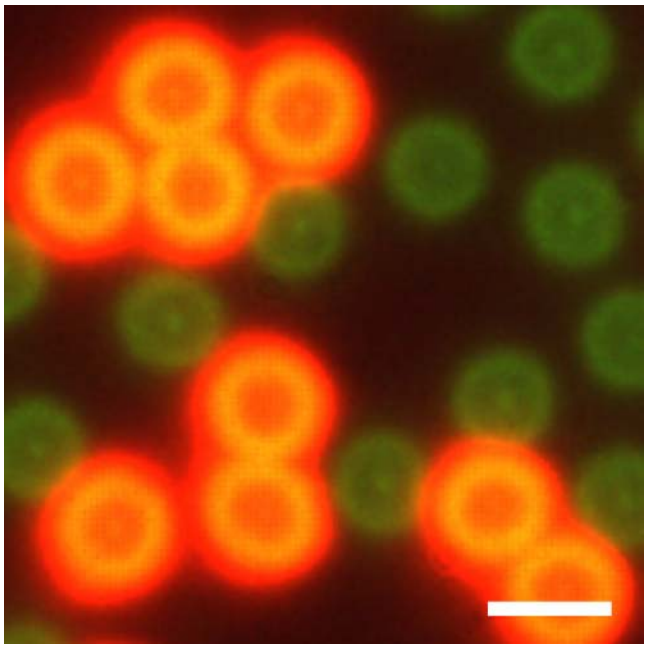

Figure 5-3. Wider view fluorescence microscopy images of hydrogel microlenses in 1 μM avidin in 10 mM PBS. Note that the microgel is labeled with 4-acrylamidofluorescein (green) and avidin (red) is conjugated with Texas red. Biotin-avidin binding is observed by the formation of red circles only on the biotinylated microgel and not on the non-biotinylated microgel at the tested avidin concentration. The scale bar is 2 μm.

As described above, we propose that the [avidin] dependent microlens response is caused by an increase in the network cross-link density, due to the ability of avidin to bind up to four equivalents of biotin. In order to prove the requirement of multivalent binding, we investigated the sensitivity of the microlens assay to avidin that had been equilibrated with different amounts of free biotin. Figure 5-4 shows the DIC (panels a, c) and lens projection (panels b, d) images of the hydrogel microlenses exposed to avidin solutions pre-equilibrated with 1 (panels a, b) or 2 (panels c, d) equivalents of biotin. Because of the extraordinarily low dissociation constant (and hence small dissociation rate constant) of the biotin:avidin pair (K_d~$10^{-13 \text{ to } -15}$) the free biotin is not expected to exchange with the hydrogel-bound biotin on the timescale of the experiments. Thus, this experiment allows for a measure of avidin-based cross-linking as a function of the number of free binding sites. Comparing the data in Figure 5-4 with that in Figure 5-1, where free avidin is used, suggests that the hydrogel microlens is less sensitive to avidin that has been pre-equilibrated with biotin than free avidin. In the case of 1:1 biotin:avidin, the microlens is observed to "turn on" at ~200 nM (30 pmoles of avidin), while for 2:1 biotin:avidin, the lens is not switched until ~600 nM (90 pmoles of avidin). This behavior can be reasonably understood by the fact that the free avidin statistically will have more opportunities to form cross-links than avidin with partially occupied binding sites.

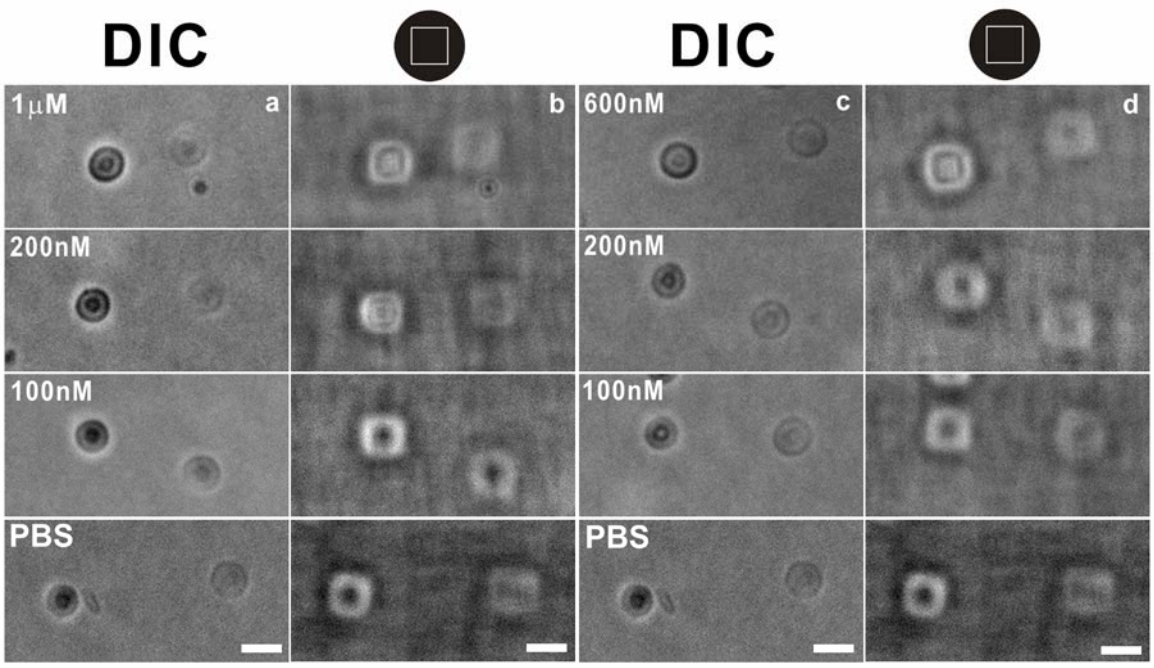

Figure 5-4. Sensitivity of the hydrogel microlens assay to the number of the active binding sites on avidin. The different number of the active sites were prepared by equilibrating avidin with different stoichiometric ratios of biotin. (a) DIC images of the hydrogel microlenses exposed to 1:1 biotin:avidin solutions in 10 mM PBS buffer as a function of total avidin concentration. (b) Projection of the single square pattern (top) through the hydrogel microlenses under the same conditions as described for column (a). (c) DIC images of the hydrogel microlenses exposed to 2:1 biotin:avidin solutions in 10 mM PBS buffer as a function of total avidin concentration. (d) Projection of the single square pattern (top) through the hydrogel microlenses under the same conditions as described for column (c). Note that 150 μL of each solution was used for this experiment (100 nM is equivalent to 15 pmoles). The scale bar is 2 μm.

To eliminate the possibility that the focal length change is caused by monovalent binding and/or nonspecific binding of avidin, we exposed microlens arrays to solutions of avidin pre-equilibrated with 3 (monovalent avidin) and 5 (excess biotin) equivalents of biotin (Figure 5-5). Under these conditions, we observe no discernable change in lens focal length due to the statistical improbability of protein-based cross-linking under conditions where one or fewer binding sites are available on the protein.

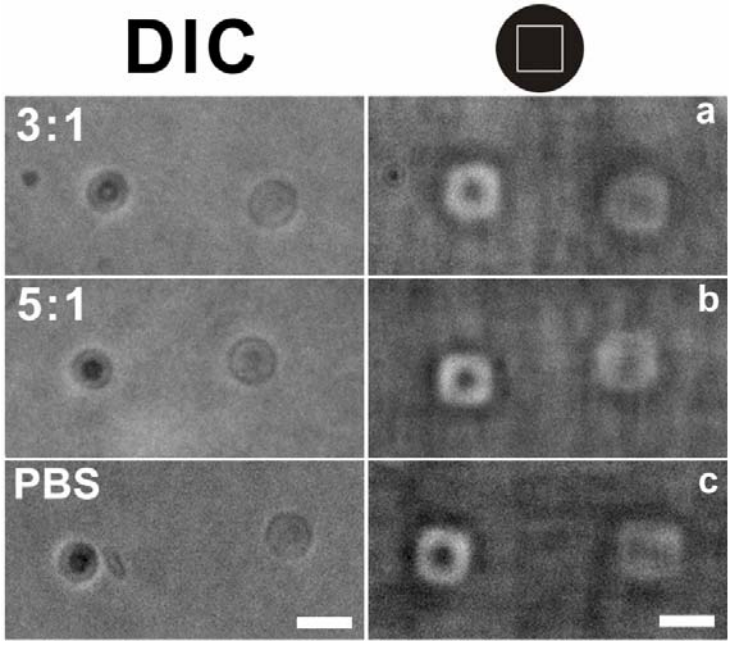

Figure 5-5. Effects of the monovalent binding and the nonspecific adsorption. (Left column) DIC images of the hydrogel microlenses and (Right column) projected square pattern images through the hydrogel microlenses in 1 μM of biotin-equilibrated avidin solutions with the ratio of (a) 3:1, (b) 5:1 biotin:avidin, and (c) 10 mM PBS buffer. The bare microgels (right element in each panel) and the biotylated microgels (left element in each panel) are unchanged under these conditions. Note that 150 μL of each solution was used for this experiment (100 nM is equivalent to 15 pmoles). The scale bar is 2 μm.

To evaluate the generality of the assay for protein detection, we investigated a weaker binding protein-ligand interaction. In this case, a polyclonal antiserum (IgG fraction) raised in goat against biotin was used as the cross-linking protein. Note that an IgG is different from avidin in a number of ways. It has a higher molecular weight (~150 kDa vs. ~66 kDa for avidin), it has only 2 binding sites (paratopes) for biotin, and it is expected to have a much higher dissociation constant than avidin. Typical effective (ensemble) dissociation constants for polyclonal antisera are on the order of $K_d \sim 10^{-9}$ M. Figures 5-6 (a) and (b) show the DIC images and the projected pattern images as a function of anti-biotin concentration, respectively. The hydrogel microlens assay displays a focal length change at a concentration above 367 nM (equivalent to 55 pmoles), with the general microlens appearance being very similar to that observed for avidin binding. If one compares Figures 5-4 (c) and (d) with Figures 5-6 (a) and (b) where the effective number of binding sites to biotin is same but the K_d values are different, we find that the microlens assay is more sensitive to anti-biotin than it is to avidin, despite avidin's lower K_d value. While it is possible that this arises from the higher molecular weight of the IgG, it is also reasonable to consider the larger distance between binding sites in the IgG. It may be the case that the IgG is statistically a better cross-linker simply because it can access more biotins than the smaller avidin. Also, it should be pointed out that the anti-biotin assay is less sensitive than the avidin assay in Figures 5-4 (a) and (b), where the avidin has three active binding sites. Thus, the sensitivity of the cross-linking assay will be due to the protein:ligand affinity, the number of ligand binding sites, and the distance between binding sites on the protein.

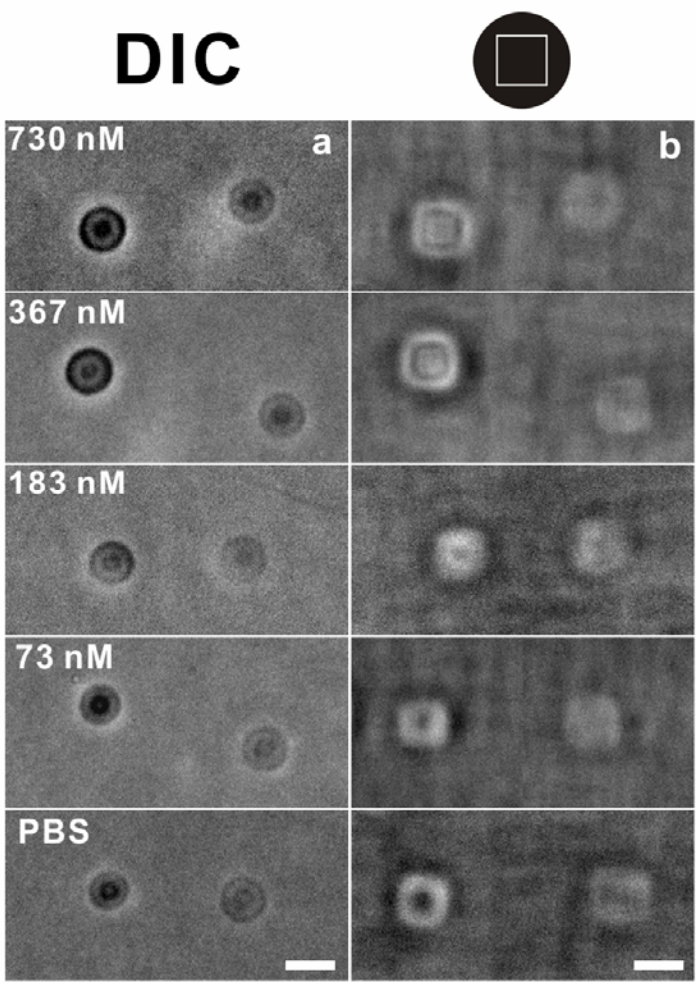

Figure 5-6. Influence of polyclonal anti-biotin on the hydrogel microlenses in 10 mM PBS buffer solution as a function of anti-biotin concentration at room temperature. a) DIC microscopy images of bare microgels (right element in each panel) and biotylated microgels (left element in each panel) at the indicated anti-biotin concentrations. b) Projection of the single square pattern (top right) through the hydrogel microlenses under the same conditions as described for column a. As the anti-biotin concentration increases, only the biotinylated hydrogel microlenses form dark circles in DIC images (a) and tightly focused square images in projection mode (b). Note that 150 μL of each solution was used for this experiment (367 nM is equivalent to 55 pmoles). The scale bar is 2 μm.

The reversibility of the hydrogel microlens assay is shown in Figure 5-7. The hydrogel microlenses were stepwise exposed to PBS buffer (Row (a)), polyclonal anti-biotin solution (Row (b)), and biotin solution (Row (c, d)). As shown, when the antibody-bound microlenses are exposed to a solution of the free ligand, the focal length of the microlens reverts back to its original state, suggesting that the protein-based cross-links have been disrupted. This result suggests that this construct could potentially be used in a displacement-type assay. For example, each microlens could contain both a tethered protein and a tethered ligand, where association between the two results in a cross-linking point and hence a decrease in focal length. However, upon exposure to the free ligand or protein (depending on what is to be assayed), these cross-links would be disrupted, thereby increasing the lens focal length, which can be visualized on a simple optical microscope. A displacement assay of this type would have the advantage of being reversible, since the displaced moiety would remain tethered to the microlens. Following washing, the protein:ligand cross-link would be re-formed, thereby resetting the microlens in the "on" state. Furthermore, if one were able to tune either the dissociation constant of the tethered protein:ligand pair, or the critical number of cross-links required for microlens modulation, the sensitivity of the assay to the solution concentration of analyte could be tuned to a level appropriate for a particular application.

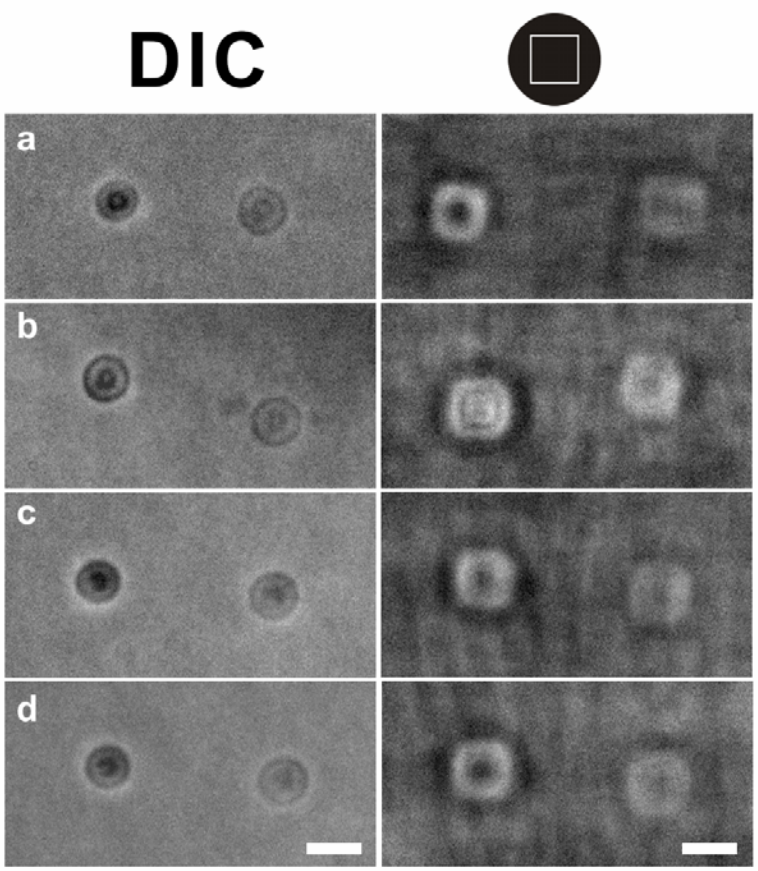

Figure 5-7. Reversibility of the hydrogel microlens assay. (Left column) DIC images of the hydrogel microlenses and (Right column) projected square pattern images through the hydrogel microlenses. The hydrogel microlenses were stepwise exposed to 10 mM PBS buffer (Row (a)), 667 nM polyclonal anti-biotin solution (Row (b)), and 1 mM free biotin solution (Row (c) after 3 hrs and, (d) after 22 hrs). The bare microgels are the right elements in each panel and biotinylated microgels are left elements in each panel. Note that 150 μL of each solution was used for this experiment (667 nM is equivalent to 100 pmoles). The scale bar is 2 μm.

5.4 Conclusions

This chapter has demonstrated that biotin-functionalized hydrogel microlenses can be used to assay avidin and polyclonal anti-biotin using a brightfield optical microscopy technique.[*] The hydrogel microlens assay can be easily constructed in inexpensive, simple, and rapid fashion, with high selectivity. The unique characteristics of the assay technology include the ability to determine the presence of an expected protein by monitoring the focal length of the microlens without the need for covalent tagging of the protein of interest. Furthermore, these microlenses could individually represent pixels in a biochip-type format, where such a chip could be read-out by simple optical microscopy coupled with image recognition software, again in a label-free format. These fundamental advantages make this new technique attractive for the future development of a displacement type protein assay where "on" and "off" signals are sufficient for primary affinity screening. However, it should be noted that the present materials platform represents a non-optimized format for biological sensing, as the polymers used here may be sensitive to changes in ionic strength in the physiological range and will be sensitive to changes in ambient temperature. Thus, this chapter has demonstrated the first steps towards practically applicable bioresponsive materials, with further optimization required before true applications result.

[*] We thank Prof. J. Fourkas (University of Maryland) for helpful discussions during the course of this work.

5.5 References

(1) Lutolf, M. P.; Lauer-Fields, J. L.; Schmoekel, H. G.; Metters, A. T.; Weber, F. E.; Fields, G. B.; Hubbell, J. A., Synthetic matrix metalloproteinase-sensitive hydrogels for the conduction of tissue regeneration: Engineering cell-invasion characteristics. *Proc. Natl. Acad. Sci. USA* **2003**, *100*, 5413-5418.

(2) Shimoboji, T.; Larenas, E.; Fowler, T.; Kulkarni, S.; Hoffman, A. S.; Stayton, P. S., Photoresponsive polymer-enzyme switches. *Proc. Natl. Acad. Sci. USA* **2002**, *99*, 16592-16596.

(3) Hu, Z.; Chen, Y.; Wang, C.; Zheng, Y.; Li, Y., Polymer gels with engineered environmentally responsive surface patterns. *Nature* **1998**, *393*, 149-152.

(4) Holtz, J. H.; Asher, S. A., Polymerized colloidal crystal hydrogel films as intelligent chemical sensing materials. *Nature* **1997**, *389*, 829-832.

(5) Liu, L.; Li, P.; Asher, S. A., Entropic trapping of macromolecules by mesoscopic periodic voids in a polymer hydrogel. *Nature* **1999**, *397*, 141-144.

(6) Langer, R.; Tirrell, D. A., Designing materials for biology and medicine. *Nature* **2004**, *428*, 487-492.

(7) Kim, J.; Singh, N.; Lyon, L. A., Label-free biosensing with hydrogel microlenses. *Angew. Chem. Intl. Ed.* **2006**, *45*, 1446-1449.

(8) Miyata, T.; Jige, M.; Nakaminami, T.; Uragami, T., Tumor marker-responsive behavior of gels prepared by biomolecular imprinting. *Proc. Natl. Acad. Sci. USA* **2006**, *103*, 1190-1193.

(9) Plunkett, K. N.; Berkowski, K. L.; Moore, J. S., Chymotrypsin Responsive Hydrogel: Application of a Disulfide Exchange Protocol for the Preparation of Methacrylamide Containing Peptides. *Biomacromolecules* **2005**, *6*, 632-637.

(10) Dong, L.; Agarwal Abhishek, K.; Beebe David, J.; Jiang, H., Adaptive liquid microlenses activated by stimuli-responsive hydrogels. *Nature* **2006**, *442*, 551-554.

(11) Serpe, M. J.; Yarmey, K. A.; Nolan, C. M.; Lyon, L. A., Doxorubicin Uptake and Release from Microgel Thin Films. *Biomacromolecules* **2005**, *6*, 408-413.

(12) Atencia, J.; Beebe, D. J., Controlled microfluidic interfaces. *Nature* **2005**, *437*, 648-655.

(13) Nayak, S.; Lyon, L. A., Soft nanotechnology with soft nanoparticles. *Angew. Chem. Intl. Ed.* **2005**, *44*, 7686-7708.

(14) Pelton, R., Temperature-sensitive aqueous microgels. *Adv. Colloid. Interface Sci.* **2000**, *85*, 1-33.

(15) Tanaka, T.; Fillmore, D. J., Kinetics of Swelling of Gels. *J. Chem. Phys.* **1979**, *70*, 1214 - 1218.

(16) Dusek, K.; Patterson, K., Transition on swollen polymer networks induced by intramolecular condensation. *Journal of Polymer Science, Polymer Physics Edition* **1968**, *6*, 1209-16.

(17) Heskins, M.; Guillet, J. E., Solution properties of poly(N-isopropylacrylamide). *J. Macromol. Sci. Chem.* **1968**, *A2*, 1441-1455.

(18) Arotcarena, M.; Heise, B.; Ishaya, S.; Laschewsky, A., Switching the inside and the outside of aggregates of water-soluble block copolymers with double thermoresponsivity. *J. Am. Chem. Soc.* **2002**, *124*, 3787-3793.

(19) Gan, D.; Lyon, L. A., Tunable Swelling Kinetics in Core-Shell Hydrogel Nanoparticles. *J. Am. Chem. Soc.* **2001**, *123*, 7511-7517.

(20) Nayak, S.; Lee, H.; Chmielewski, J.; Lyon, L. A., Folate-mediated cell targeting and cytotoxicity using thermoresponsive microgels. *J. Am. Chem. Soc.* **2004**, *126*, 10258-10259.

(21) Nayak, S.; Lyon, L. A., Photoinduced Phase Transitions in Poly(N-isopropylacrylamide) Microgels. *Chem. Mater.* **2004**, *16*, 2623-2627.

(22) Wang, C.; Flynn, N. T.; Langer, R., Controlled structure and properties of thermoresponsive nanoparticle-hydrogel composites. *Adv. Mater.* **2004**, *16*, 1074-1079.

(23) Wang, C.; Stewart, R. J.; Kopecek, J., Hybrid hydrogels assembled from synthetic polymers and coiled-coil protein domains. *Nature* **1999**, *397*, 417-420.

(24) Miyata, T.; Asami, N.; Uragami, T., A reversibly antigen-responsive hydrogel. *Nature* **1999**, *399*, 766-769.

(25) Tauro, J. R.; Gemeinhart, R. A., Matrix Metalloprotease Triggered Delivery of Cancer Chemotherapeutics from Hydrogel Matrixes. *Bioconjugate Chem.* **2005**, *16*, 1133-1139.

(26) Kim, J.; Serpe, M. J.; Lyon, L. A., Photoswitchable Microlens Arrays. *Angew. Chem. Intl. Ed.* **2005**, *44*, 1333-1336.

(27) Nayak, S.; Lyon, L. A., Ligand-functionalized core/shell microgels with permselective shells. *Angew. Chem. Intl. Ed.* **2004**, *43*, 6706-6709.

(28) Jones, C. D.; Serpe, M. J.; Schroeder, L.; Lyon, L. A., Microlens formation in microgel/gold colloid composite materials via photothermal patterning. *J. Am. Chem. Soc.* **2003**, *125*, 5292-5293.

(29) Nolan, C. M.; Serpe, M. J.; Lyon, L. A., Thermally modulated insulin release from microgel thin films. *Biomacromolecules* **2004**, *5*, 1940-1946.

(30) Kikuchi, A.; Okano, T., Pulsatile drug release control using hydrogels. *Adv. Drug Deliv. Rev.* **2002**, *54*, 53-77.

(31) Jeong, B.; Bae, Y. H.; Lee, D. S.; Kim, S. W., Biodegradable block copolymers as injectable drug-delivery systems. *Nature* **1997**, *388*, 860-862.

(32) Lutolf, M. P.; Raeber, G. P.; Zisch, A. H.; Tirelli, N.; Hubbell, J. A., Cell-responsive synthetic hydrogels. *Adv. Mater.* **2003**, *15*, 888-892.

(33) Suh, K. Y.; Langer, R.; Lahann, J., A novel photoderinable reactive polymer coating and its use for microfabrication of hydrogel elements. *Adv. Mater.* **2004**, *16*, 1401-1405.

(34) Yu, Q.; Bauer, J. M.; Moore, J. S.; Beebe, D. J., Responsive biomimetic hydrogel valve for microfluidics. *Appl. Phys. Lett.* **2001**, *78*, 2589-2591.

(35) Beebe, D. J.; Moore, J. S.; Bauer, J. M.; Yu, Q.; Liu, R. H.; Devadoss, C.; Jo, B.-H., Functional hydrogel structures for autonomous flow control inside microfluidic channels. *Nature* **2000**, *404*, 588-590.

(36) Arndt, K.-F. K., D.; Richter, A., *Polymers for Advanced Technologies* **2000**, *11*, 496-505.

(37) Eddington, D. T.; Beebe, D. J., Flow control with hydrogels. *Adv. Drug Deliv. Rev.* **2004**, *56*, 199-210.

(38) Kim, J.; Serpe, M. J.; Lyon, L. A., Hydrogel Microparticles as Dynamically Tunable Microlenses. *J. Am. Chem. Soc.* **2004**, *126*, 9512-9513.

(39) Yoshimura, I.; Miyahara, Y.; Kasagi, N.; Yamane, H.; Ojida, A.; Hamachi, I., Molecular recognition in a supramolecular hydrogel to afford a semi-wet sensor chip. *J. Am. Chem. Soc.* **2004**, *126*, 12204-12205.

(40) Lee, M.-C.; Kabilan, S.; Hussain, A.; Yang, X.; Blyth, J.; Lowe, C. R., Glucose-Sensitive Holographic Sensors for Monitoring Bacterial Growth. *Analytical Chemistry* **2004**, *76*, 5748-5755.

(41) Hermanson, G. T. *Bioconjugate Techniques*; Academic Press: San Diego, 1996.

(42) Murphy, D. B. *Fundamentals of Light Microscopy and Electronic Imaging*; Wiley-Liss: New York, 2001.

CHAPTER 6

LABEL-FREE BIOSENSING WITH HYDROGEL MICROLENSES

This chapter is divided into three main sections, all describing the use of bioresponsive hydrogel microlenses as a label-free biosensing scaffolding. The first section describes the design and application of multifunctional hydrogel microlenses to the problem of label-free biosensing and bioanalysis. These microstructures simultaneously act as the biosensor's scaffolding/immobilization architecture, transducer, amplifier, and also allow for broad tunability of the analyte concentration to which the microlens is sensitive. The second section describes investigations of the response rates of bioresponsive hydrogel microlenses in order to gain a deeper understanding of their potential utility as a new label-free biosensing construct. The response rates of the hydrogel microlenses are strongly coupled to analyte concentrations at a equilibrium number of antigen:antibody binding on the hydrogel microlenses. The third section describes studies of specific and nonspecific adsorption effects on bioresponsive hydrogel microlenses in order to better understand the utility and potential advantages of this bioresponsive material. The technique described here does not suffer from false signals by nonspecific adsorption, mainly due to the fact that the microlensing is predominantly modulated by cross-linking formation/deformation of antibody:antigen (and/or protein:ligand) binding rather than by simple protein adsorption.

6.1 Introduction

Recent efforts in the field of bioresponsive materials have focused on the design of novel structures that intelligently respond to biological stimuli.[1-29] In this paradigm, Chapter 5 has shown bioresponsive hydrogel microlenses in which specific protein binding events were monitored as changes in the microlens focal length via brightfield optical microscopy.[2] In that study, we observed that the microlens focal length could be tuned by multivalent protein binding, where the protein:ligand association formed a cross-link in the hydrogel network. In this chapter, we take advantage of that fundamental observation by coupling an antigen:antibody pair directly to the microlens, thereby providing for a *reversibly* switchable cross-link on the microlens. This forms the basis of a new biosensing construct that is reversible, and simultaneously acts as the biosensor scaffolding/immobilization architecture, transducer, and amplifier, while providing for broad *tunability* of the analyte concentration to which the microlens is sensitive. Furthermore, this construct is exceedingly resistant to spurious signals due to non-specific binding, since the microlens bioresponsivity is dependent on the *reversible displacement* of protein:ligand interactions.

To achieve these goals, we fabricated hydrogel microparticles (>1 micron in diameter) composed of poly(*N*-isopropylacrylamide-*co*-acrylic acid) (pNIPAm-*co*-AAc) via aqueous free-radical precipitation polymerization. Previous Chapters demonstrated that similar particles can be used to create self-assembled arrays of hydrogel microlenses on solid supports.[2,30-32] To render the microgels antibody reactive, a portion of the AAc groups are used to couple an antigen (biotin, as H_2N-Biotin) and aminobenzophenone (ABP) via EDC and DCC coupling, respectively.[33] Functionalization by ABP allows for

photo-tethering of anti-biotin after it is associated to the microlens via native antibody:antigen association. The biotin/ABP-functionalized microgels are then Coulombically assembled onto a 3-aminopropyltrimethoxysilane (APTMS)-functionalized glass substrate to form supported microlenses. Bioresponsive microlenses are then prepared by exposure to a buffered solution of polyclonal anti-biotin, which binds to the microlenses via antibody:antigen interactions. Photoligation of the surface-tethered ABP to the antigen-bound antibody is accomplished via UV irradiation. Thus, the microlens surface is decorated with multiple antibody:antigen-based cross-links, which can then be disrupted by introduction of free antigen to the surrounding medium. Since the antibody is covalently tethered to the microlens surface, washing with antigen-free media results in re-assembly of the tethered antibody:antigen pairs, thereby providing for a reversible biosensing microlens. This approach is diagrammed in Scheme 6-1.

Scheme 6-1. The general strategy for label-free biosensing using bioresponsive hydrogel microlenses. (a) pNIPAm-*co*-AAc hydrogel microparticles assembled as microlenses on a glass substrate. (b) Conjugation of biotin and ABP to the microlenses. (c) Assembly of antibodies followed by photoligation. (d) Reversible displacement of the antibody:antigen cross-link with antigen.

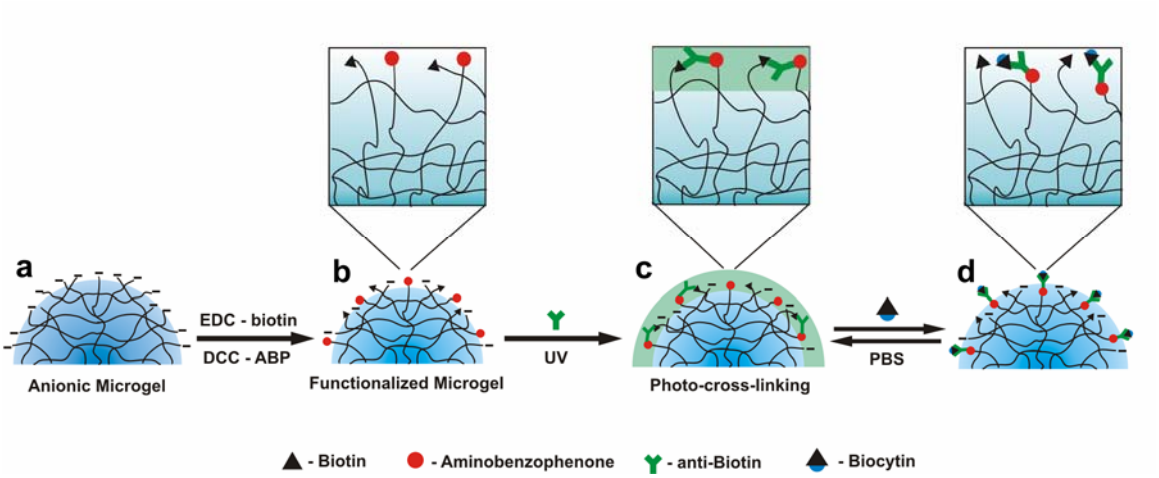

6.2 Experimental Section

Materials

All reagents, materials, and water were purchased and/or prepared as previously described in the Chapter 2 unless otherwise specified. 1-ethyl-3-(3-dimethylaminopropyl) carbodiimide (EDC) and biotin hydrazide were purchased from Pierce. Dimethyl sulfoxide (DMSO) was obtained from J.T. Baker. Polyclonal anti-avidin (raised in rabbit)

and polyclonal anti-biotin (raised in goat) were purchased from Sigma-Aldrich. Labled anti-goat IgG (Alexa Fluor 594, raised in rabbit) was obtained from Molecular Probes.

Microgel Synthesis

The same batch of microgels was used throughout this investigation and was the exact same microgels used in the Chapter 2.

Microgel Functionalization

The anionic microgel was functionalized with biotin and 4-aminobenzophenone by 1-ethyl-3-(3-dimethylaminopropyl) carbodiimide (EDC) and dicyclohexylcarbodiimide (DCC) coupling reactions respectively.[33] The functionalization was planned by assuming the consumption of 50% of the carboxyl groups on the particles by biotin and other 50% by 4-aminobenzophenone (ABP). Since the reaction efficiency of the coupling is <100 %, some portion of AAc groups are expected to remain available for binding to the cationic glass substrate.

First, the biotinylation of 10-fold 2-[*N*-morpholino]ehtanesulfonic acid (MES) (pH 4.7) diluted anionic microgel (1 mL) was done by adding biotin hydrazide (3.8 mg dissolved in 0.5 mL of dimethyl sulfoxide (DMSO), 50 % of the total amount of acrylic acid in the microgel solution) to the dilute microgel solution. EDC (15 mg) was added to the microgel and biotin solution to activate the coupling reaction. The solution was stirred overnight at 4 °C and the unreacted biotin hydrazide was removed by several cycles of centrifugation followed by resuspension in phosphate buffered saline (PBS) (pH 7.5).

For the modification of the biotinylated pNIPAm-AAc particles with aminobenzophenone (ABP), the microgel particle solution (1 mL) was centrifuged 5 times and the resulting white pellet was redispersed in 700 μL DMSO. To this was added

150 μL each of 0.01 M ABP and 0.01 M DCC solution in DMSO. The reaction solution was stirred overnight at room temperature in the dark, following which 0.5 mL de-ionized water was added. The white solid precipitate of *N,N'*-dicyclohexylurea thus formed was filtered off. The resultant filtrate was centrifuged at 14000 RPM for 15 minutes and the pellet was redispersed in DMSO followed by four additional centrifugation cycles and redispersion in PBS buffer (pH 7.5). Note that the synthetic scheme employs an equal stoichiometric amount of biotin and ABP for coupling with the carboxyl groups. Also the reaction efficiency of the carbodiimide coupling is <100 %, hence the unreacted carboxyl groups can be further used for binding to the cationic glass substrate.

Reversibly Bioresponsive Hydrogel Microlens Substrate

To prepare bioresponsive hydrogel microlenses, Glass cover slips were cleaned in an Ar plasma (Harrick Scientific) and functionalized in an ethanolic (absolute ethanol) 1% APTMS solution as previously described in the Chapter 2. Two different microgel substrates were used to investigate the properties of the bioresponsive hydrogel microlens in this Chapter. Biotin-modified microgel assembly was formed by exposing the silane-modified substrate to a biotin-modified microgel solution in 10 mM PBS buffer (pH 7.5). After a 30 min exposure, the substrate was immersed in DI water for 2 hrs, rinsed with DI water, and dried with nitrogen gas to leave behind microgels that are strongly attached to the substrate by Coulombic interactions. The second type of substrate consists of the biotin/ABP modified microgels. Silane functionalized glass substrate was exposed to an aqueous biotin/ABP modified microgel solution buffered by 10 mM PBS buffer pH 7.5. After 30 min, the substrate was rinsed with DI water, and dried with N_2 gas to leave

behind microgels strongly attaching to the substrate. As an internal reference substance, non-functionalized microgels were also attached to the substrate in similar way.

After attachment of the microgels, a microlens array/silicone gasket/coverslip sandwich assembly was prepared. At this state, bioresponsive hydrogel microlens for direct protein binding study in section 6.4 is acquired. For reversible bioresponsive microlens studies in this Chapter, buffered solution of polyclonal anti-biotin was introduced into the void space for. After 3 hrs of incubation, the substrates were rinsed and the medium was replaced with PBS buffer pH 7.5. Photoligation of the microgel-tethered ABP to the antigen-bound antibody was accomplished via UV irradiation using a 100W longwave UV lamp for 30 min while cooling the coverslip on an ice bath. For microscopic investigations of microlens response to competitive protein binding, 150 μL of various biocytin, anti-avidin, and anti-goat IgG solutions buffered in 10 mM PBS were introduced into the void space of the assembly.

A microlens array/silicone gasket/coverslip sandwich assembly was prepared using the microgel functionalized glass slides in similar fashion as previously described in this chapter. The assembly is then incubated with a solution of polyclonal anti-biotin diluted with pH 7.5 PBS and irradiated using a 100W longwave UV lamp as previously described in this chapter For microscopic investigations as the microlenses response to competitive antigen:antibody binding, various concentrations (100 μL aliquots) of biotin, alexa fluor labeled avidin, IgG, biocytin and antibiotin buffered in 10 mM PBS were introduced into the void space of the assembly.

Microscopy

The bioresponsivity of hydrogel microlenses were monitored using brightfield and fluorescence optical microscopies as described in the Chapter 5. The details of image projection through microlenses via optical microscopy have been described in previous Chapters. The same microscope setup as shown in the Chapter 5 (Scheme 5-1) was used in the studies described in this Chapter.

6.3 Reversible Biosensing with Hydrogel Microlenses

This study demonstrates a label-free biosensor/bioassay technique based on bioresponsive hydrogel microlenses. The elasticity (or cross-link density) of the *outer surface* of a microgel is coupled to an antibody:antigen association-dissociation equilibrium. In the bound state, the degree of cross-linking at the microgel surface is increased, resulting in hydrogel deswelling at the surface. In the presence of soluble antigen, the bound antibody:antigen cross-link is disrupted, resulting in swelling at the microgel-solution interface. Reversible antibody:antigen cross-links at the microlens surface allow for microlens focal length tuning in response to soluble antigen without interference from non-specific adsorption. As the method is based on a displacement event in the context of gel swelling changes, the sensitivity can be tuned by controlling the number of cross-links required to elicit a specific swelling response.

6.3.1 Results and Discussion

The behavior of microlenses formed following incubation with different concentrations of polyclonal anti-biotin is shown in Figure 6-1 (a,b). Under these

conditions, microlenses not only show antibody concentration dependence in the differential interference contrast (DIC) images, with the formation of a dark circle at the particle periphery, but also show changes in the image projection through the microlenses. Above a critical antibody concentration, the lens is in the "on" configuration, while below that concentration the lens is "off". These optical effects are due to the local refractive index (RI) change of the hydrogel microlenses caused by the formation of biotin:anti-biotin based cross-links at the microlens surface. The critical anti-biotin concentration represents the point at which the number of cross-linking points is sufficient to cause the microgel periphery to deswell. Below that concentration, the elastic restoring force of the network exceeds the free energy change associated with multivalent antibody binding. In this fashion, the intrinsic binding affinity of the antibody:antigen pair is modulated by the negative entropy associated with gel restriction.

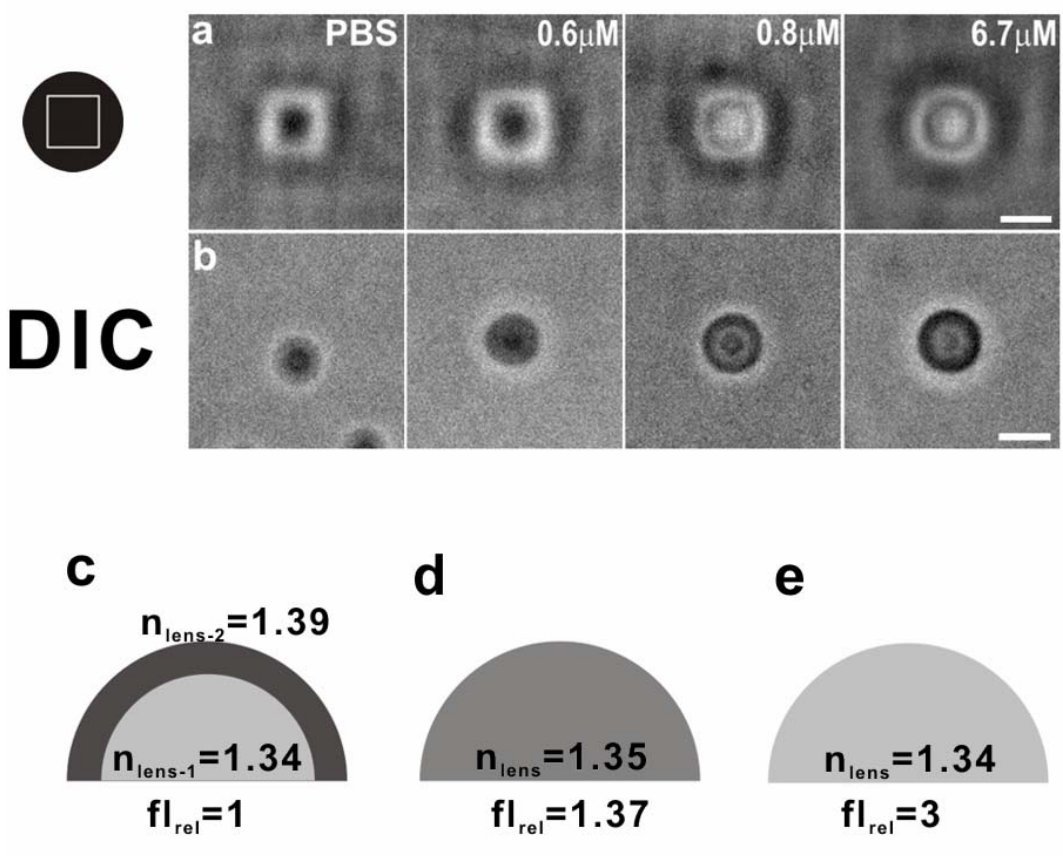

Figure 6-1. Influence of polyclonal anti-biotin concentration on lensing and the optical model of lens structure. (a) Projection of a square pattern (left) through a biotin/APB modified hydrogel microlens after photo-irradiation during incubation with the indicated anti-biotin concentrations. (b) DIC microscopy images taken under the same conditions as in (a). The scale bars are 2 μm. (c-e) Results of raytracing simulations of the relative microlens focusing powers: (c) a meniscus+plano-convex compound lens arising from the formation of antibody:antigen cross-links at the microgel periphery; (d) a simple plano-convex lens arising from uniform distribution of the two refractive indices in (c); and (e) a uniform plano-convex lens lacking antibody:antigen cross-links. The relevant refractive indices (*n*) and the relative focal lengths (fl_{rel}) are indicated. Note that the refractive index of medium is considered to be n=1.33.

To illustrate the effect of microlens surface deswelling on the overall optical properties, a series of 2-D optical raytracing simulations (Raytrace v.2.18) were performed in a medium with n=1.33 (refractive index of water). In the lens "on" state (Figure 1c), the microlens is modeled as meniscus + plano-convex compound lens with slightly higher refractive index at the periphery (n=1.39 vs. 1.34 in the bulk) due to a surface localized binding of biotin:anti-biotin. The simulations show that the compound lens structure produces a significantly shorter relative focal length (fl_{rel}=1.00) as compared to the unmodified hydrogel microlens modeled as a uniform plano-convex lens (n=1.34; fl_{rel}=3.00; Figure 6-1(e)). In the compound lens, we have somewhat arbitrarily assumed that antibody:antigen binding, and hence the RI increase, is limited to the outer 25% of the lens volume (~170 nm deep into the particle). It is clear that the dimensions of the dark circle at the particle periphery are at or below the diffraction limit for visible light imaging (~250 nm), so this is a reasonable initial guess. The Chapter 5 have also illustrated that avidin can diffuse into the periphery of microgels with a similar cross-linking density. In this figure, we also compare the surface localized binding case to a plano-convenx lens where the increase in the refractive index due to antibody:antigen binding is uniformly distributed over the entire optic (n=1.35; fl_{rel}=1.37; Figure 1d). In light of the simulation results, it is clear that by limiting the hydrogel responsivity to the particle periphery, one can potentially have a higher sensitivity to binding events due to a concomitant localization of the refractive index changes. Furthermore, these structures should display fast response times due to the short mass transport distance required to elicit an optical response.

The lens bioresponsivity is highly reversible, as shown in Figure 6-2. In this example, the biotin-ABP-functionalized hydrogel microlenses were incubated with a 6.7 μM solution (equivalent to 670 pmol) of polyclonal anti-biotin, followed by UV irradiation to covalently tether the antigen-associated antibodies to the microlens. The changes in the microlens-projected image were then monitored during exposure to 10 mM PBS (panels a, c, and e) and 1 mM biocytin (panels b, d, and f) solutions. Biocytin is a water-soluble analogue of biotin. The microlens is initially observed be in the "on" state in PBS buffer, which we characterize as the formation of a double square image in image projection mode and the dark circle at the particle periphery in DIC image. When the microlenses are then exposed to a solution of free biocytin, the microlenses are observed to switch to the "off" state, as characterized by a single square image (projection mode) and the disappearance of the black circle (DIC mode). This change in microlens focal length arises from disruption of the bound antibody:antigen pairs by competitive displacement with free antigens from solution. When the microlens is returned to an antigen-free buffer, the tethered antibody:antigen pairs re-assemble as the free antigens dissociate from the microlens. This response can then be cycled by repeated exposures to either antigen-containing or antigen-free buffer. These results indicate that (1) the microlens response is thermodynamically reversible, i.e., the initially photo-coupled state is a relatively low energy state and (2) the antibodies are indeed coupled to the microlens, as we would not expect reversibility if the first displacement interaction led to dissolution of antibody from the microlens surface.

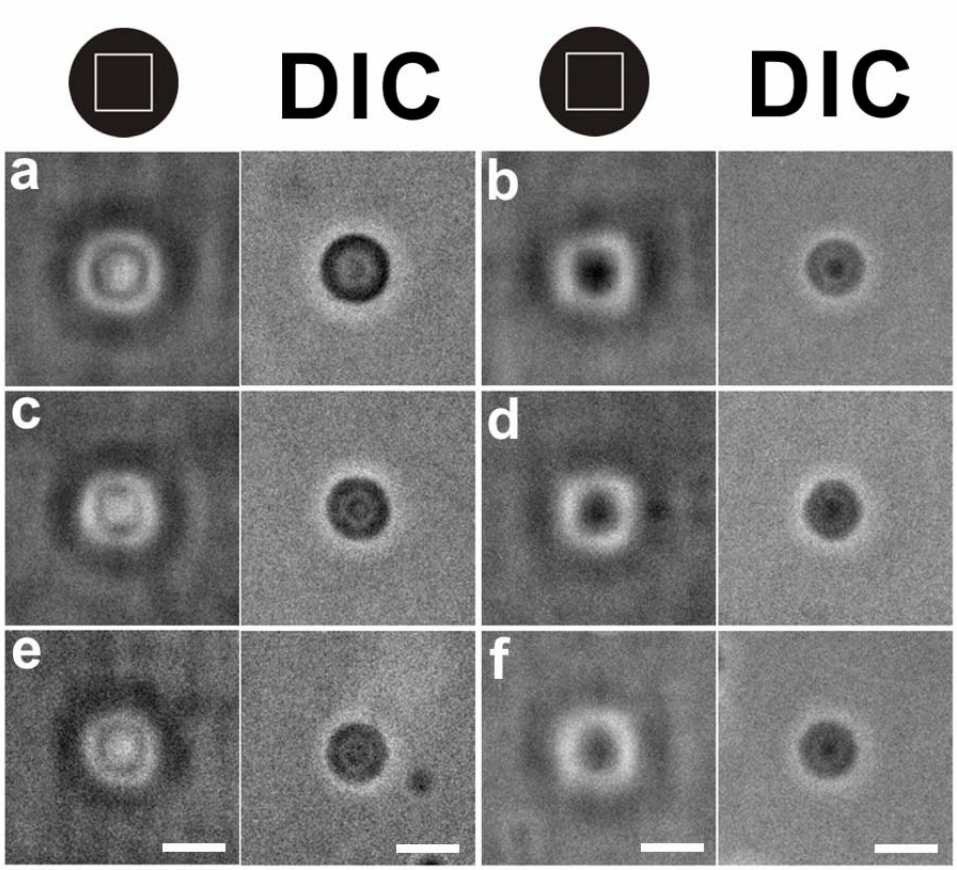

Figure 6-2. Reversibility of the bioresponsive microlenses. In each panel, the left image is the projection of the square pattern and the right image is the DIC image of the microlens. (a) Initial "on" state; (b) the lens turned "off" with 1 mM biocytin; (c, e) the lens reverts to the "on" state upon washing with PBS; (d, f) the same conditions as (b), which turns the lens "off". The scale bars are 2 μm.

It is also interesting to note that this displacement-based mode of action yields microlenses that are insensitive to non-specific binding, as well as secondary specific binding events. Figure 6-3a shows the DIC and image projection views of a single microlens in PBS. After introducing a solution of anti-avidin, which should not bind to the microlens via the tethered antibody or antigen, (Figure 6-3b) there is no discernable change in the microlens appearance or focal length. If the microlens is then exposed to anti-goat IgG (raised in rabbit), which should bind the tethered antibody (Figure 6-3c), but will do so by binding to non-paratope regions and will therefore not disrupt antibody:antigen interactions, we find again that the microlens is unperturbed. Fluorescence microscopy further reveals that the secondary antibody is indeed bound to the particle periphery.

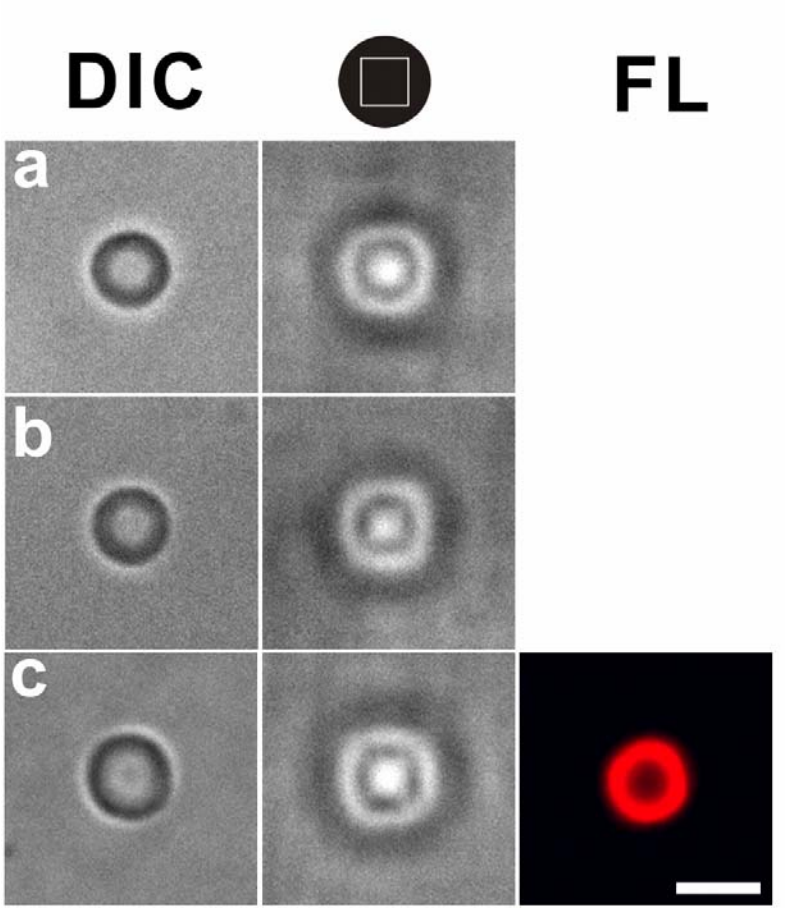

Figure 6-3. Effects of nonspecific adsorption on the optical properties of bioresponsive microlenses prepared with 1 μM anti-biotin: (left column) DIC image of the hydrogel microlens and (right column) projected square pattern images through the hydrogel microlens in: (a) 10 mM PBS buffer pH 7.5, (b) 5.5 μM anti-avidin and, (c) 5.5 μM rabbit anti-goat IgG conjugated with Alexa Fluor 594. The fluorescence microscopy image of hydrogel microlens (FL) is also shown in the extra panel. Note that 150 μL of each solution was used for this experiment. The scale bar is 2 μm.

In designing any sensor system, selectivity, sensitivity, and dynamic range are the key factors to realize a sensor for real world utilization. In the light of above results, one is able to prepare bioresponsive hydrogel microlenses, which have high specificity in a label-free format due to the use of a displacement/competitive binding scheme. However, the response is essentially a binary (on/off) one, which does not allow for quantitative analysis over a wide range of analyte concentrations. Therefore, it should be possible to tune the sensitivity of the microlenses by changing the number of antibody:antigen cross-links present on the microlens, an hence the number that must be displaced to induce a response. This can be trivially accomplished by changing the concentration of polyclonal anti-biotin used in the photo-cross-linking step to set initial lens "on" state. These data are shown in Figure 6-4. As expected, the minimum concentration of biocytin required to switch the microlens state is inversely dependent on the concentration of antibody used in the photo-cross-linking step. This can be understood by considering the thermodynamics of the system. In the tethered antibody:antigen system, the thermodynamics of hydrogel swelling are intimately coupled with those of the biological affinity pair. That is, the effective affinity of an individual binding pair must be reduced in the case where the gel is deswollen relative to its equilibrium state. Essentially, this is a state where the total free energies of antibody:antigen binding overcome the required reduction of network entropy required for deswelling. Thus, there should be a critical number of cross-linking points that result in observable hydrogel deswelling. If the hydrogel microlenses are prepared with excess binding pairs above that critical point, then the individual hydrogel microlenses will reswell only after a suitably large number of displacement events have occurred. However, if the number of cross-linking points is just slightly above this

critical point, only a few displacement events will result in gel swelling. Also, note that row (d) shows a lens incubated with 0.6 μM anti-biotin, which is insufficient to turn the lens "on", even in PBS that is lacking added biocytin. These results suggest that the digital nature of an individual microlens response can be overcome by creating microlens arrays where individual array elements possess differing analyte sensitivities.

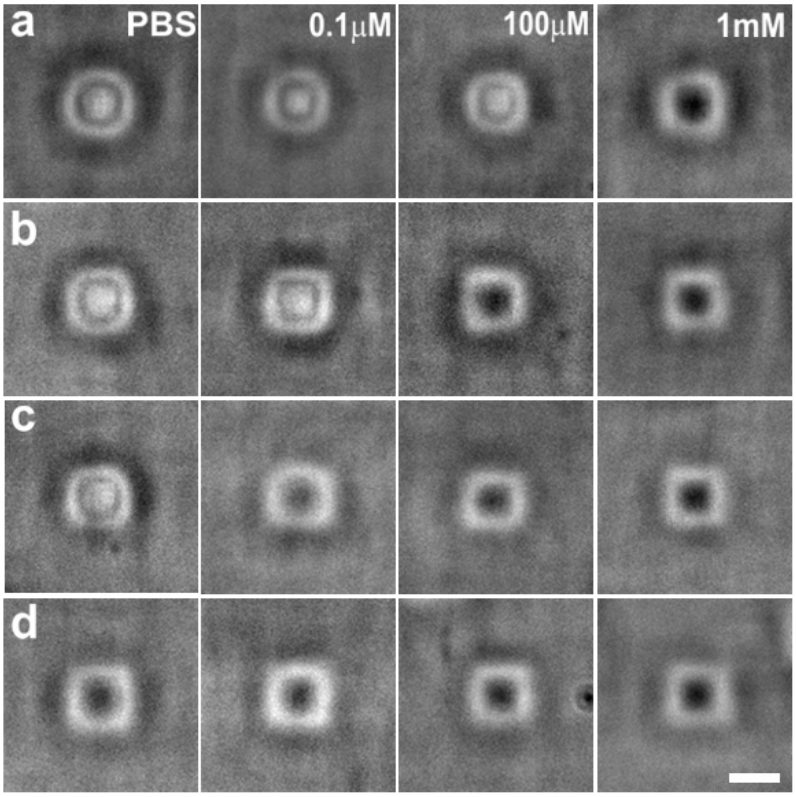

Figure 6-4. Tuning the microlens sensitivity. (Row a) Projection of the square pattern through a microlens incubated with 6.7 μM anti-biotin before photo-cross-linking. The biocytin concentrations are indicated at the top of each column. Incubation with: (row b) 2 μM anti-biotin, (row c) 1 μM anti-biotin, and (row d) 0.6 μM anti-biotin.

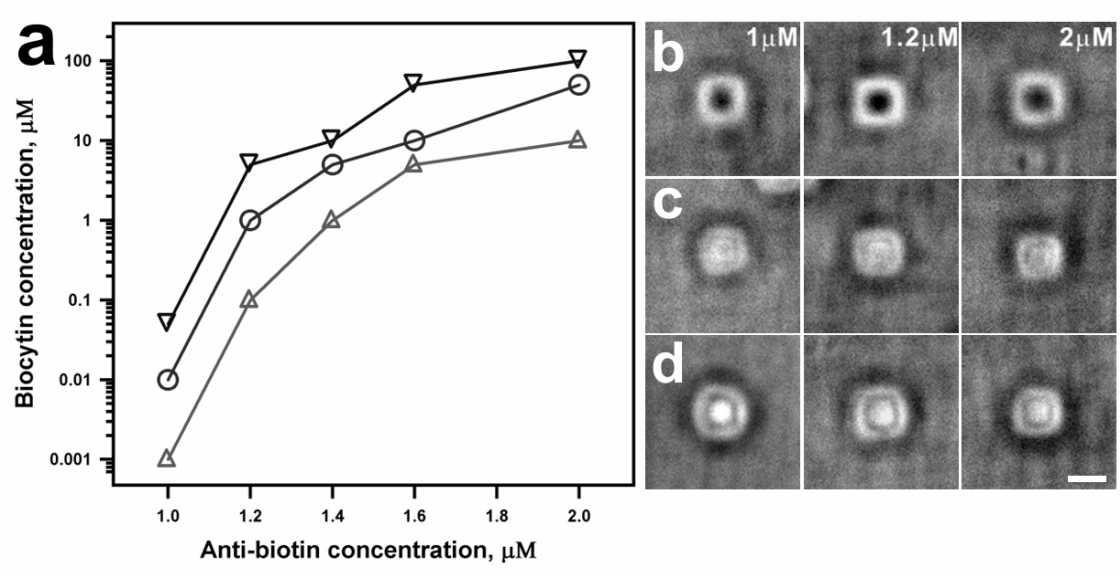

Figure 6-5. (a) Graph of the microlens focusing "state" as a function of solution biocytin concentration and initial anti-biotin concentration. Triangles represent the fully "on" state (as shown in row b), circles represent the transition point (row c), and inverse triangles represent the fully "off" state (row d). Note that 150 μL of each biocytin solution was used for this experiment (10 nM is equivalent to 1.5 pmol). The scale bars are 2 μm.

To observe microlens switching in more detail, we exposed the hydrogel microlenses to a narrower range of biocytin concentrations in Figure 6-5. These experiments reveal that hydrogel microlenses show at least three distinct image projection modes, which we refer to here as "off", "intermediate", and "on", in response to different anti-biotin concentrations in Figure 6-5(b, c, and d). Figure 6-5(a) shows the occurrence of each state upon changing the biocytin concentration as a function of the initial concentration of anti-biotin. From this it is clear that the bioresponsive microlenses

do display a transition range of finite width and are hence not purely binary response elements, thereby making the ultimate sensitivity of the element coupled to our ability to observe subtle changes in microlens focal length. Most importantly, Figure 6-5(a) shows a modulation of microlens sensitivity over ~4 orders of magnitude, clearly illustrating the potential for using gel swelling thermodynamics to modulate the sensitivity of a bioaffinity based sensor element.

6.3.2 Conclusions

This section have demonstrated a new paradigm in label-free biosensing by combining antibody:antigen cross-linked hydrogel microlenses with a simple brightfield optical microscopy technique. The utility of the construct for small molecule detection, its resistance to interferences from non-specific adsorption, the ability to tune the sensitivity, small sample volume requirement, and the inexpensive, rapid and simple fabrication method make this a potentially powerful and generalizable biosensing construct. Furthermore, these fundamental advantages make this material attractive for the future development of bioresponsive materials in applications far beyond bioanalysis.

6.4 Displacement Induced Switching Rates of Bioresponsive Hydrogel Microlenses

This section describes investigations of the response rates of bioresponsive hydrogel microlenses in order to gain a deeper understanding of their potential utility as a new label-free biosensing construct. The same bioresponsive hydrogel microlens construct as previously described in this chapter were used for this study. The response rates of the microlenses to biocytin binding (bound antibody-antigen displacement) were studied by monitoring the microlens optical properties via brightfield optical microscopy. The response rates of the hydrogel microlenses are strongly coupled to analyte concentrations at a equilibrium number of antigen:antibody binding on the hydrogel microlenses.

6.4.1 Results and Discussion

The main purpose of this study is to investigate the response rate of the bioresponsive hydrogel microlenses on label-free biosensing. To accomplish this goal, a bioresponsive hydrogel microlens construct containing biotin:anti-biotin-labeled pNIPAm-*co*-AAc microparticles and non-labeled pNIPAm-*co*-AAc microparticles is prepared, which is shown in Scheme 6-1.

The focusing power of microlenses as a function of the polyclonal anti-biotin concentration is shown in Figure 6-6. Here, we have prepared a microlens assembly containing pNIPAm-AAc microlenses (left element in each column as an internal reference) and biotin/ABP functionalized pNIPAm-AAc microlenses (right element in each column as the responsive element) in Figure 6-6 (a,c). The microlenses were

incubated with a 1 μM solution of anti-biotin solution and then irradiated with UV light allowing for photo-tethering of anti-biotin to microlens surface (Figure 6-6 b,d). As in the previous studies, the biotin/ABP functionalized microlens not only shows in the differential interference contrast (DIC) images (Figure 1b), with the formation of a dark circle at the particle periphery, but also shows changes in the image projection through the microlenses (Figure 6-6 d). However, there is no discernable change in the optical properties of the pNIPAm-*co*-AAc microlenses after antibody incubation. These results suggest that above a antibody concentration, the only biotin/ABP functionalized microlenses deswell by formation of biotin:anti-biotin cross-links at the microlens surface, undergo change in the local refractive index (RI), and is in the so called "on" configuration. These results are also confirmed by measuring an effective focal length of the microlens "on" or "off" state. To this end, we measured the distance between the focusing point of light source and the surface plane of the microlens substrate by using a brightfield microscope setup. The effective focal lengths of the "on" and "off" states are determined as 3.07 μm and 6.18 μm, respectively.[*] It is clear that the bioresponsive microlenses are able to show significant changes in the optical properties for the each state, although the measured focal length of the microlenses may be shorter than that of the actual microlens component mainly due to microscope setup, and/or other compartments of the substrate assembly.

[*] We thank Prof. M. Srinivasarao for helpful discussion during the focal length measurements of this work.

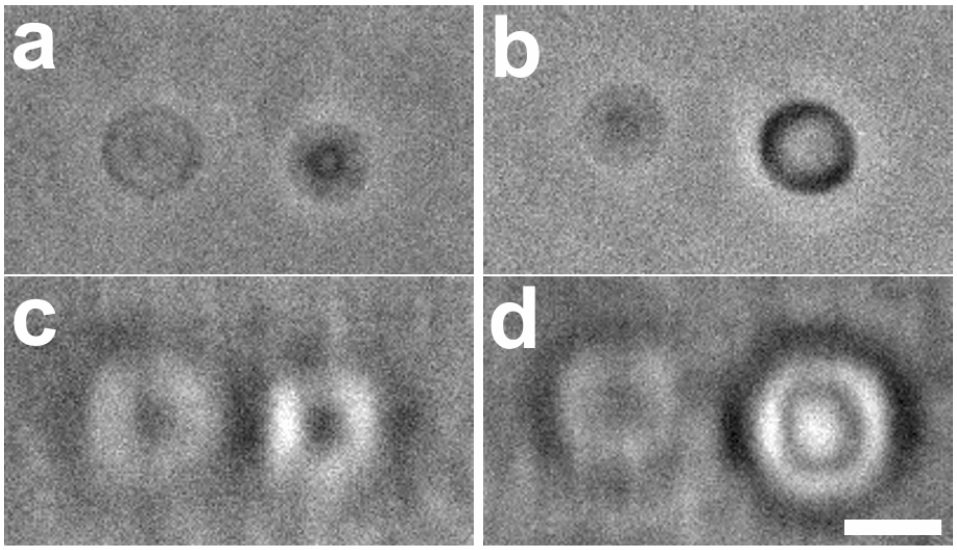

Figure 6-6. The responsive behavior of hydrogel microlenses to polyclonal anti-biotin incubation. DIC microscopy images of pNIPAm-*co*-AAc hydrogel microlenses (left element in each column) and biotin/ABP functionalized hydrogel microlenses (right element in each column) before (a) and after (b) 1 μM anti-biotin incubation. Projected square-pattern (shown in Scheme 1) images (c) and (d) through the hydrogel microlenses under same condition as described in (a) and (b), respectively. The scale bar is 2 μm.

To investigate the time dependent response of the bioresponsive microlenses, they were exposed to the various antigen concentrations in 10 mM phosphate buffered saline (PBS), and the focusing power was monitored over time. Figure 6-7 shows the focusing power of the microlenses as a function of antigen incubation time. The results show that the characteristic timescale for microlens swelling is a function of the solution antigen concentration. As one would expect, the response is rapid (<10 min) under higher antigen concentrations, (row d), while low antigen concentrations do not induce swelling on the timescale of this experiment (row a). We interpret these results by considering that hydrogel swelling is induced by displacing a critical number of tethered antibody-antigen binding pairs. The time required for antibody:antigen displacement will be dependent on the intrinsic dissociation rate constant of this pair, the intrinsic association rate between the free antigen and the bound antibody, and the concentration of free antigen. Under the conditions that gave rise to Figure 6-7, where the bound antibody:antigen concentration is held constant, the free antigen concentration remains the only tunable variable. In the light of these results, we expect that the response rate of the microlenses will be related to the microlens sensitivity, which is determined by the number of bound antibody:antigen pairs.

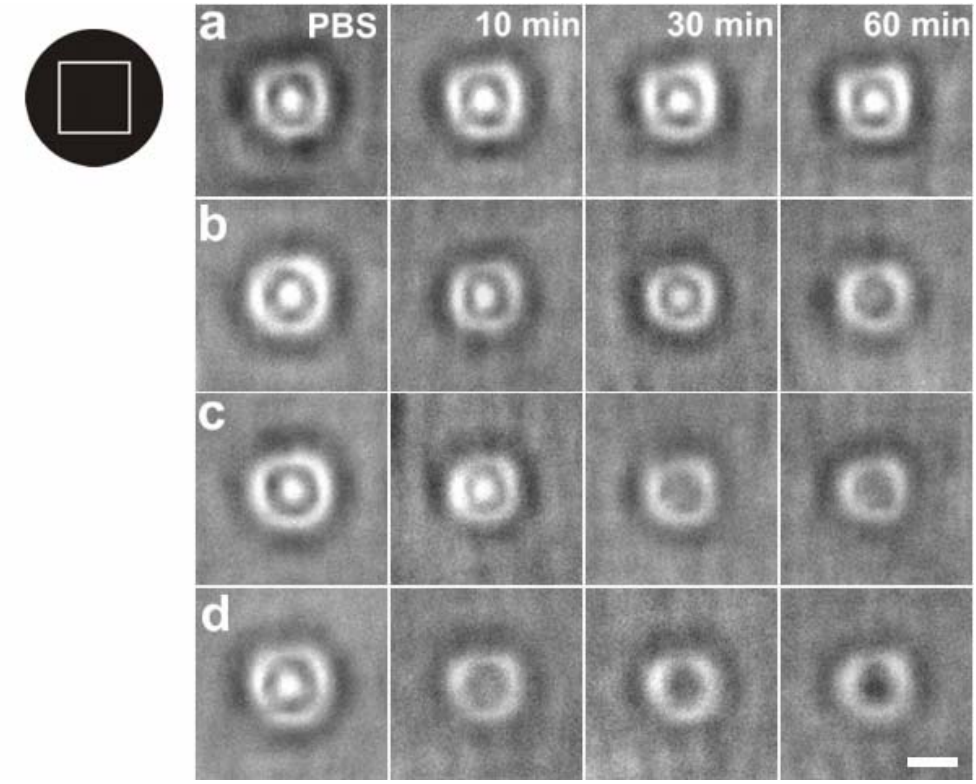

Figure 6-7. Lens switching times as a function of free biocytin concentration. Projection of a square pattern (shown on top left) through a hydrogel microlens prepared via incubation with 2.0 μM anti-biotin. The [biocytin] is: (a) 10 μM (b) 50 μM (c) 100 μM (d) 500 μM. The contact times are indicated at the top of each column, with the initial image in PBS shown in the first column. The scale bar is 2 μm.

The ability to determine the antigen concentration in both equilibrium and kinetic modes may allow us to apply this behavior to multi-dimensional antigen sensing. For example, Figure 6-8 shows the microlens state in response to free antigen as a function of time and tethered antibody concentration. It is interesting to note that the different number of "on" or "off" lenses serves to form a response pattern, which is a function of the solution antigen concentration (10 μM (left), 50 μM (center), 100 μM (right)). Such time-evolving patterns may be of use in increasing our ability to discriminate between small differences in antigen concentration and may also increase the dynamic range with respect to antigen sensitivity.

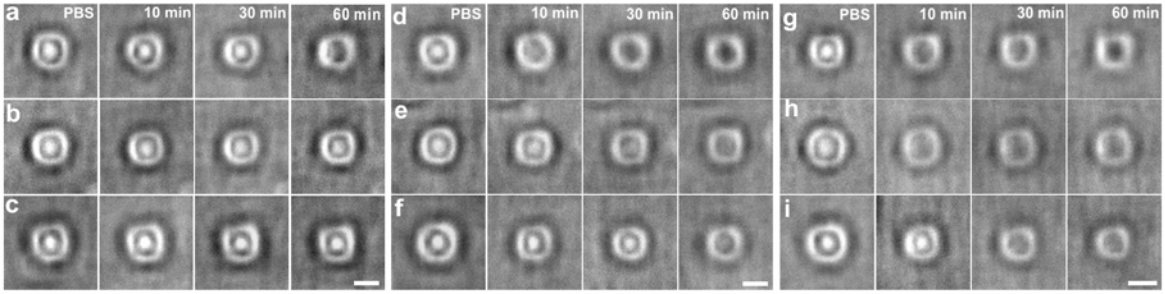

Figure 6-8. Microlens response time as a function of sensitivity. Projection of the square pattern (shown in Figure 6-7) through a microlens incubated with anti-biotin solutions of 0.7 μM (row a,d,g), 1 μM (row b,e,h), and 2 μM (row c,f,i). Number of "on" or "off" state in projected images was measured as a function of response time to biocytin concentrations (left (a,b,c) = 10 μM biocytin, center (d,e,f) = 50 μM biocytin, right (g,h,i) = 100 μM biocytin). The contact times are indicated at the top of each column, with the initial image in PBS shown in the first column. The scale bar is 2 μm.

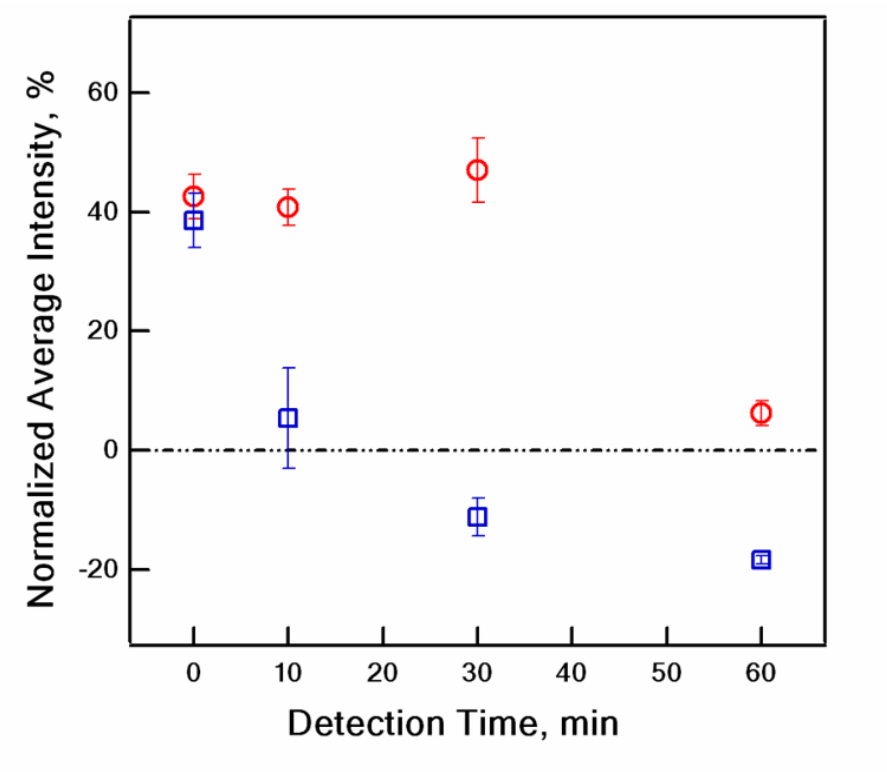

Figure 6-9. Normalized average intensity of the projected images as a function of lens time. The average intensity of central region (0.55 μm^2) in the projected images was normalized against the background intensity as a function of free biocytin concentration: (red circles) 50 μM and (blue squares) 500 μM. The error bars represent ±1σ about the average intensity of 4 microlens images.

The microlens focusing state in response to antigen concentration as a function of times is shown in Figure 6-9. The normalized average intensity (in percentile) was determined by subtracting the average background intensity of the captured images from the average intensity of the central region (0.55 μm^2) of the image projected through the microlens. Thus, a positive value can be considered as a lens "on" state, where the central region of the projected square image (see Figures 6-6 to 6-9) is brighter than the background. As expected from the images shown in Figure 6-7(b,d), the projected image intensity allows one to distinguish between the lens "off" and lens "on" states. These results suggest that the bioresponsive microlens response to the target antigen can be monitored by quantitative image analysis as opposed to qualitative inspection of the image fidelity.

As described above, we propose that the response time of the microlenses will be related to the number of antibody:antigen cross-links. This behavior is shown in Figure 6-10. For these experiments, the sensitivity of the microlenses was modulated by changing number of antibody-antigen cross-links present on the microlens. The microlenses were then exposed to different concentrations of antigen, after which the microlenses were continually observed on the optical microscope. As expected, the response rates of the microlenses (detection time for biocytin analysis through the lens state "on" to off") is faster in the higher biocytin concentration than that in the lower concentration at an antibody:antigen cross-linking degree on the microlenses. Thus, the results clearly show that the time required for lens switching is closely related to both the microlens sensitivity, and the solution concentration of the antigen.

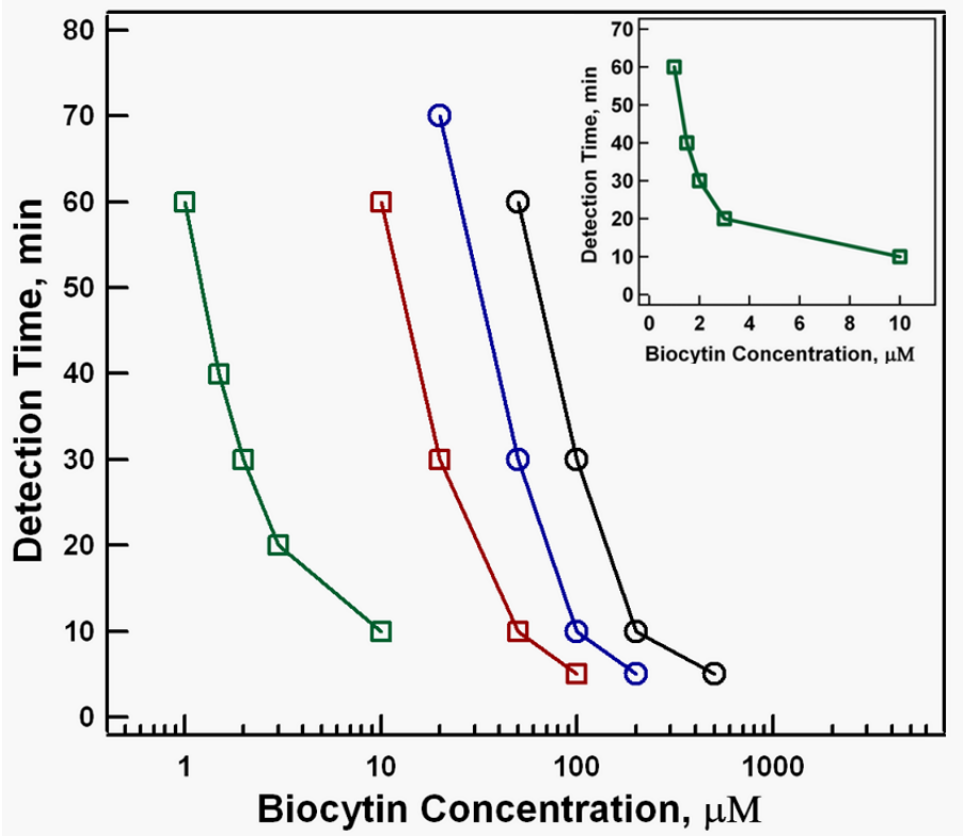

Figure 6-10. Lens switching rate was measured as a function of free biocytin concentration for microlenses prepared from a range of solution concentrations of anti-biotin. The anti-biotin concentrations used were: (green square) 0.3 μM, (red square) 0.7 μM, (blue circle) 1.0 μM, and (black circle) 2.0 μM. The inset shows the 0.3 μM anti-biotin incubated case with the x-axis on a linear scale.

6.4.2 Conclusions

This section has demonstrated that the response rates of antibody-antigen modified hydrogel microlenses are strongly tied to the equilibrium sensitivities of those materials. We also show that the sensitivity of the each microlens is tunable, and can be read-out by simple optical microscopy with image analysis software in quantitative fashion. Finally, we measured the effective focal lengths of the hydrogel microlenses, experimentally by optical microscopy. The hydrogel microlens construct can be prepared in simple, rapid, and inexpensive method for the detection of antigen, where surface localization of the binding pairs may offer advantages with respect to reversibility and switching speed. Thus, these advantages make this bioresponsive material useful not only for label-free biosensing but also for a variety of other applications where direct responsivity to the surrounding biological environment is advantageous.

6.5 Influence of Ancillary Binding and Nonspecific Adsorption on Bioresponsive Hydrogel Microlenses

In this section, I will describe the investigation on the intrinsic selectivity of the bioresponsive microgel construct to a target molecule, such as antigen and protein, in the microlensing methodology. For this study, specific (but ancillary) and nonspecific binding effects on the bioresponsive microlenses were evaluated by observing the optical properties of the microlenses when they are exposed to a solution of a secondary IgG (for specific binding) and a solution of antigen dissolved in reconstituted human serum (for nonspecific binding). These approaches enable one to deeply understand the utility and potential advantages of the bioresponsive microlens construct not only for advanced label-free biosensing but also for new stimuli-responsive biomaterials. The technique described here does not suffer from false signals by nonspecific adsorption, mainly due to the fact that the microlensing is predominantly modulated by cross-linking formation/deformation of antibody:antigen (and/or protein:ligand) binding rather than by simple protein adsorption.

6.5.1 Results and Discussion

The main purpose of this study is to examine specific and nonspecific adsorption effects on bioresponsive hydrogel microlenses to comprehend the utility and potential advantages of this bioresponsive material. To accomplish this aim, pNIPAM-*co*-AAc hydrogel microparticles were first functionalized with biotin via EDC coupling (Scheme 5-2) or with biotin-ABP via EDC and DCC coupling (Scheme 6-1).[2,19] For direct protein binding study (Scheme 5-2), the biotinylated hydrogels are used to prepare bioresponsive

hydrogel microlens constructs as described in previous studies. Also, reversibly bioresponsive hydrogel microlenses (Scheme 6-1) are prepared by using biotin-ABP functionalized hydrogels via anti-biotin incubation and photoligation. The reversible microlenses are then exposed to antigen in reconstituted human serum for nonspecific binding effects and secondary IgG solutions for specific/ancillary binding effects. By taking the advantage from our previous reports, a specific and/or nonspecific binding effect on the bioresponsive hydrogel microlenses is investigated by utilizing the engineered hydrogel microlensing in conjunction with the brightfield optical microscopy and fluorescence microscopy.

To develop bioresponsive materials for a specific application, the selective binding between the trigger and the material is highly required even though a nonspecific adsorption is somehow coexistent in any case. For that reason, specific biotin-avidin binding to the hydrogel microlenses is investigated by using fluorescence microscope, and the results are shown in Figure 6-11. Note that the microgels and avidin are fluorescently labeled by fluorescein and Texas red, respectively to determine avidin binding to the microgels via red and green emission spectra. One group of microgels is non-biotinylated as an internal reference (right element in each panel). Red fluorescence at the outer surface of the biotinylated microgels is observed when the microgels are exposed to various concentrations of avidin solution (Figure 6-11b-d). Nonspecific adsorption of avidin to the non-biotinylated microgels is apparently negligible. Note that both microgels show same results at the same experiment conditions when they are placed on the substrate in homogeneous population (data not shown).

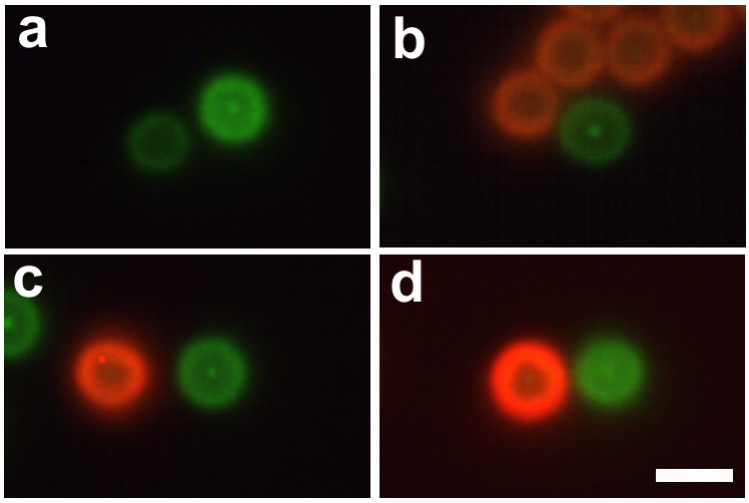

Figure 6-11. Selective binding of avidin on biotinylated hydrogel microlenses in (a) no avidin, (b) 10 nM avidin, (c) 100 nM avidin, and (d) 1 μM avidin dissolved in 10 mM PBS buffer solution. Note that avidin (red) is labeled with Texas red, and the microgel (green) is labeled with 4-acrylamidofluorescein. The fluorescence microscopy images reveal that the biotin-avidin binding is only observed on the biotinylated microgels in the various concentrations of avidin solution. Note that nonspecific adsorption of avidin on the nonbiotinylated microgels is not observed. The scale bar is 2 μm.

In applying a biosensing/bioassay platform to a realistic application, the platform and materials are mostly required to be insensitive to interferences in complex media such as serum. To investigate the reliability of the bioresponsive microgels in such complex media, the hydrogel microlenses were prepared by the route b in Scheme 6-3 and then are exposed to various antigen concentrations dissolved in reconstituted

ImmunoPure Normal Human Serum (Figure 6-12). These microlenses display their typical sensitivities to biocytin concentration in reconstituted human serum, where the hydrogel microlenses undergo lens "on" to "off" state with increasing the biocytin concentration. The results suggest that the bioresponsivity of the hydrogel microlenses is highly resistant to nonspecific interference due to the use of a displacement/competitive binding scheme.

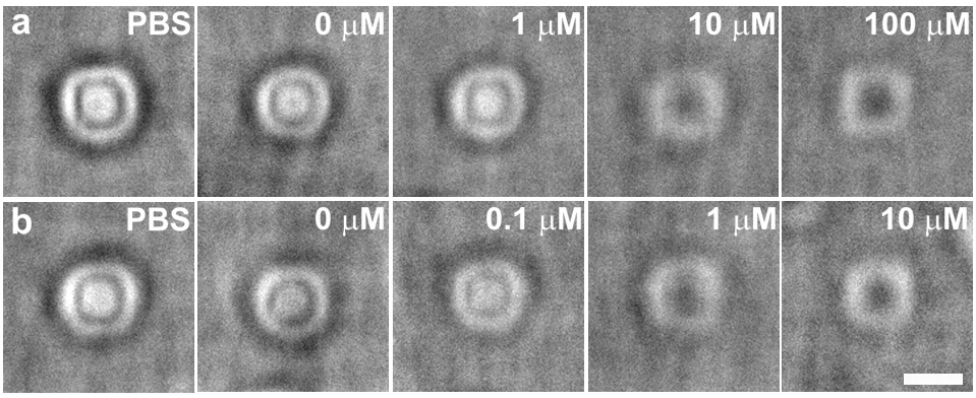

Figure 6-12. The sensitivity of hydrogel microlenses to various antigen concentrations in normal human serum. The hydrogel microlenses are incubated in (a) 1 μM antibody solution, and (b) 0.3 μM antibody solution. Note that antibiotin and biocytin was selected as an antibody and antigen, respectively, and reconstituted normal human serum (protein concentration, 60 mg/ml) was used for false negative control experiment. PBS buffer solution was used for a reference medium in the experiment. The biocytin concentrations in the human serum are indicated at the top right of each column. The scale bar is 2 μm.

We also find that these microlenses are insensitive to secondary specific binding events, such as those involving anti-IgG binding. Figure 6-13a shows the DIC and image projection views of a single bioresponsive microlens in PBS. A solution of anti-goat IgG (raised in rabbit, and labeled with Alexa fluor 594), which should bind the tethered antibody but should do so by binding to non-paratope regions, was exposed to the microlenses. Since this protein should not disrupt antigen-antibody interactions, there is no discernable change in the microlens appearance or microlens-projected images (Figure 6-13b). Fluorescence microscopy further reveals that the secondary antibody is indeed bound to the particle periphery. Subsequently, the microlenses were exposed to 100 μM concentration of an antigen solution dissolved in PBS buffer, which results in shift in the lensing properties from "on" to "off", as seen in both the DIC and image projection modes (Figure 6-13c). The fluorescence microscopy image confirms that the secondary antibody is still bound to the tethered anti-biotin, while biotin:anti-biotin binding at the microlens surface is disrupted by the displacement action as described above. Green emission from biotin-4-fluoresein is not observed in the tested concentration probably due to a relatively weak intensity and/or photobleaching.

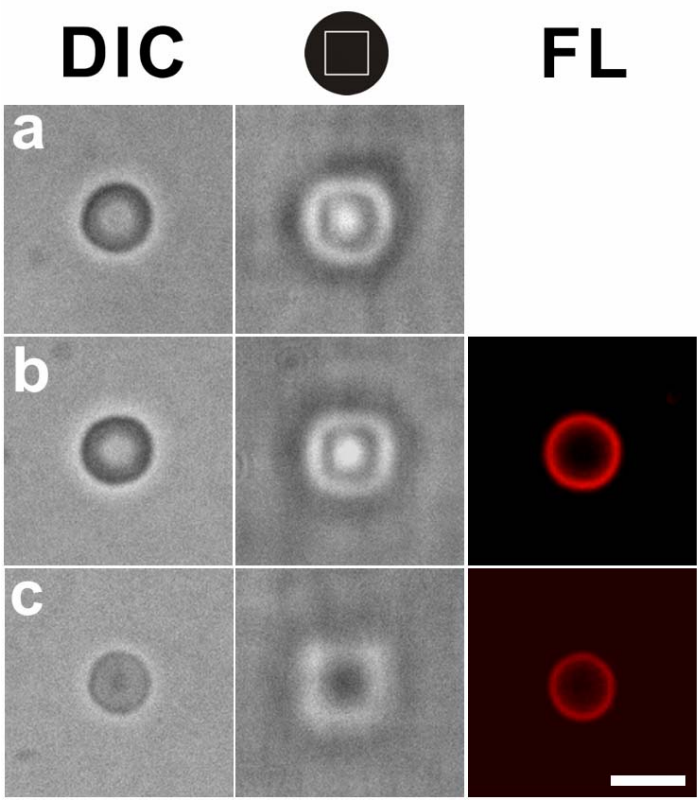

Figure 6-13. Effects of secondary specific adsorption on the sensitivity of bioresponsive microlenses prepared with 1 μM anti-biotin (raised in goat): (left column) DIC image of the hydrogel microlens, (center column) projected square pattern images through the hydrogel microlens, and (right column) fluorescence microscopy images in: (a) 10 mM PBS buffer pH 7.5, (b) 0.1 μM rabbit anti-goat IgG conjugated with Alexa Fluor 594, (c) 100 μ M biotin-4-fluorecein in sequence fashion. The scale bar is 2 μm.

Table 6-1. Effects of secondary specific adsorption on the utility of bioresponsive microlenses. DIC images of the hydrogel microlenses (DIC) and fluorescence microscopy images (FL) were investigated and characterized as lens "on" or "off" in the same method as described in Figure 6-13. Note that the bioresponsive microlenses are incubated in 1 μM anti-biotin (raised in goat) and then observed in10 mM PBS buffer pH 7.5 in the first step; next, the microlenses are exposed to 1 μM, 0.5 μM, or 0.1 μM rabbit anti-goat IgG conjugated with Alexa Fluor 594 (IgG); finally, the microlenses were observed in 1 mM biocytin.

[anti-biotin] (DIC)	1 μM (on)	1 μM (on)	1 μM (on)
[anti-IgG] (DIC, FL)	1 μM (on, Ab bound)	0.5μM (on, Ab bound)	0.1μM (on, Ab bound)
[antigen] (DIC, FL)	1 mM (on, Ab bound)	1 mM (on, Ab bound)	1 mM (off, Ab bound)

By considering the fact that the secondary IgG can form additional cross-links by means of binding to the tethered antibody at microlens periphery, it is worthwhile to investigate the binding of the secondary IgG on microlenses for a specific, but undesired binding event. For this study, the microlensing is investigated in the same method as described in Figure 6-13, but the microlenses were exposed to higher concentration of the secondary IgG. Table 6-1 shows that the microlens biosensing can be perturbed by the formation of the secondary cross-links. If the microlenses are exposed to 0.5 μM or 1 μM solution of the secondary IgG, a sufficient number of Ab:Ab cross-links are formed for

lens “on” state to persist even in the presence of antigen. These microlenses will switch to the “off” state when exposed to 50 μM biotin solution, and microlenses in “off” state are switched to “on” state with introduction of 1 μM solution of the secondary IgG. These results suggest that the secondary IgG can form secondary cross-links by coupling tethered antibody at the microlens periphery and thus influence the bioresponsive microlensing. Note that the fluorescent microscopy reveals that the secondary IgG are bound to the microlens surface throughout this experiment after introduced.

6.5.2 Conclusions

This section has demonstrated that the responsive behavior of the bioresponsive hydrogel microlenses is exclusively triggered by the formation/disruption of cross-links via ligand-protein or antigen-antibody pair. I also show that the hydrogel microlensing is highly resistant to interference by simple protein adsorption in a negative control study. Furthermore, the positive control experiment with the secondary IgG again confirms that biosensing/bioassay in applying the hydrogel microlens construct is strongly dependant on the cross-link formation/deformation and not on the nonspecific protein adsorption. The bioresponsive hydrogel microlens can be simply prepared in rapid and inexpensive method as well as in scalable and highly selective fashion. This study suggests that the hydrogel microlens construct can be applied to prepare a highly selective biosensor and also to develop smart biomaterials in directly response to the surrounding biological stimuli.

6.6 References

(1) Miyata, T.; Jige, M.; Nakaminami, T.; Uragami, T., Tumor marker-responsive behavior of gels prepared by biomolecular imprinting. *Proc. Natl. Acad. Sci. USA* **2006**, *103*, 1190-1193.

(2) Kim, J.; Nayak, S.; Lyon, L. A., Bioresponsive Hydrogel Microlenses. *J. Am. Chem. Soc.* **2005**, *127*, 9588-9592.

(3) Plunkett, K. N.; Berkowski, K. L.; Moore, J. S., Chymotrypsin Responsive Hydrogel: Application of a Disulfide Exchange Protocol for the Preparation of Methacrylamide Containing Peptides. *Biomacromolecules* **2005**, *6*, 632-637.

(4) Ehrick, J. D.; Deo, S. K.; Browning, T. W.; Bachas, L. G.; Madou, M. J.; Daunert, S., Genetically engineered protein in hydrogels tailors stimuli-responsive characteristics. *Nature Materials* **2005**, *4*, 298-302.

(5) Tauro, J. R.; Gemeinhart, R. A., Matrix Metalloprotease Triggered Delivery of Cancer Chemotherapeutics from Hydrogel Matrixes. *Bioconjugate Chem.* **2005**, *16*, 1133-1139.

(6) Rizzi, S. C.; Hubbell, J. A., Recombinant protein-co-PEG networks as cell-adhesive and proteolytically degradable hydrogel matrixes. Part I: Development and physicochemical characteristics. *Biomacromolecules* **2005**, *6*, 1226-1238.

(7) Nayak, S.; Lyon, L. A., Soft nanotechnology with soft nanoparticles. *Angew. Chem. Intl. Ed.* **2005**, *44*, 7686-7708.

(8) Kim, S.; Chung, E. H.; Gilbert, M.; Healy, K. E., Synthetic MMP-13 degradable ECMs based on poly(N-isopropylacrylamide-co-acrylic acid) semi-interpenetrating polymer networks. I. Degradation and cell migration. *Journal of Biomedical Materials Research, Part A* **2005**, *75A*, 73-88.

(9) Eddington, D. T.; Beebe, D. J., Flow control with hydrogels. *Adv. Drug Deliv. Rev.* **2004**, *56*, 199-210.

(10) Nayak, S.; Lee, H.; Chmielewski, J.; Lyon, L. A., Folate-mediated cell targeting and cytotoxicity using thermoresponsive microgels. *J. Am. Chem. Soc.* **2004**, *126*, 10258-10259.

(11) Nayak, S.; Lyon, L. A., Ligand-functionalized core/shell microgels with permselective shells. *Angew. Chem. Intl. Ed.* **2004**, *43*, 6706-6709.

(12) Lutolf, M. P.; Raeber, G. P.; Zisch, A. H.; Tirelli, N.; Hubbell, J. A., Cell-responsive synthetic hydrogels. *Adv. Mater.* **2003**, *15*, 888-892.

(13) Drury, J. L.; Mooney, D. J., Hydrogels for tissue engineering: scaffold design variables and applications. *Biomaterials* **2003**, *24*, 4337-4351.

(14) Metters, A. T.; Anseth, K. S.; Bowman, C. N., Fundamental studies of a novel, biodegradable PEG-b-PLA hydrogel. *Polymer* **2000**, *41*, 3993-4004.

(15) Miyata, T.; Asami, N.; Uragami, T., Preparation of an Antigen-Sensitive Hydrogel Using Antigen-Antibody Bindings. *Macromolecules* **1999**, *32*, 2082-2084.

(16) Lutolf, M. P.; Lauer-Fields, J. L.; Schmoekel, H. G.; Metters, A. T.; Weber, F. E.; Fields, G. B.; Hubbell, J. A., Synthetic matrix metalloproteinase-sensitive hydrogels for the conduction of tissue regeneration: Engineering cell-invasion characteristics. *Proc. Natl. Acad. Sci. USA* **2003**, *100*, 5413-5418.

(17) Holtz, J. H.; Asher, S. A., Polymerized colloidal crystal hydrogel films as intelligent chemical sensing materials. *Nature* **1997**, *389*, 829-832.

(18) Kim, S.; Healy, K. E., Synthesis and Characterization of Injectable Poly(N-isopropylacrylamide-co-acrylic acid) Hydrogels with Proteolytically Degradable Cross-Links. *Biomacromolecules* **2003**, *4*, 1214-1223.

(19) Kim, J.; Singh, N.; Lyon, L. A., Label-free biosensing with hydrogel microlenses. *Angew. Chem. Intl. Ed.* **2006**, *45*, 1446-1449.

(20) Asher, S. A.; Alexeev, V. L.; Goponenko, A. V.; Sharma, A. C.; Lednev, I. K.; Wilcox, C. S.; Finegold, D. N., Photonic crystal carbohydrate sensors: Low ionic strength sugar sensing. *J. Am. Chem. Soc.* **2003**, *125*, 3322-3329.

(21) Alexeev, V. L.; Sharma, A. C.; Goponenko, A. V.; Das, S.; Lednev, I. K.; Wilcox, C. S.; Finegold, D. N.; Asher, S. A., High ionic strength glucose-sensing photonic crystal. *Analytical Chemistry* **2003**, *75*, 2316-2323.

(22) Miyata, T.; Uragami, T.; Nakamae, K., Biomolecule-sensitive hydrogels. *Adv. Drug Deliv. Rev.* **2002**, *54*, 79-98.

(23) Hoffman, A. S., Hydrogels for biomedical applications. *Adv. Drug Deliv. Rev.* **2002**, *54*, 3-12.

(24) Ogawa, K.; Wang, B.; Kokufuta, E., Enzyme-Regulated Microgel Collapse for Controlled Membrane Permeability. *Langmuir* **2001**, *17*, 4704-4707.

(25) Metters, A. T.; Bowman, C. N.; Anseth, K. S., Verification of scaling laws for degrading PLA-b-PEG-b-PLA hydrogels. *AIChE J.* **2001**, *47*, 1432-1437.

(26) Lee, K. Y.; Mooney, D. J., Hydrogels for Tissue Engineering. *Chem. Rev.* **2001**, *101*, 1869-1879.

(27) Holtz, J. H.; Holtz, J. S. W.; Munro, C. H.; Asher, S. A., Intelligent Polymerized Crystalline Colloidal Arrays: Novel Chemical Sensor Materials. *Analytical Chemistry* **1998**, *70*, 780-791.

(28) Jeong, B.; Bae, Y. H.; Lee, D. S.; Kim, S. W., Biodegradable block copolymers as injectable drug-delivery systems. *Nature* **1997**, *388*, 860-862.

(29) Aggeli, A.; Bell, M.; Boden, N.; Keen, J. N.; Knowles, P. F.; McLeish, T. C.; Pitkeathly, M.; Radford, S. E., Responsive gels formed by the spontaneous self-assembly of peptides into polymeric beta-sheet tapes. *Nature* **1997**, *386*, 259-262.

(30) Kim, J.; Serpe, M. J.; Lyon, L. A., Hydrogel Microparticles as Dynamically Tunable Microlenses. *J. Am. Chem. Soc.* **2004**, *126*, 9512-9513.

(31) Serpe, M. J.; Kim, J.; Lyon, L. A., Colloidal hydrogel microlenses. *Adv. Mater.* **2004**, *16*, 184-187.

(32) Kim, J.; Serpe, M. J.; Lyon, L. A., Photoswitchable Microlens Arrays. *Angew. Chem. Intl. Ed.* **2005**, *44*, 1333-1336.

(33) Hermanson, G. T. *Bioconjugate Techniques*; Academic Press: San Diego, 1996.